



TUNNEL IMPACT ASSESSMENT

HARTFIELD PLACE RESIDENTIAL DEVELOPMENT

SWORDS ROAD

IMPACT OF CONSTRUCTION OF THE DEVELOPMENT

ON DUBLIN PORT TUNNELS

Scheme No. 472

for

Eastwise Construction Swords Limited

Station Mews,
Lindsay Grove,
Dublin 9,
D09 W8W8
Ireland

By

AGL Consulting

Suite 2, The Avenue
Beacon Court, Sandyford
Dublin 18
Tel: (01) 295 6532
Fax: (01) 295 6533

March, 2022




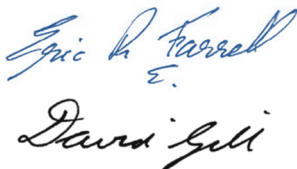
Document Approval Form

TUNNEL IMPACT ASSESSMENT HARTFIELD PLACE RESIDENTIAL DEVELOPMENT SWORDS ROAD

IMPACT OF CONSTRUCTION OF THE DEVELOPMENT ON DUBLIN PORT TUNNELS

Scheme No. 472

Revision	Description	Date	Notes
0		08/09/2020	
1		11/02/2021	
2		25/03/2022	Clarification on Foundation Design for Block G & Update for comments on SHD application

Document No:	19-196-R05	Rev 2
Made:	Niamh Farrell	
Checked:	Dr. Eric Farrell/ Dr. David Gill	

This document has been prepared for the titled project and should not be relied upon or used for any other project without an independent check being carried out as to its suitability and prior written authority of AGL being obtained. AGL accepts no responsibility or liability for the consequences of this document being used for a purpose other than the purposes for which it was commissioned. Any person using or relying on the document for such other purposes agrees and will by such use or reliance be taken to confirm his agreement to indemnify AGL for all loss or damage resulting therefrom. AGL accepts no responsibility or liability for this document to any other party other than the person by whom it was commissioned.

TABLE OF CONTENTS

1	INTRODUCTION	1
2	THE DEVELOPMENT	3
2.1	Introduction	3
2.2	Details of Development	3
2.3	Position of Development Relative to Dublin Port Tunnels.....	3
2.4	Building Finished Floor Levels & Bearing Pressures.....	4
3	PLANNING APPLICATION HISTORY	11
4	TUNNEL DETAILS	13
4.1	Tunnel Type and Chainages	13
4.2	The Tunnel Boring Machine (TMB)	16
4.3	Tunnel Lining Details (Gillarduzzi, 2013)	16
4.4	Tunnel Design Limits	17
4.5	Pedestrian Cross Passage.....	18
4.6	Guidance Notes for Developers (TII)	20
5	GROUND & GROUNDWATER CONDITIONS	22
5.1	Available Ground Investigation Information.....	22
5.2	Ground Conditions	22
5.3	Ground Water Conditions.....	28
6	CHARACTERISTIC SOIL PROPERTIES	31
6.1	Upper Brown Boulder Clay	31
6.2	Upper Black, Lower Brown and Lower Black Boulder Clay	31
6.3	Hardening Soil model with small-strain stiffness (HSS) material parameters.....	32
7	PLAXIS 3D FINITE ELEMENT ANALYSIS	35
7.1	Introduction	35
7.2	Design Philosophy.....	35
7.3	Plaxis Ground Model.....	36
7.4	Ground Water Model.....	39
7.5	Site Model	39
7.6	Characteristic Loads	40
7.7	Tunnel Details & Material Properties	41
7.8	Design Situations.....	43
7.9	Plaxis 3D Results.....	47
7.10	Discussion	61
8	STRUCTURAL ASSESSMENT ON TUNNEL LINING.....	63
8.1	Change in Vertical Total Stress on the Tunnel Lining	63
8.2	Tunnel Lining Bending Moments and Axial forces	63
8.2.1	Transverse Joints.....	63
8.2.2	Longitudinal Joints.....	67
8.3	Tunnel Lining Shear Forces	70
8.3.1	Transverse Joints.....	70
8.3.2	Longitudinal Joints.....	70
8.4	Tunnel Lining Ovalisation & Joint Rotation & Eccentricity	70
8.5	Tunnel Lining Longitudinal Curving & Joint Opening	71
9	ASSESSMENT OF PEDESTRIAN CROSS PASSAGE.....	71
10	CONSTRUCTION SEQUENCE	72

11	SUMMARY & CONCLUSION	73
12	REFERENCES	75

APPENDICES

- **Appendix A:** Calculations
- **Appendix B:** As-Built Drawings of Dublin Port Tunnels
- **Appendix C:** Plaxis 3D Results
- **Appendix D:** Comparison of Mohr Coulomb (MC) and Hardening Soil model with small-strain stiffness (HSS) material model
- **Appendix E:** Punch Consulting Characteristic Bearing Pressures below Buildings & Basement
- **Appendix F:** Plaxis 3D Results – Construction Sequence
- **Appendix G:** GII 2010 Ground Investigation Report
- **Appendix H:** GII 2020 Ground Investigation Report

TABLE OF FIGURES

Figure 1-1: Location of Proposed Residential Development	2
Figure 1-2: Location of development and Dublin Port Tunnels	2
Figure 2-1: Location of Buildings and Basement Relative to Dublin Tunnels.....	4
Figure 2-2: Finished Floor levels for Blocks A-G of proposed development	7
Figure 2-3: Finished Floor levels for basement proposed below Blocks A to E.....	7
Figure 2-4: Topographical Survey, carried out in February, 2020 (DOB Surveys Ltd)	8
Figure 2-5: Plan Layout of Attenuation Tanks on the site (shown as blue hatched areas)	8
Figure 2-6: Characteristic Bearing Pressures for development (Provided by Punch Consulting) – included in Appendix E.....	9
Figure 2-7: Proposed attenuation tank design	9
Figure 2-8 Plan View of location of proposed basement access ramp (outlined in blue).....	10
Figure 3-1: Development granted planning permission by Dublin City Council in 2010 (DCC Reg. Ref. 3269/10 / ABP Ref. PL29N.238685).....	12
Figure 4-1: Plan View of DPT in the vicinity of the site showing tunnel chainages (site shown in red).....	14
Figure 4-2: Profile View of View of DPT in the vicinity of the site showing tunnel chainages (Northbound tunnel).....	15
Figure 4-3: Tunnel Lining Details (extract from Dwg No. DR/HA/BT/C11/41018/07/X)	17
Figure 4-4: Design N-M Interaction Chart of the lining of the Dublin Tunnels	18
Figure 4-5: Cross Passage Design Details (as-built drawing No. DR/HA/BH/C11/41061/05/X)	19
Figure 4-6: Cross section through Cross Passage Design Details (as-built drawing No. DR/HA/BH/C11/41061/05/X).....	19
Figure 4-7: Dublin Port Tunnels - Zones 1 and 2.....	21
Figure 5-1: SI location Plan along Dublin Port Tunnels, from 1995 to 1996	24
Figure 5-2: SI location Plan Ground Investigations Ireland, 2010	24
Figure 5-3: SI location Plan Ground Investigations Ireland, 2020	25
Figure 5-4: Subsurface ground profile along northbound tunnel within site	26
Figure 5-5: SPT N-Values vs Depth	27

Figure 5-6: SPT N-Values vs Elevation	27
Figure 5-7: Groundwater Depth readings taken from standpipes (Oct, 1995 to May, 1997)	29
Figure 5-8: Groundwater Elevation readings taken from standpipes (Oct, 1995 to May, 1997)	29
Figure 5-9: Groundwater Depth readings taken from standpipes (June to August, 2020)	30
Figure 5-10: Groundwater Elevation readings taken from standpipes (June to August, 2020)	30
Figure 6-1: Drained stiffness of Boulder Clays showing increase with Elevation.....	33
Figure 6-2: Drained stiffness stiffness of Boulder Clays showing increase with depth	33
Figure 7-1: Plaxis 3D model of site (see Figure 7-9 for basement access ramp and attenuation tanks)	35
Figure 7-2: 3D Ground Model with locations of GP-A to GP-C	37
Figure 7-3: Ground Profile GP-A (level of tunnel varies)	37
Figure 7-4: Ground Profile GP-B & GP-C (level of tunnel varies)	38
Figure 7-5: Profile showing transition of tunnel into rock along the northbound and southbound tunnels.....	38
Figure 7-6: Profile showing transition of tunnel into rock along the northbound and southbound tunnels.....	38
Figure 7-7: Interpolated Ground water level below excavations (i.e. Blocks F and G, underground carpark and attenuation tanks).....	39
Figure 7-8: Global Ground Water Level.....	39
Figure 7-9: Final excavation levels for Blocks F and G, the basement, the attenuation tanks and the access ramp in the Plaxis program.....	40
Figure 7-10: Profile view of tunnels (facing west) showing drop of tunnel from north to south	42
Figure 7-11: 3D view of tunnels showing Pedestrian Cross Passage	42
Figure 7-12: 3D Plaxis Model showing Design Situation DS-1	44
Figure 7-13: 3D Plaxis Model showing Design Situation DS-2	44
Figure 7-14: 3D Plaxis Model showing Design Situation DS-3	45
Figure 7-15: 3D Plaxis Model showing Design Situation DS-4	45
Figure 7-16: 3D Plaxis Model showing Design Situation DS-5	46
Figure 7-17: 3D Plaxis Model showing the Dublin Port Tunnels model (southern side of site)	46
Figure 7-18: Orientation of axes along tunnel plate.....	50
Figure 7-19: Min. Vertical Tunnel Displacements (settlement) (DS-5 SB MC)	54
Figure 7-20: Max. Vertical Tunnel Displacements (heave) (DS-4 SB MC)	55
Figure 7-21: Min. Horizontal Tunnel Displacements (DS-3 NB MC).....	55
Figure 7-22: Max. Horizontal Tunnel Displacements (DS-1 SB MC).....	56
Figure 7-23: Max Axial Force on DPTs (N1 i.e. Longitudinal Force) (DS-1 NB MC).....	56
Figure 7-24: Max Axial Force on DPTs (N2 i.e. Hoop Force) (DS-2 NB MC).....	57
Figure 7-25: Max Bending Moment on DPTs (M11 i.e. Longitudinally along tunnel) (DS-1 SB MC)	57
Figure 7-26: Max Bending Moment on DPTs (M22 i.e. transversely across tunnel) (DS-1 SB MC)	58
Figure 7-27: Max Shear Force on DPTs (Q23 i.e. Transversely across tunnel) (DS-1 SB -MC)	58
Figure 7-28: Max Shear Force on DPTs (Q13 i.e. Longitudinally along tunnel) (DS-1 NB MC)	59

Figure 7-29: Vertical Total Stress (Initial conditions with Tunnels installed, at $y = 71$ i.e. max increase in stress on tunnels).....	59
Figure 7-30: Vertical Total Stress @ max change in total stress on tunnel lining i.e. at $y=71$ (DS-2 SB MC).....	60
Figure 7-31: Location of max change in total stress on tunnel lining i.e. $y = 71.0$ (DS-2 SB MC) – Section A-A.....	60
Figure 8-1: Design N-M Interaction Chart for tunnel lining along transverse direction with Plaxis 3D results plotted - MC NB.....	65
Figure 8-2: Design N-M Interaction Chart for tunnel lining along transverse direction with Plaxis 3D results plotted - MC SB	65
Figure 8-3: Design N-M Interaction Chart for tunnel lining along transverse direction with Plaxis 3D results plotted - HSS NB	66
Figure 8-4: Design N-M Interaction Chart for tunnel lining along transverse direction with Plaxis 3D results plotted - HSS SB.....	66
Figure 8-5: Design N-M Interaction Chart for tunnel lining along longitudinal direction with Plaxis 3D results plotted - MC NB.....	68
Figure 8-6: Design N-M Interaction Chart for tunnel lining along longitudinal direction with Plaxis 3D results plotted - MC SB	68
Figure 8-7: Design N-M Interaction Chart for tunnel lining along longitudinal direction with Plaxis 3D results plotted - HSS NB	69
Figure 8-8: Design N-M Interaction Chart for tunnel lining along longitudinal direction with Plaxis 3D results plotted - HSS SB.....	69

TABLE OF TABLES

Table 2-1: Finished floor level and Excavation levels for Blocks F & G	5
Table 2-2: Finished Floor Levels & Excavation levels for the basement	6
Table 2-3: Attenuation Tank Design Details	6
Table 4-1: Summary of Tunnel Details within the site.....	13
Table 4-2: Summary of information relating to the design of the lining for the Dublin Tunnels	17
Table 5-1: Summary of ground water levels taken from standpipes on the site (Detailed SI 2000).....	28
Table 5-2: Summary of ground water levels taken from standpipes on the site (GII 2020) ..	29
Table 5-3: Summary of ground water strikes in the boreholes(Detailed SI 2000 & GII 2020) ..	29
Table 6-1: Summary of geotechnical design parameters & ground model for site*	34
Table 6-2: Summary of geotechnical design parameters for HSS Model (after Lawler et al 2011)	34
Table 7-1: Summary of Ground Models GM-A to GM-C.....	36
Table 7-2: Summary of Tunnel Details in 3D Plaxis Model	41
Table 7-3: Material properties of the DPT tunnel lining & cross passage.....	42
Table 7-4: Design Situations for Plaxis 3D analysis.....	43
Table 7-5: Excavation Levels and Loads for Design Situations DS-1 to DS-5.....	43
Table 7-6: Change in Total Stress on the tunnel lining crown & invert (NB MC)	48
Table 7-7: Change in Total Stress on the tunnel lining crown & invert (NB HSS).....	49
Table 7-8: Change in Total Stress on the tunnel lining crown & invert (SB MC)	49
Table 7-9: Change in Total Stress on the tunnel lining crown & invert (SB HSS)	49

Table 7-10: Change in Total Stress on the crown of the Pedestrian Cross Passage (MC & HSS)	50
Table 7-11: Summary of the characteristic bending moments and axial and shear forces on the tunnels (NB MC).....	51
Table 7-12: Summary of the characteristic bending moments and axial and shear forces on the tunnels (NB HSS)	51
Table 7-13: Summary of the characteristic bending moments and axial and shear forces on the tunnels (SB MC)	52
Table 7-14: Summary of the characteristic bending moments and axial and shear forces on the tunnels (SB HSS).....	52
Table 7-15: Change in horizontal and vertical deformations on the tunnels (NB MC)*	53
Table 7-16: Change in horizontal and vertical deformations on the tunnels (NB HSS)*	53
Table 7-17: Change in horizontal and vertical deformations on the tunnels (SB MC)*	53
Table 7-18: Change in horizontal and vertical deformations on the tunnels (SB HSS)*	54
Table 10-1: Construction Sequences analysed (see notes 1 & 2)	72



EXECUTIVE SUMMARY

The 3D finite element program, PLAXIS, has been used to assess the impact on the Dublin Port Tunnels due to the excavation and building loads for the Hartfield Place Development.

The Plaxis 3D program enables structural elements as well as soils to be modelled to develop sophisticated soil/structure interaction analyses and the 3D modelling allows for the combined effect of the development on the Dublin Port Tunnels (DPTs) to be analysed. The assessment takes into account all aspects of the development including the excavation for the basement carpark under Blocks A to E, the loads for the buildings Blocks A to G and the unloading due to construction of the attenuation tanks.

The Hardening Soil model with small-strain stiffness (HSS) and the Mohr Coulomb (MC) material models have been used to model the behaviour of the Boulder Clays. The latter model (MC) provides a more conservative estimate of the impact of the development on the tunnel, however, the HSS model has been shown to closely model the behaviour of the very stiff Dublin Boulder Clays (Lawlor et. al, 2011).

The NRA (now TII) has set out criteria to be met for any development proposed to be constructed in the vicinity of the Dublin Port Tunnels in the document titled *Guidance Notes for Developers, The assessment of surface and sub-surface developments in the vicinity of the Dublin Port Tunnel*.

The analysis carried out in this report assesses the results with respect to the criteria set out in the TII document for surcharge loading of the tunnels. In addition, checks of the tunnel lining for Ultimate Limit and Serviceability Limit State have been made in respect to tunnel distortion such as ovalisation/squatting and longitudinal tunnel deformations, as well as shear force, axial force and bending moment in the tunnel lining (both in the longitudinal and transverse directions) and the tunnel lining bolt connections.

The analysis has been carried out for various design situations (DS-1 to DS-5) to account for the different excavation depths and loading combinations for the development that would have an impact on the Dublin Port Tunnels. The following is a summary of the results of the assessment of the proposed development on the tunnels from the numerical analysis presented herein:

1. The analyses showed that the increase in vertical total stress on the tunnel lining does not exceed the TII limit of 22.5 kN/m^2 at any point on the main tunnels or pedestrian cross passage. The maximum increase in stress on the tunnel lining is calculated to be 19.3 kN/m^2 for Design Situation DS-2 for the Mohr Coulomb material model. We note that TII does not require any further assessment of the tunnel lining and its components (i.e., in respect to the *Ultimate Limit and Serviceability Limit States*) where the surcharge loading on the tunnel does not exceed 22.5 kN/m^2 .
2. The design bending moments and axial forces derived from the Plaxis 3D model indicate that the combined design axial forces and bending moments plot within the design envelope for the tunnel lining both in the transverse and longitudinal directions and are therefore acceptable.
3. The design shear forces exerted on the tunnel lining in the transverse and longitudinal directions are less than the design shear resistance of the tunnel lining and are therefore acceptable.
4. The change in ovalisation, joint rotation, radial joint eccentricity and longitudinal curving of the tunnel due to the proposed development are considered to have negligible effect on the integrity of the Dublin Tunnels.
5. Consideration has been given to the impact on the tunnel of the different construction sequences that could be adopted during construction. The construction sequences analysed as part of this report must be adopted by the Contractor during the works. No other construction sequences shall be permitted.

In conclusion, it is found that the construction of the proposed residential development at Hartfield Place does not exceed the TII surcharge limit on the tunnels and is also found to have no detrimental effect on tunnel lining.



1 INTRODUCTION

A residential development is proposed to be constructed at Swords Road, Whitehall, Co. Dublin. The proposed development consists of 7 no. blocks in heights up to 8 storeys (over single level basement) comprising 472 no. apartment units, a creche, café unit, and internal residential amenity space and is referred to as Scheme No. 472. The location and layout of the development is shown on Figure 1-1 and Figure 1-2. An underground carpark is proposed to be constructed below Blocks A to E. The Dublin Port Tunnels cross the eastern part of the site in a roughly north-northwesterly direction. Block F and G are located partially above or directly above the DPTs, as shown on Figure 1-2.

Planning permission for the entire development was granted by Dublin City Council in 2010. However, some changes have been made since that submission. A revised planning application was issued for Block F in August 2019 and has been approved by Dublin City Council. The principal changes to Block F from the previous design comprised a change in the layout of the apartments and changes of the building foundations from strip foundations to a raft foundation.

Changes have also been made to the design for Block G, which are addressed in this report. The principal changes to Block G includes a change in the layout of the apartments and the removal of the underground carpark from below the proposed building. Further changes were also made to the layout of the development based on comments received during the SHD application process.

AGL Consulting was requested by Eastwise Construction Swords Ltd. (Eastwise) to carry out an assessment of the impact of construction of the proposed development on the Dublin Port Tunnels.

This report is an assessment of the impact that the construction of the development will have on the Dublin Port Tunnels. The entire development has been modelled using the 3D finite element model, Plaxis, to ensure that the combined impact of the overall development on the Dublin Port Tunnels has been assessed. This report shall form part of the planning application.

The NRA (now TII) has set out criteria to be met for any development proposed to be constructed in the vicinity of the Dublin Port Tunnels in the document titled *Guidance Notes for Developers, The assessment of surface and sub-surface developments in the vicinity of the Dublin Port Tunnel*. This document recommends that a development does not incur a surcharge loading on the tunnel in excess of 22.5kPa and that the method and sequencing of construction of the development minimises or eliminates the potential for tunnel deformation.

A 3D finite element analysis of the development has been carried out in this report and models various construction stages. The analysis indicates that the increase in vertical total stress on the tunnel lining does not exceed the TII recommended limit of 22.5kPa. The assessment also indicates that the impact on the tunnel deformations, bending moments and axial and shear forces are negligible. Therefore, it is considered that the construction of the Hartfield Place Development will have negligible effect on the Dublin Port Tunnels.



Figure 1-1: Location of Proposed Residential Development

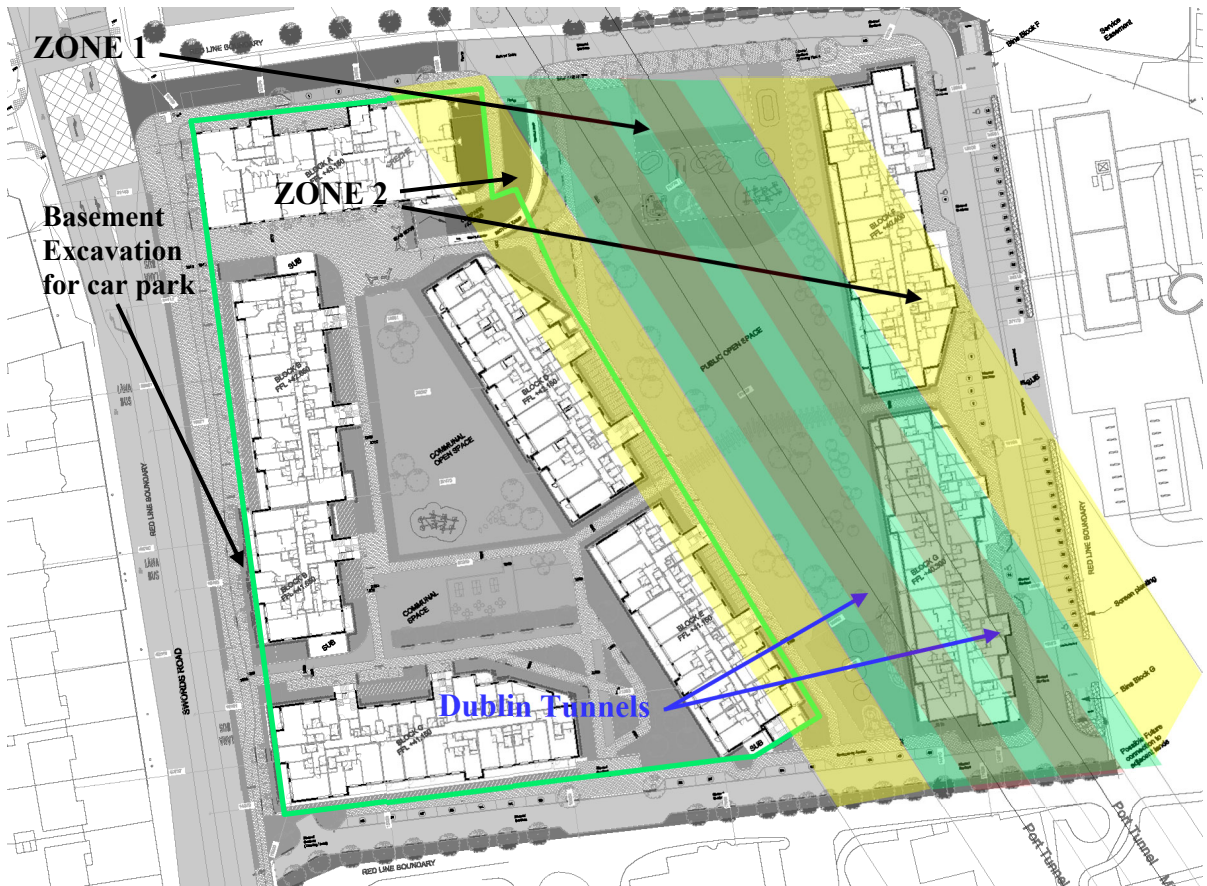


Figure 1-2: Location of development and Dublin Port Tunnels

2 THE DEVELOPMENT

2.1 Introduction

The development involves the construction of 7 No. apartment blocks, namely Blocks A to G, on a greenfield site located off the Swords road in north county Dublin. The details of the development are outlined in this section.

2.2 Details of Development

The proposed development will consist of the construction of 7 no. blocks in heights up to 8 storeys (over single level basement) comprising 472 no. apartment units, a creche, café unit, and internal residential amenity space. The proposal also includes car, cycle, and motorcycle parking, public and communal open spaces, landscaping, bin stores, plant areas, substations, switch rooms, and all associated site development works and services provision. Access is provided from the development from Swords Road with associated upgrades to the existing public road and footpaths. A full description of the development is provided in the statutory notices and in Chapter 3 of the EIAR submitted with the application.

2.3 Position of Development Relative to Dublin Port Tunnels

The Dublin Port Tunnels cross the central-eastern part of the site in a roughly northerly direction.

TII has produced the *Guidance Notes for Developers, The assessment of surface and sub-surface developments in the vicinity of the Dublin Port Tunnel* which defines zones of potential impact of development in relation to the Dublin Port Tunnels, i.e. Zone 1 and Zone 2 – see Figure 4-7. These guidance notes are discussed in detail in Section 4.6 of this report.

Apartment blocks B and C are located beyond Zone 2, Blocks A, D and E are partially within Zone 2, Block G is directly above the north and southbound tunnels and Block F partially overlies the southbound tunnel. Both Block F and G are within Zone 1. The position of the development in relation to the Dublin Port Tunnels (and Zone 1 and Zone 2) is shown on Figure 2-1.

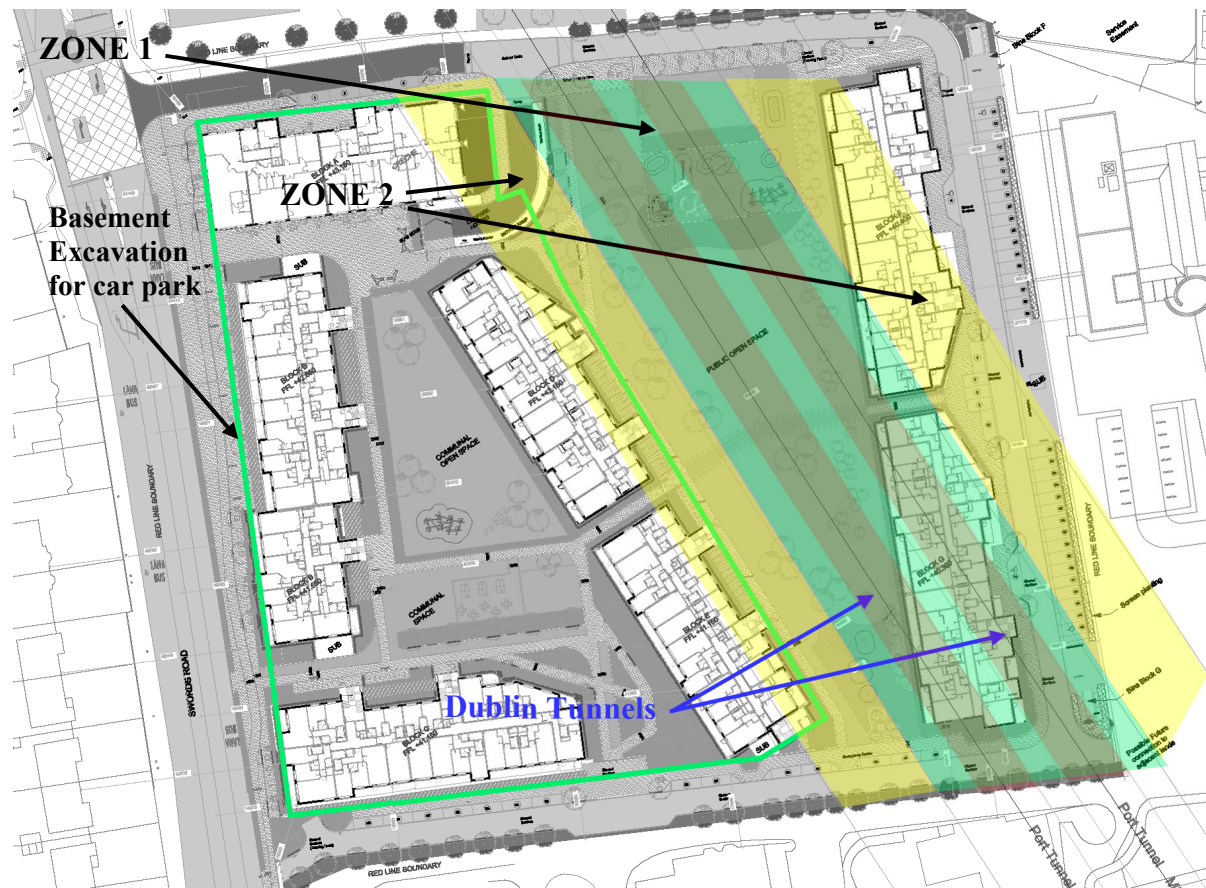


Figure 2-1: Location of Buildings and Basement Relative to Dublin Tunnels

2.4 Building Finished Floor Levels & Bearing Pressures

The finished floor levels for Blocks A to G are shown on Figure 2-2 and the finished floor levels for the basement proposed under Blocks A to E are shown on Figure 2-3. A topographical survey of the site carried out in February 2020, is shown on Figure 2-4.

The foundation formation levels and bearing pressures below the buildings and within the carpark area are outlined in this section.

Derivation of Characteristic Bearing Pressures for Blocks A to G and the Basement

The characteristic bearing pressures below Blocks A to G and the Basement were determined by Punch Consulting. The pressures assigned to each area is shown on Figure 2-6 and the drawing is included in Appendix E. This section provides information on how the bearing pressures were calculated which are as follows:

- The foundations of the individual units are designed to distribute the loadings at the respective formation levels onto the boulder clay.
- The foundation pressure magnitudes are an accumulation of the following loadings:
 - Lift weight roof structure
 - Suspended floor levels of the superstructure are 75mm structural screed with 200mm precast concrete hollow core slab
 - Loadbearing walls which are typically 200mm solid concrete walls
 - The outer leaf façade which are a combination of brick, block and lightweight cladding

- Imposed loadings are in accordance with IS EN 1991, with permitted imposed load reduction for multistorey buildings
- External ground floor areas above the basement are designed for the landscape and vehicular loading

Block A to G Design Details

Block A to Block G are to be supported on raft foundations. The characteristic bearing pressures below Blocks A to Block G were determined by Punch consulting and the pressures assigned to each area is shown on Figure 2-6. The bearing pressures include the weight of the foundations. The characteristic bearing pressures on the blocks vary due to the different storey heights over the footprint of the building.

For Clarification: To limit the surcharge increase on the tunnel crown to 22.5kPa, a void is included below the ground floor slab for Block G. Thus, the foundation formation for Block G is taken as 37.85mOD which is between 1.6m and 2.8mbgl. The design of the foundation for Block G was carried out by Punch Consulting. This is not a design change from previous versions of the Tunnel Impact Assessment.

The finished floor levels for Blocks A to E are shown on Figure 2-2, however, these buildings are located above the basement, therefore, these levels do not relate to the levels at which the bearing pressures apply. The finished floor level and foundation formation levels for the foundations are shown on Table 2-1 for Block F and Block G.

Table 2-1: Finished floor level and Excavation levels for Blocks F & G

Block ID	Finished Floor level (mOD)	Slab Thickness *(m)	Insulation (m)	Foundation Formation Level (mOD)	Existing Ground Level (mOD)	Excavation Depth (m)
Block F	40.4	0.7	0.25	39.45	40.3-40.6	0.9-1.2
Block G	40.3	0.7	0.25	37.85 Note 1	39.4-40.6	1.6-2.8

Note 1: Assumes formation for Block G is at 37.85mOD with a void below the ground floor incorporated into the design.

Basement Design Details

The proposed basement lies below Blocks A to E to the west of the Dublin Tunnels, generally at a distance of approx. 17m from the outermost edge of the northbound tunnel but locally approx. 11.5m at the most northern part of the site, adjacent to Block A. The basement is to be used as an underground carpark. The location of the basement with respect to the Dublin Tunnels is shown on Figure 2-1.

The characteristic bearing pressures below Blocks A to Block G and within the carpark were determined by Punch consulting and the pressures assigned to each area is shown on Figure 2-6. The bearing pressure applied to the basement carpark outside the Blocks A to E is 50kPa and is applied at the underside of the raft foundation.

The finished floor levels and foundation formation levels for the basement carpark is summarised on Table 2-2. The finished floor levels for the basement ranges from 39.0mOD in Block A at the north of the site to 36.95mOD to the west of Block E at the south – see Figure 2-3. The ground levels within the footprint of the basement range from approx. 43.0m to 41.7mOD along the northern site boundary dropping to 41.5m to 40.2mOD at the southern site

boundary – see Figure 2-4. The ground levels along the eastern side of the basement range from approx. 41.9mOD at the north to 40.2mOD at the south, giving depths to finished floor level ranging from 3.5m to 4.4mmbgl, and is typically deepest (4.2m to 4.4m) below Blocks D and E. The depth to finished floor level increases to a max. of 5.25m below Block B at the west of the site.

Table 2-2: Finished Floor Levels & Excavation levels for the basement

Location of Basement Perimeter Wall	Finished Floor level (mOD)	Slab Thickness (m)	Insulation (m)	Foundation Formation Level (mOD) ^{Note 1}	Existing Ground Level (mOD)	Excavation Depth (m)
Northern Boundary	39	0.7	0.25	38.05	41.8-43.0	3.8-5.0
Western boundary	37.05-39.0	0.7	0.25	36.1-38.05	43.0-41.4	5.0-5.3
Southern boundary	37.05-37.1	0.7	0.25	36.1-36.15	40.3-41.4	4.2-5.3
Eastern boundary	37.1-39.0	0.7	0.25	36.15-38.05	40.3-41.9	3.9-4.2

Basement Access Ramp

There is an access ramp to the basement car park located to the east of Block A as shown on Figure 2-8. The access ramp runs along the eastern end of Block A in a southwestern direction and it enters the basement south of Block A. The finished road level of the ramp ranges from 41.711mOD at the northeastern end of the basement reducing gradually to 38.245mOD at the basement entrance at Block A. Assuming a road pavement and pavement foundation thickness of 0.75m gives a corresponding excavation level of 41.0mOD and 37.5mOD, respectively. The ground level in the area of the ramp is approx. 41.7mOD, therefore, the excavation is between 0.7m and 3.5m below ground level.

Attenuation Tank Design Details

It is proposed to construct 3 No. attenuation tanks, Tanks 1 to 3, at the locations along the perimeter of the site as shown on Figure 2-5. The design comprises an underground reinforced concrete tank with inner void of approx 1.5m height and upper and lower slab thicknesses of approx. 250mm. The design details for the tanks are given on Table 2-3 and the proposed design for Tank 3 is shown on Figure 2-7. The tanks are to be embedded approx. 350mm below the ground and includes a void of 1.5m height for Tanks 2 & 3 and 1.45m void height for Tank 1.

In the case of Tank 3, the total load of soil above formation which is to be excavated for the construction of the tanks is approx. 68 kPa (i.e.3.4*20). The total load of the attenuation tanks above formation in the permanent condition is 54.2kPa, this includes the 1.5m high void full with water. Therefore, there is a net unloading effect of approx. 13.8kPa in the permanent condition. This unloading effect is the same in magnitude for the remaining Tanks 2 and 3.

Table 2-3: Attenuation Tank Design Details

Tank ID	Existing Ground level (mOD)	Length (m)	Width (m)	Min Formation Level (mOD)	Excavation Level (mOD)	Excavation depth (m)
Tank 1	40.3	102.0	3.4	37.160	36.94	3.4
Tank 2	40.0	68.8	6.3	37.622	37.40	2.6
Tank 3	40.1	54.0	6.3	37.610	37.39	2.7



Figure 2-2: Finished Floor levels for Blocks A-G of proposed development

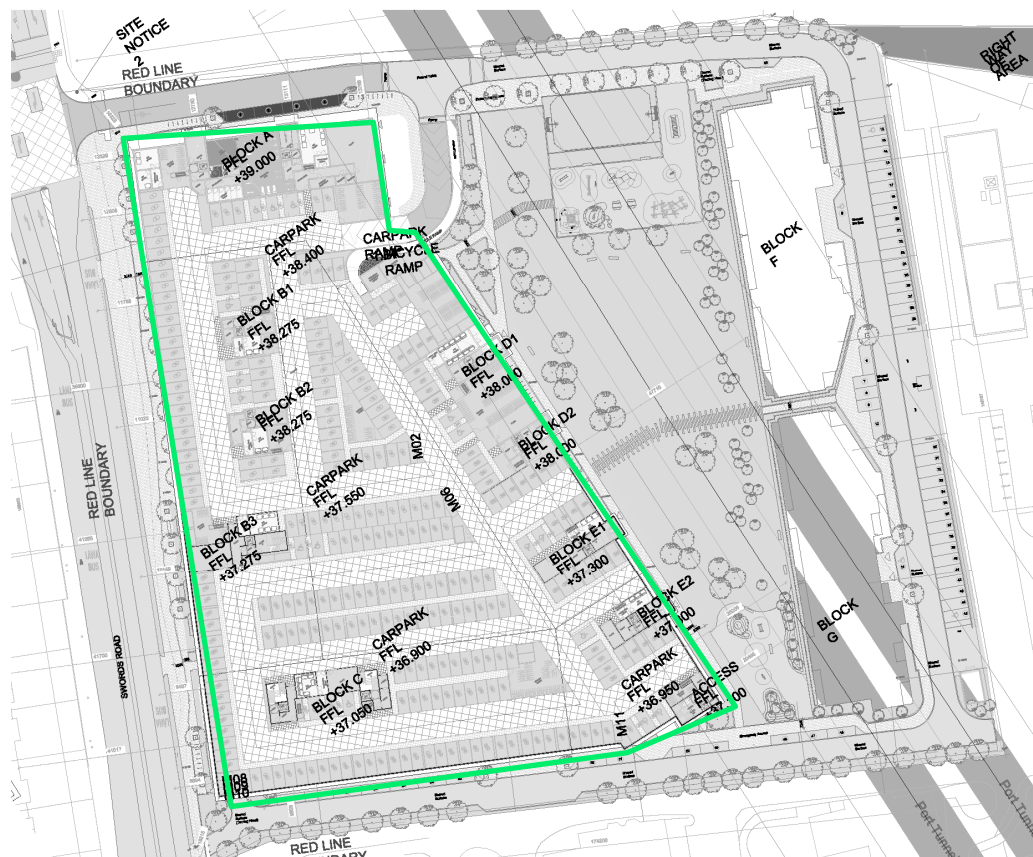


Figure 2-3: Finished Floor levels for basement proposed below Blocks A to E

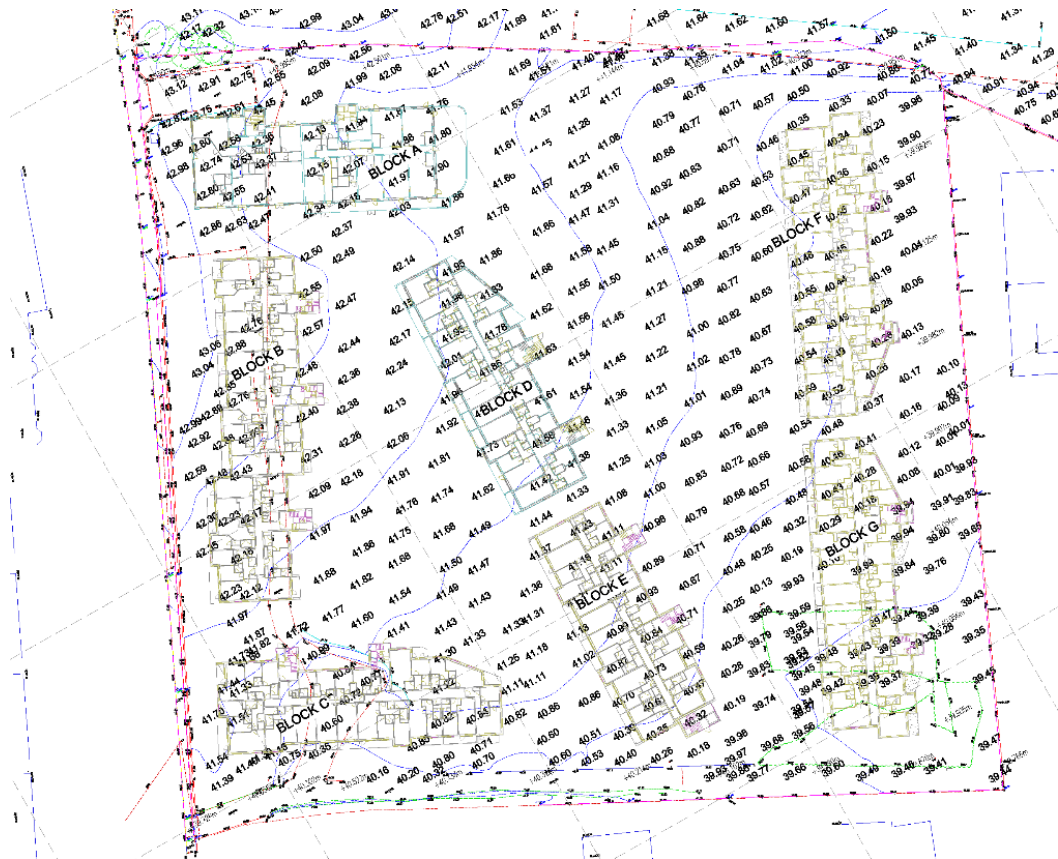


Figure 2-4: Topographical Survey, carried out in February, 2020 (DOB Surveys Ltd)

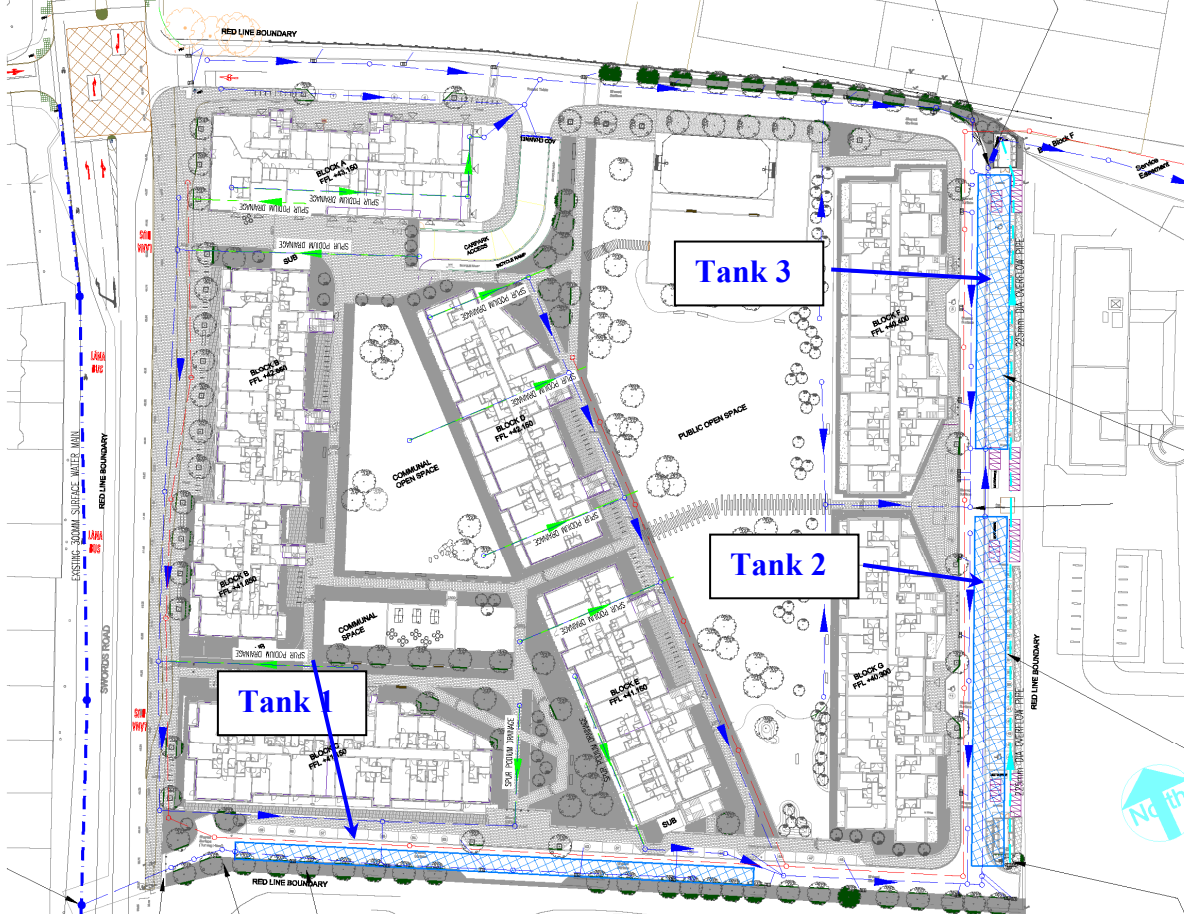


Figure 2-5: Plan Layout of Attenuation Tanks on the site (shown as blue hatched areas)

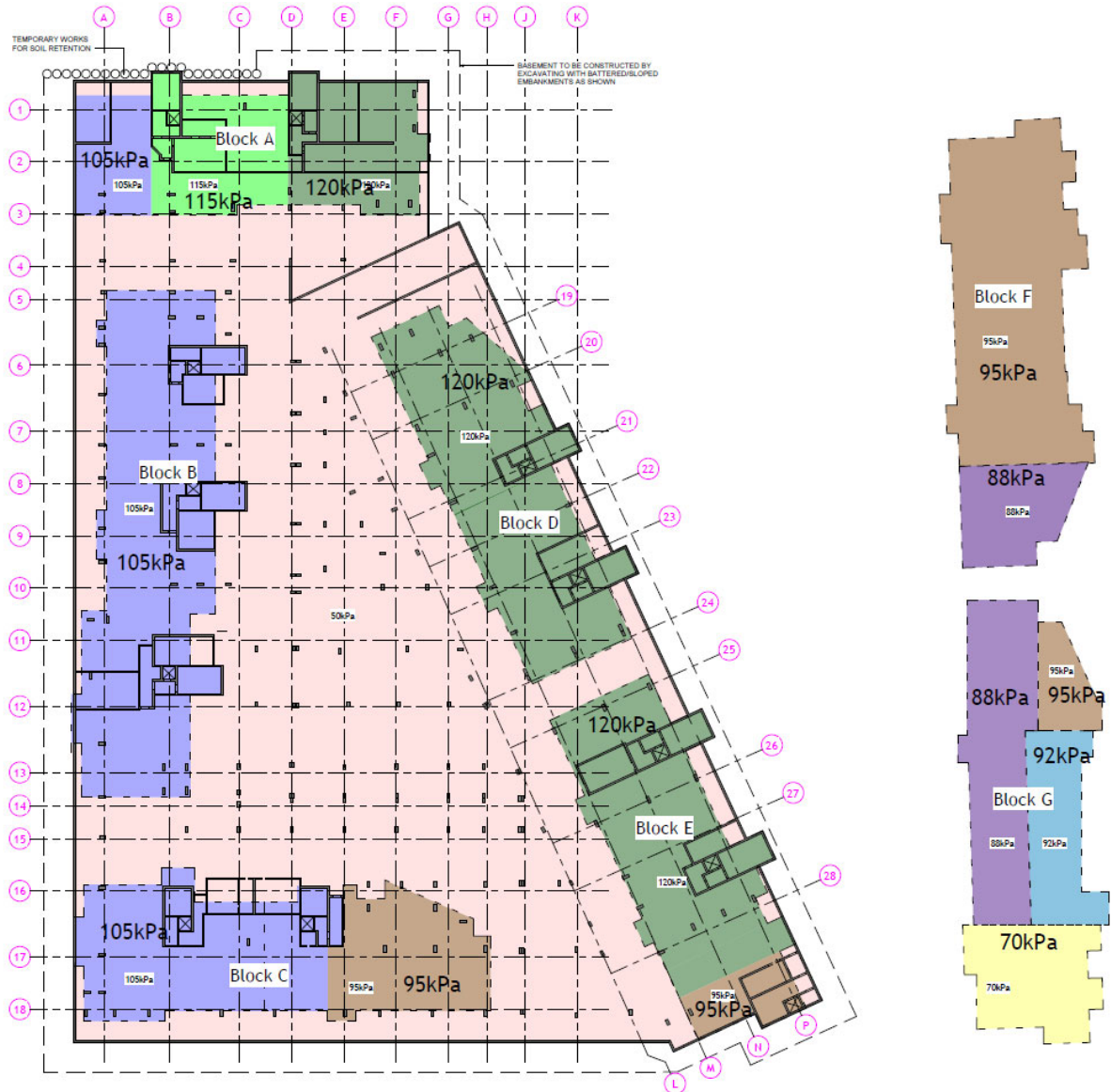


Figure 2-6: Characteristic Bearing Pressures for development (Provided by Punch Consulting) – included in Appendix E

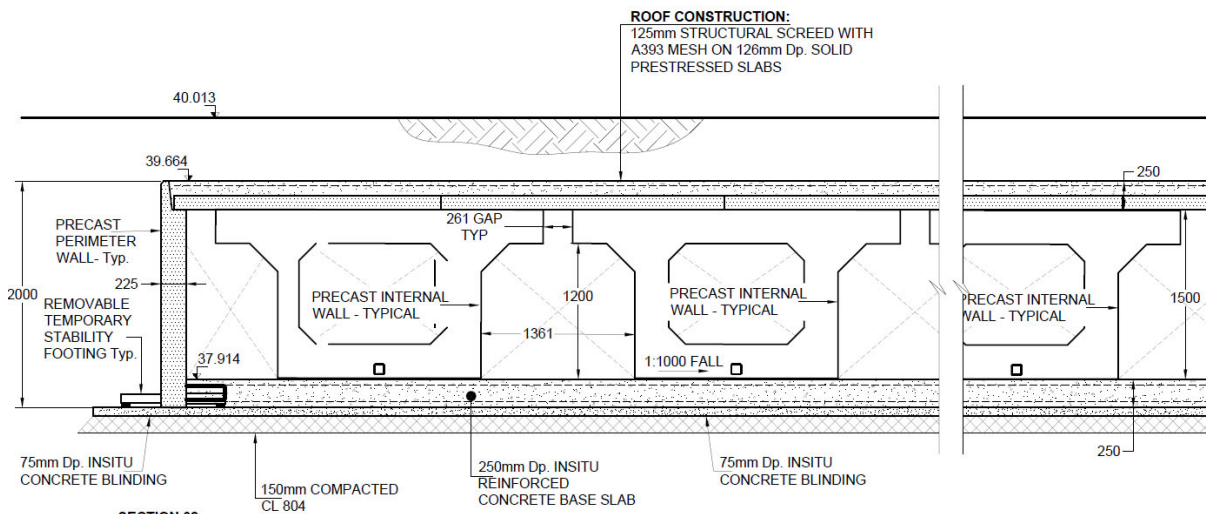


Figure 2-7: Proposed attenuation tank design

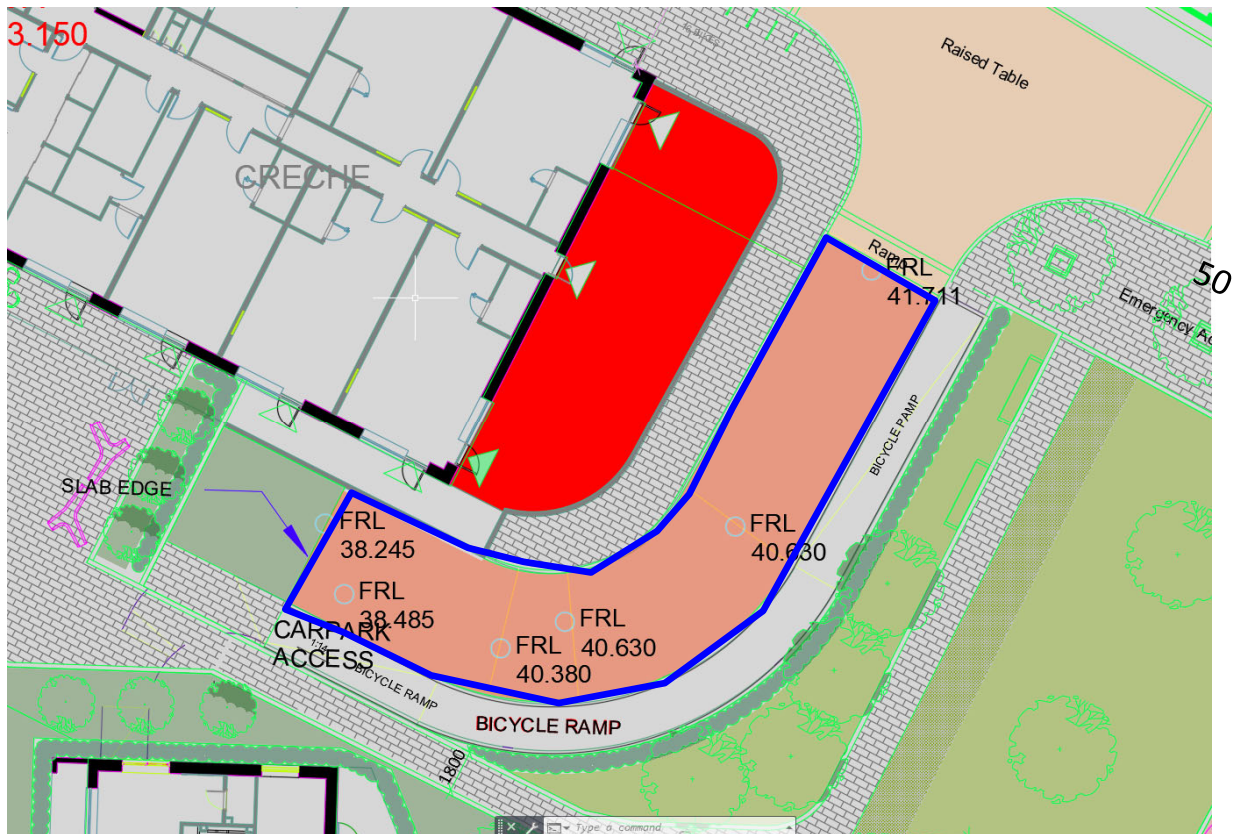


Figure 2-8 Plan View of location of proposed basement access ramp (outlined in blue)

3 PLANNING APPLICATION HISTORY

Planning permission was granted in 2010 by Dublin City Council for seven multi-storey apartment blocks (Blocks A to G), an underground carpark and a creche (DCC reference no. 3269/10 and An Bord Pleanála Reference Number: PL 29N.238685). The layout of the development is shown on Figure 3-1. As can be seen from Figure 2-1, the Dublin Port Tunnels pass through the eastern part of the site, with Block G of the development directly above the Dublin Port Tunnels and Block F partially above the tunnels.

As part of the planning application process in 2010, an assessment of the impact of the development on the Dublin Port Tunnels was carried out by DBFL/Mott MacDonald. The findings of this indicated that the proposed development would not have a detrimental impact on the lining of the Dublin Port Tunnels. This report was reviewed by Jacobs, acting on behalf of the NRA (now called TII), who concluded that the assessment methodology undertaken by Mott MacDonald was both appropriate and in compliance with NRA guidelines.

On 16th August, 2019, a revised planning application was submitted to Dublin City Council (DCC) for Block F of the development (DCC reference no. 3405/19). The principal changes to Block F from the previous design comprised a change in the layout of the apartments and changes of the building foundations from strip foundations to a raft foundation. A Request for Further Information issued by Dublin City Council on 30th August, 2019, indicated that an impact assessment on the Dublin Port Tunnels (DPTs) was required to be carried out for the proposed construction of Block F to ensure the revised design did not adversely impact the integrity of the DPTs.

An impact assessment was carried out by AECOM in February, 2020, which concluded that the impact of the proposed redesign for Block F did not adversely affect the tunnels. This was reviewed by Mott MacDonald who were acting on behalf of Transport Infrastructure Ireland (TII). The planning permission was granted for the amendment to Block F in June 2020 provided conditions 3 and 7 of the grant of permissions are complied with. These conditions relate to compliance with the terms and conditions for the original development and to the submission of a Construction management plan prior to construction, respectively.

This report forms part of the pre-planning application to An Bord Pleanála for the proposed development. The principal changes to the previously accepted planning application for the development in 2010 comprises a change in the layout of the apartments for Block G and the removal of the underground carpark from below the proposed building.

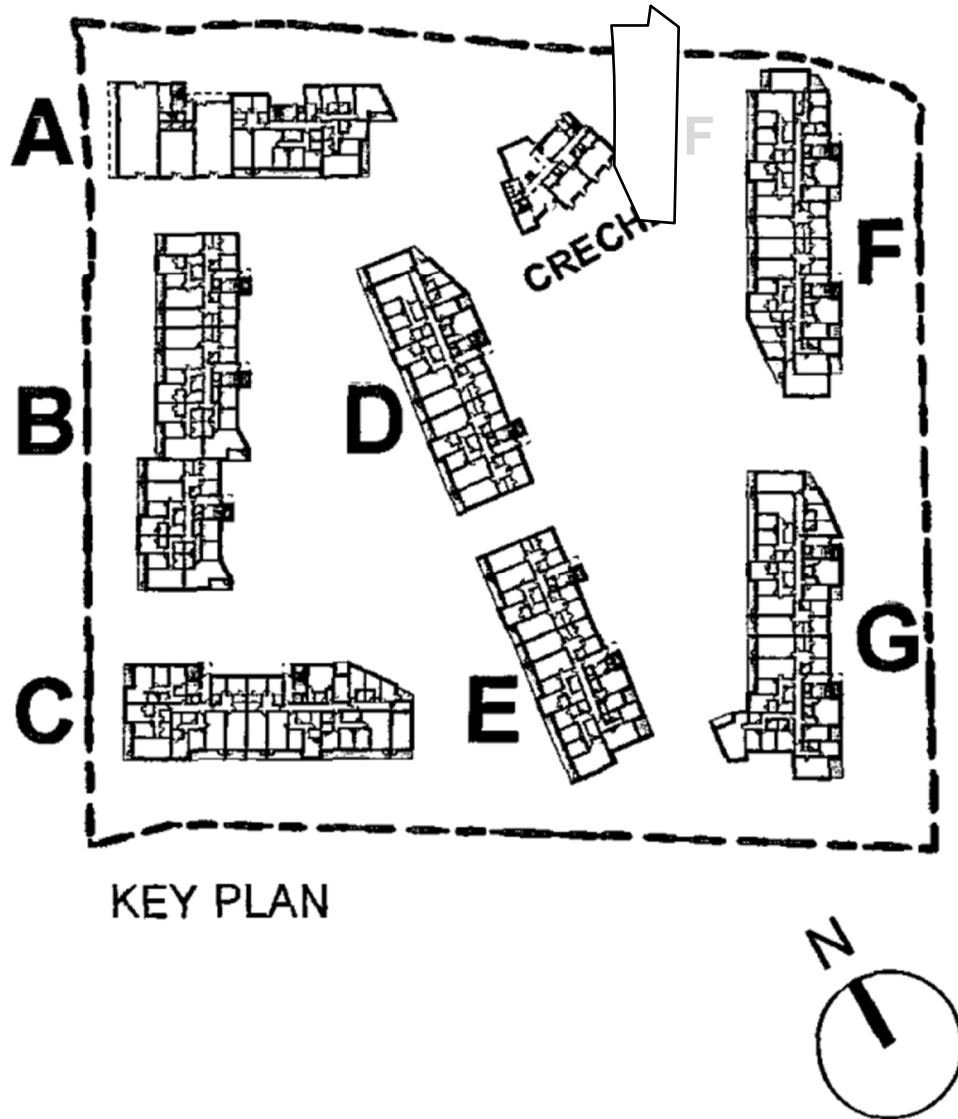


Figure 3-1: Development granted planning permission by Dublin City Council in 2010 (DCC Reg. Ref. 3269/10 / ABP Ref. PL29N.238685)

4 TUNNEL DETAILS

4.1 Tunnel Type and Chainages

The Dublin Port Tunnels (DPTs) comprises 5.6km of motorway linking the Irish motorway network around Dublin to the northern part of Dublin Port. The DPTs comprise 1.1km of surface motorway and 4.7 km of twin tunnels, of which 2.8km are bored and 1.9km are cut and cover. The chainages of the cut and cover and bored sections of the tunnels are as follows:

- Ch. 0+600 to 1+900: Cut and cover
- Ch. 1+900 to 4+537: Twin Bored tunnels
- Ch. 4+537 to 5+112: Cut and cover

From Ch. 1+900 to Ch. 4+537 at Fairview Park, the tunnel was constructed as twin bored tunnels and is overlain by green-field sites and densely populated housing/retail development. These tunnels were driven by tunnel boring machines (TBMs) from a 56m diameter shaft, centred at Ch. 2+250 which was subsequently backfilled.

The section of tunnel within the site was formed by tunnel boring machines (TBMs). The tunnels cross the eastern part of the site between approx. Ch. 2+360 and Ch. 2+540, a total of 180m length. There are no Vehicular Cross Passages within the proposed site. There is a Pedestrian Cross Passage (No. 07/07A) connecting the northbound and south bound tunnels located at NB Ch. 2+517 and SB Ch. 2+515. The details of the cross passage are included on the as-built drawing No. DR/HA/BH/C11/41061/05/X included in Appendix B.

The chainage system used for the southbound and northbound DPTs by TII are shown on Figure 4-1. The as-built drawings for the centreline of the northbound and southbound carriageways along the tunnels were provided to AGL by TII and cross checked with those provided by Eastwise. A plan and profile view of the northbound tunnel within the region of the site is shown on Figure 4-1 and Figure 4-2, respectively.

A summary of the tunnel details within the site is given on Table 4-1.

Table 4-1: Summary of Tunnel Details within the site

Tunnel	Northbound	Southbound
Tunnel Chainage	2+360 to 2+540	2+360 to 2+540
Ground Level **(mOD)	41.7 to 39.5	41.4 to 39.5
Tunnel Crown **Level (mOD)	22.2 to 16.0	22.63 to 15.9
Internal Tunnel Diameter (m)	10.84	10.84
Primary Tunnel Lining Thickness (mm)	350	350
Thickness of Overburden above Tunnels (m)**	19.5 to 23.5	18.7 to 23.6

*Taken from as-built drawings provided by TII (drawing no. DR/CB/PRO/C1/70033/12/X & DR-CB-PRO-C1-70041-11-X

**From north to south of tunnel alignment



Figure 4-1: Plan View of DPT in the vicinity of the site showing tunnel chainages (site shown in red)

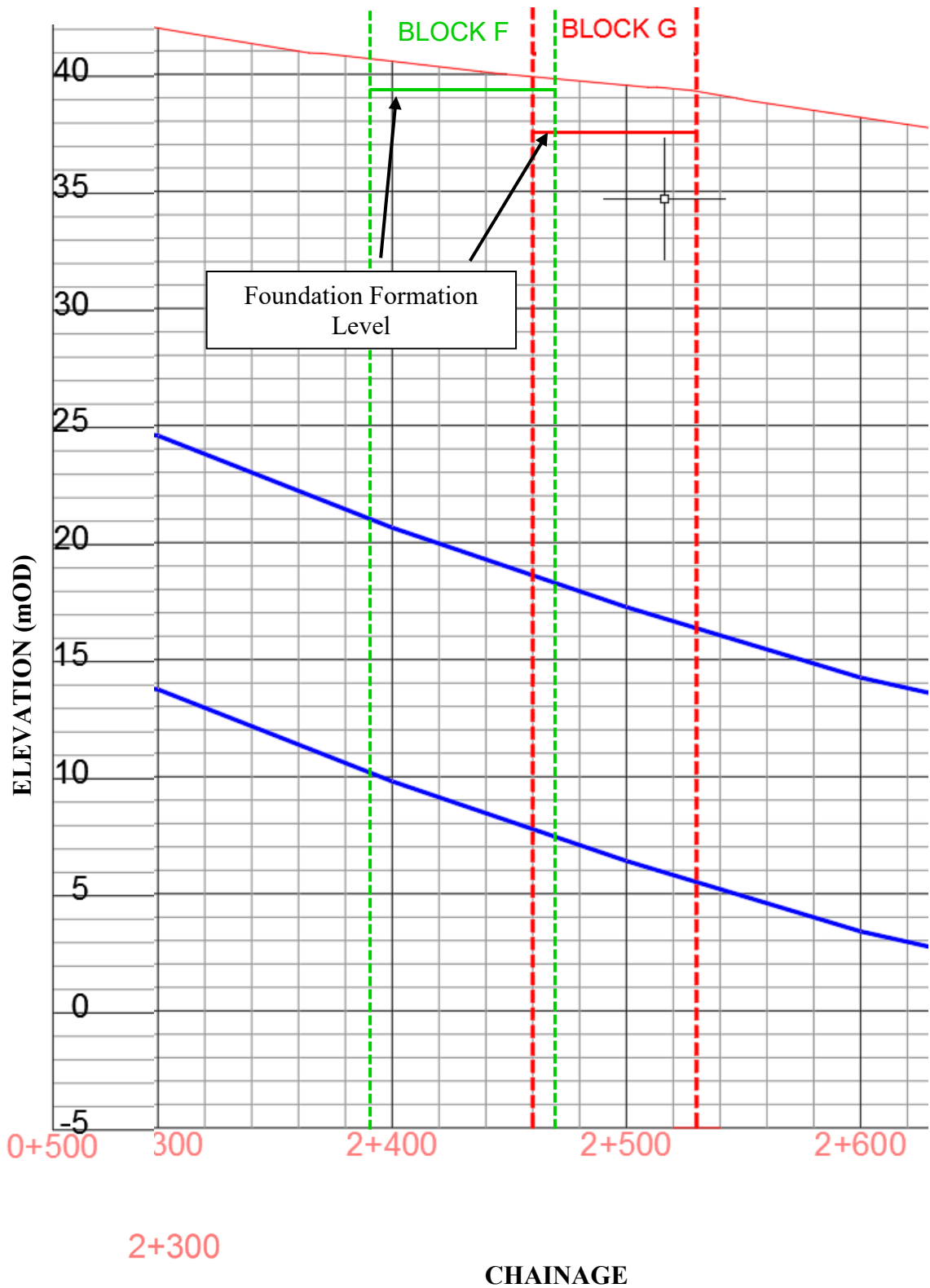


Figure 4-2: Profile View of View of DPT in the vicinity of the site showing tunnel chainages (Northbound tunnel)

4.2 The Tunnel Boring Machine (TMB)

The TMB had a full-face shield that was designed to excavate both glacial till and bedrock. The TBM was capable of conducting unidirectional boring in a clockwise direction up to a maximum speed of 4 rev/min. The shield diameter was 11.74m and had an overall length of 8.79 m and weighed 1100 t. (Gillarduzzi, 2013).

4.3 Tunnel Lining Details (Gillarduzzi, 2013)

The lining of the tunnel includes a primary and an inner secondary lining separated by a waterproof membrane. The details of these aspects of the tunnel lining have been sourced from Gillarduzzi, 2013 and are discussed below. The as-built drawing (No. DR/HA/BT/C11/41018/07/X) showing the tunnel lining details is shown on Figure 4-3.

Note the text in *italics* is directly extracted from Gillarduzzi, 2013. The text not in italics was added to provide clarity.

Primary Lining

The primary circular lining performs a structural function and constitutes the main waterproofing of the tunnel. This comprises bolted pre-cast concrete segments 1.7m wide, 350 mm thick and 9.6t each (made of C60 concrete with approximately 90 kg/m³ conventional reinforcement bars), with six principal segments and a key in each ring (Marshall and Goritshning, 2003).

A single hydrophilic (22 mm wide, 5 mm thick strip) gasket was fitted on each segment. The hydrophilic material expands when it comes in contact with water, acting as a barrier to water flow.

The primary lining reduces the inner diameter of the tunnel from approximately 11.54m to 10.84m. Immediately, as the ring emerged from the TBM tail skin, the annulus between the excavation profile (i.e. approx. 11.74m (shield diameter)) and the extrados of the tunnel lining (ideally 130mm thick) (i.e. 11.54m (primary lining diameter)) was filled in two stages, with cement-based grout. The grout was injected at a pressure between 2 and 3 bars, through an aperture located in the middle of each segment; the injection pressure was regulated taking into account the dimensions, the voids and the degree of fracturing of the bedrock.

Waterproof Membrane

A second waterproofing layer was then installed to eliminate any possibility of water entering above the tunnel carriageway and walkways level. This included a 2.1 m wide, 2 mm thick, polyvinyl chloride (PVC) membrane strips (with joints double term-welded and tested after installation at a pressure of 2 bars). The membrane was applied to the inside face of the primary lining by hot air welding onto PVC discs that were held in place by mechanical fasteners.

Secondary Lining

The secondary lining was installed above the carriageway and walkways level. This was designed to carry its own weight and that of the tunnel fixtures. This lining was cast against the waterproofing membrane from nibs realised in the primary lining. The lining included a nominal 275 mm thick layer of unreinforced, cast in situ, C40 concrete, with 1 kg of 18 mm monofilament polypropylene fibres per cubic metre of concrete. The minimum structural thickness, after the specified tolerance, was 200 mm. The secondary lining was installed to

achieve a smooth finishing surface (to improve air flow, painting and cleaning), to protect the primary lining from tunnel fires and damage (due to impacts), and as a further waterproofing barrier to prevent water infiltrating above the carriageway. The finished internal tunnel diameter, including the secondary lining, was 10.29 m.

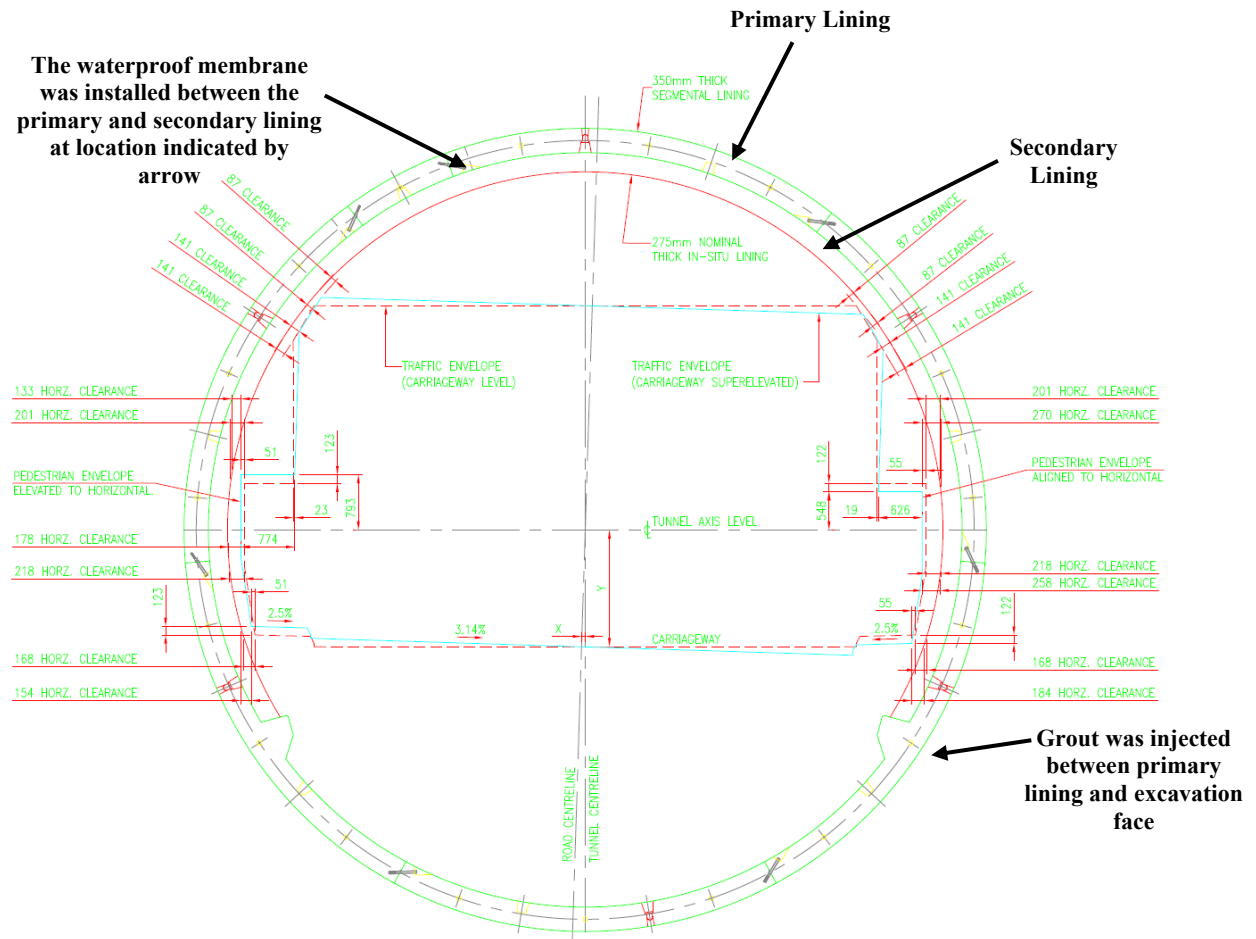


Figure 4-3: Tunnel Lining Details (extract from Dwg No. DR/HA/BT/C11/41018/07/X)

4.4 Tunnel Design Limits

Table 4-2 gives a summary of the information provided to AGL by TII relating to the design of the lining for the Dublin Port Tunnels. This information was obtained from the TII document CA/HA/BT/C11/54026/02/O titled *Bored Tunnel Lining Definitive Design Calculations*.

Table 4-2: Summary of information relating to the design of the lining for the Dublin Tunnels

Design Calculation	Design Values/Limits
Design Bending moment & Axial Forces – ref 1 page 4/11	see N-M Plot shown on Figure 4-4
Max. Construction Tolerance as per BTS Tunnel Specification (1987) – ref 1 page 4/3	50mm Using this maximum tolerance, the following has been calculated: <ul style="list-style-type: none"> Joint Rotation between two segments (ref 1 page 4/3) = 0.581 degrees Radial Joint Eccentricity (ref page 4/8A) = 41mm

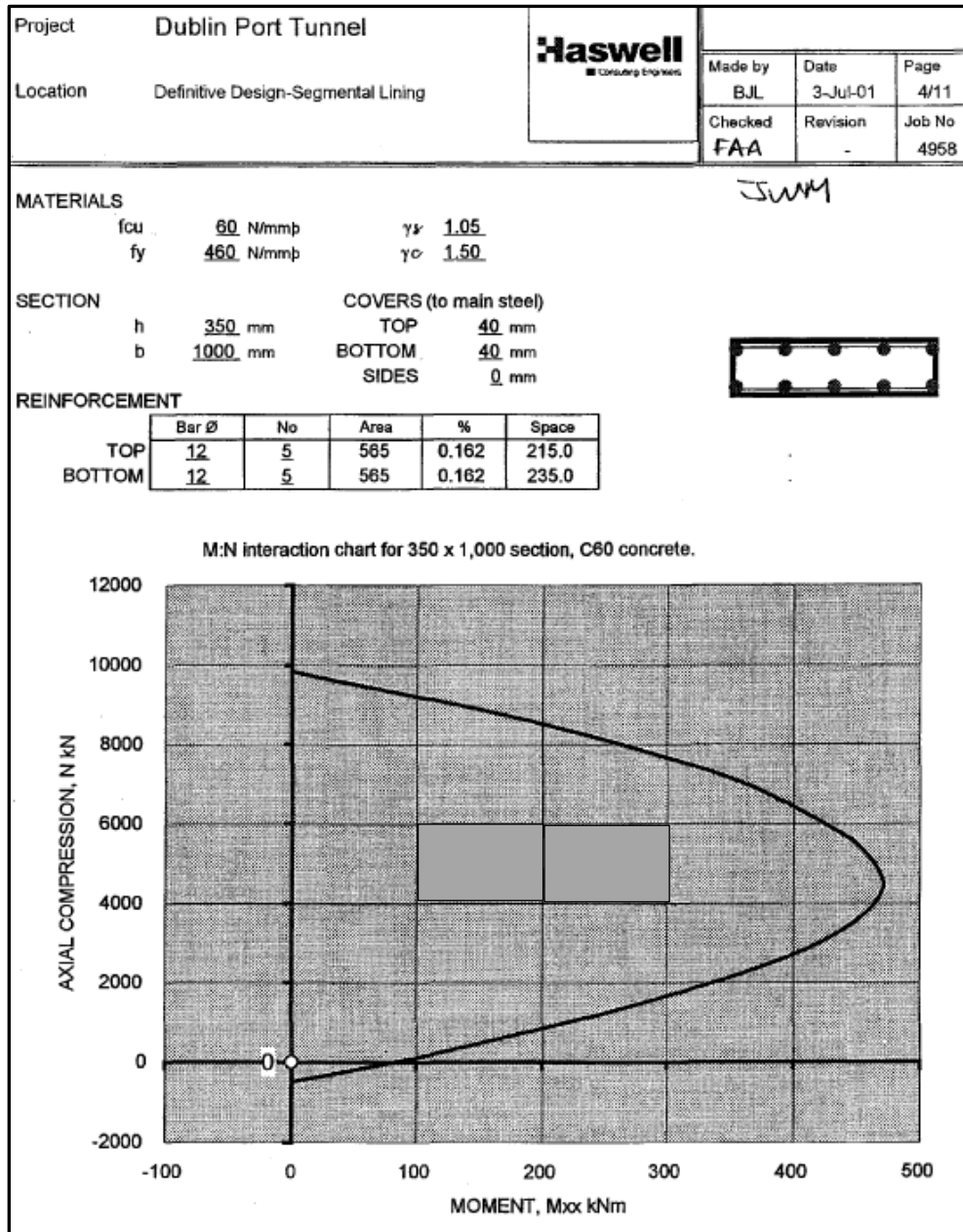


Figure 4-4: Design N-M Interaction Chart of the lining of the Dublin Tunnels

4.5 Pedestrian Cross Passage

The Pedestrian Cross Passage (PCP) comprises a shotcrete primary lining, the details of which are not available, and a 350mm thick in-situ concrete secondary lining with a hydrolite sealing strip separating the two – see Figure 4-5. There is additional reinforcement, comprising a 356x406x634 UC steel I-beam Section, at the connection to the primary lining of the TBM tunnel sections, to take the locally higher shear forces and bending moments that would occur at these locations. Up to 550mm of concrete is placed at the base of the tunnel to form a level floor. The cross section profile of the PCP is a roughly oblong shape as shown in Figure 4-6.

The details of the cross passage are included on the as-built drawing No. DR/HA/BH/C11/41061/05/X included in Appendix B.

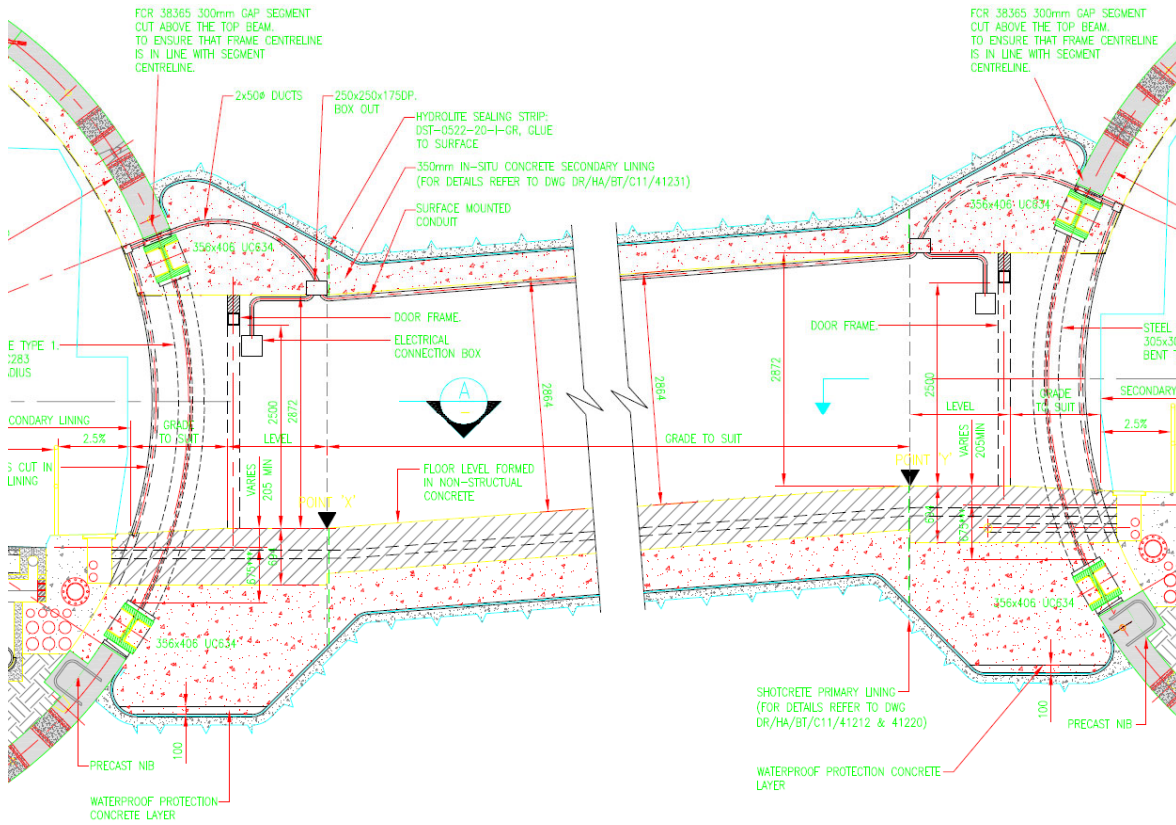


Figure 4-5: Cross Passage Design Details (as-built drawing No. DR/HA/BH/C11/41061/05/X)

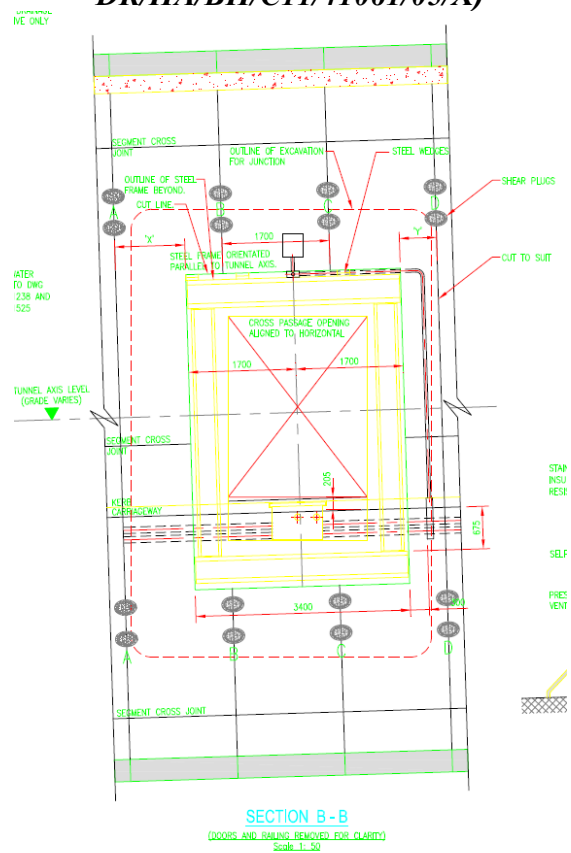


Figure 4-6: Cross section through Cross Passage Design Details (as-built drawing No. DR/HA/BH/C11/41061/05/X)

4.6 Guidance Notes for Developers (TII)

In accordance with the *Guidance Notes for Developers, The assessment of surface and sub-surface developments in the vicinity of the Dublin Port Tunnel (GND)*, an assessment of the impact of a development on the Dublin Port Tunnels is to be carried out where the development lies within Zone 1 or Zone 2 of the tunnels as shown on Figure 4-7. This document states the following with regards to surcharge loading and unloading of the DPTs :

- *“Surcharge Loading: The NRA requires the developer to demonstrate that a development does not incur a surcharge loading on the tunnel in excess of 22.5kNm-2 either during construction or at completion. Cognisance must be taken of any surcharge loading at depth due to anchors or piles.*
- *Unloading: The NRA requires the developer to demonstrate that the method and sequencing of construction of the development minimises or eliminates the potential for tunnel deformation”*

Section 2.5 of the GND also states the following:

- *The NRA will consider: A comprehensive submission from the developer which demonstrates that surcharge loads, during construction and on completion, exceeding 22.5kNm² are not detrimental to the lining and its components with respect to the Ultimate Limit and Serviceability Limit States*

As shown on Figure 2-1, Apartment blocks B and C are located outside Zone 2, Blocks A, D and E are partially within Zone 2, Block G is directly above the north and southbound tunnels and Block F partially overlies the southbound tunnel. Both Blocks F and G are within Zone 1.

The GND document splits the tunnel alignment into 3 No. Geographical Areas of potential future surface development, Areas A to C. The document indicates that the tunnels crosses Area B which extends from Ch. 2+210 to Ch. 4+537. This area is described as *“Green-field” land from Collins Avenue to Griffith Avenue and the housing/retail areas of Marino and Fairview.*

This area (Area B) is further subdivided based on the geological conditions and the structure of the tunnel lining. The areas of relevance to this development are as follows:

- Area B (i) Ch. 2+210 to Ch. 2+400 – Area above bored tunnel constructed within soils
- Area B (iii) Ch. 2+400 to Ch. 3+330 – Area above bored tunnel constructed within rock with low rock cover

This site addressed in this report lies between Ch. 2+370 and 2+540, therefore, it lies at the interface between the *tunnel constructed within soils* (Area B (i)) and *tunnel constructed within rock with low rock cover* sections (Area B (iii)).

It is also noted in section 2.5 that *The NRA will accept A simple load calculation to demonstrate compliance with the 22.5kNm² requirement in Area B(iii) but ONLY if the developer’s site investigation can demonstrate competent rock above the area.*

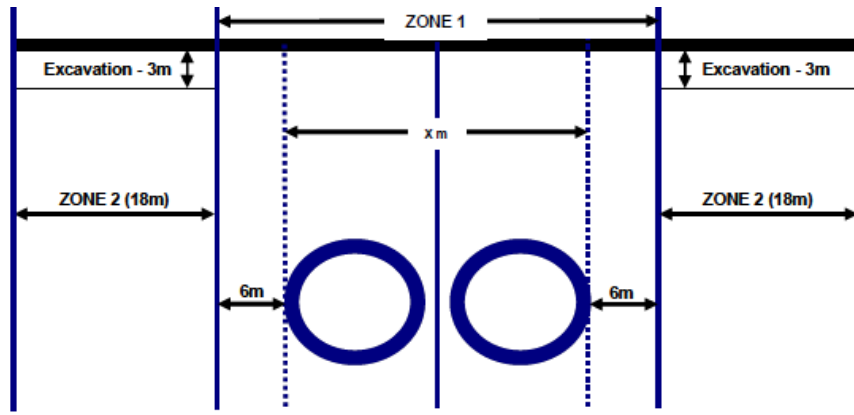


Figure 1: Bored Tunnel – Areas A&B¹

Not to scale – Depth of Tunnel varies

Figure 4-7: Dublin Port Tunnels - Zones 1 and 2

5 GROUND & GROUNDWATER CONDITIONS

5.1 Available Ground Investigation Information

The following site investigation information is available for this site:

- Dublin Port Tunnel Design and Construct Contract Site Investigation Data Reports, Volume 5 Part 1 Site Investigation Data Reports, October 2000. The relevant site investigation information includes the following:
 - 7 No. boreholes, 3 No. of which were extended using open hole drilling
 - 4 No rotary coreholes
 - 4 No. Standpipes installed in the boreholes/coreholes

The site investigation location plan is shown on Figure 5-1.

The 100 series site investigation points were carried by IGSL in 1995 and the 200 series site investigation points were carried by Geotech Specialists in 1996.

This ground investigation is referenced as *Detailed SI, 2000* in this report.

- Report on Site Investigation at Swords Road Whitehall Dublin 9, Ground Investigations Ireland, dated May 2010, Report No 2442-02-10. The relevant site investigation information includes the following:
 - 4 No. Rotary coreholes

The site investigation location plan is shown on Figure 5-2

This ground investigation is referenced as *GII, 2010* in this report. This report is included in Appendix G.

- Swords Road Ground Investigation, Ground Investigations Ireland. The relevant site investigation information includes the following:
 - 10 No. boreholes (BH01 to BH10)
 - 3 No. Geobore-S coreholes (BH04, BH05, BH09)
 - 10 No. Trial Pits (TP01 to TP10)
 - 3 No. Standpipes (BH01, BH06, BH10)

The site investigation location plan is shown on Figure 5-3.

This ground investigation is referenced as *GII, 2020* in this report. This report is included in Appendix H.

5.2 Ground Conditions

The ground conditions on the site are based on boreholes and coreholes relevant to this site, from the Detailed SI, 2000 (location plan shown on Figure 5-1), the GII 2010 site investigation (location plan shown on Figure 5-2) and the GII, 2020 site investigation (location plan shown on Figure 5-3).

A subsurface ground profile showing the ground conditions along the tunnel within the boundaries of the site is shown on Figure 5-4.

Based on the available information, the ground conditions comprise the following:

- Approx. 1m to 3m of Made Ground or a firm/firm to stiff (locally soft to firm) Sandy gravelly CLAY (Upper Brown Boulder Clay). SPT N-values recorded in exploratory holes on the site within these strata ranged from 7 to 54 within the 2m depth, increasing

to between 30 to 50 from 3-4m. This would indicate a soft to firm to a very stiff material to a depth of 2m, increasing to stiff to 3m depth using the correlation $c_u = 5 \times N_{SPT}$ (Stroud, 1989). The N_{SPT} plots are shown on Figure 5-5 and Figure 5-6 against depth and elevation respectively.

- A very stiff to hard Upper Black, Lower Black and Lower Brown Boulder Clay underlies these materials at a depth of between 0.3m and 3mbgl (39.1m and 37.0mOD). The stratum is between 17.7m and > 27.2m thick.
- The Upper Black, Lower Black and Lower Brown Boulder Clays are typically described as sandy gravelly CLAY. The SPT N-values within these strata typically range from 40 to 86 with several refusals noted. The stratum is typically described as a very stiff to hard sandy gravelly CLAY. This would indicate a very stiff to hard material with a c_u of 200kPa to 430kPa using the correlation $c_u = 5 \times N_{SPT}$ (Stroud, 1989)
- There are occasional lenses of Sands and Gravel within these strata with varying thicknesses ranging from 0.2 to 3m.
- A weathered rock zone sometimes lies below the Boulder Clay at a depth of between 18.6m and 25.5mbgl (14.6m and 20.8mOD). However, the stratum is not fully penetrated in RC2 (Ch. 2+485) which terminates at 31.0mbgl (8.5mOD). The weathered rock is described as weak to medium strong dark grey decomposed Limestone or a Fractured Limestone. The total core recovery (TCR) of the weathered rock ranges from 73% (RC2) to 95%, however, several non-intact zones were also noted. The rock quality designation (RQD) ranges from 16% (RC2) to 47%. The TCR and RQD were particularly low in RC2 where values of 15% and 8% respectively were recorded.
- The depth to top of rock within the site varies. There was no rock encountered within the site investigation points up to Ch. 2+370 where the max penetration depth of the rotary coreholes was 30mbgl (10.85m to 10.73mOD).
- Rock is encountered towards the southern part of the site from the site investigation points from Ch. 2+430 onwards. The rock is encountered at a depth of between 18m and 28.6mbgl (21.4m and 111.5mO). However, the top of rock is variable and appears to drop in RC2 at Ch. 2+485 where competent rock is not encountered to a depth of 31mbgl (8.5mOD).
- The rock is described as a strong to very strong fresh to slightly weathered dark grey LIMESTONE with interbedded layers of calcareous mudstone or a light grey Calcisiltite with frequent thin beds of black argillaceous shale.
- The TCR of the rock ranges from 43% to 100% and the RQD generally ranges from 36% to 65%.
- Without actually defining the rock, BH104 notes “*rockhead*” at 18.3mbgl (21.1mOD) and progresses using open hole drilling techniques from this depth. BH108 notes “*solid Limestone Rock*” from 24mbgl (15.4mOD) and also progresses using open hole drilling techniques. There are no rotary corehole logs to confirm the TCR, SCR and RQD of the rock, neither are there geological descriptions of the rock provided to BS 5930.
- The 4 No. additional rotary coreholes carried out in 2010 appear to indicate a lower level to the top of rock with a layer of weathered rock overlying.
- BH211 identifies a possible fault zone within the rock with the material typically described as a completely weathered argillaceous SHALE. The RQDs of this material is 0% and the associated TCR is 100%.



Figure 5-1: SI location Plan along Dublin Port Tunnels, from 1995 to 1996



Figure 5-2: SI location Plan Ground Investigations Ireland, 2010



Figure 5-3: SI location Plan Ground Investigations Ireland, 2020

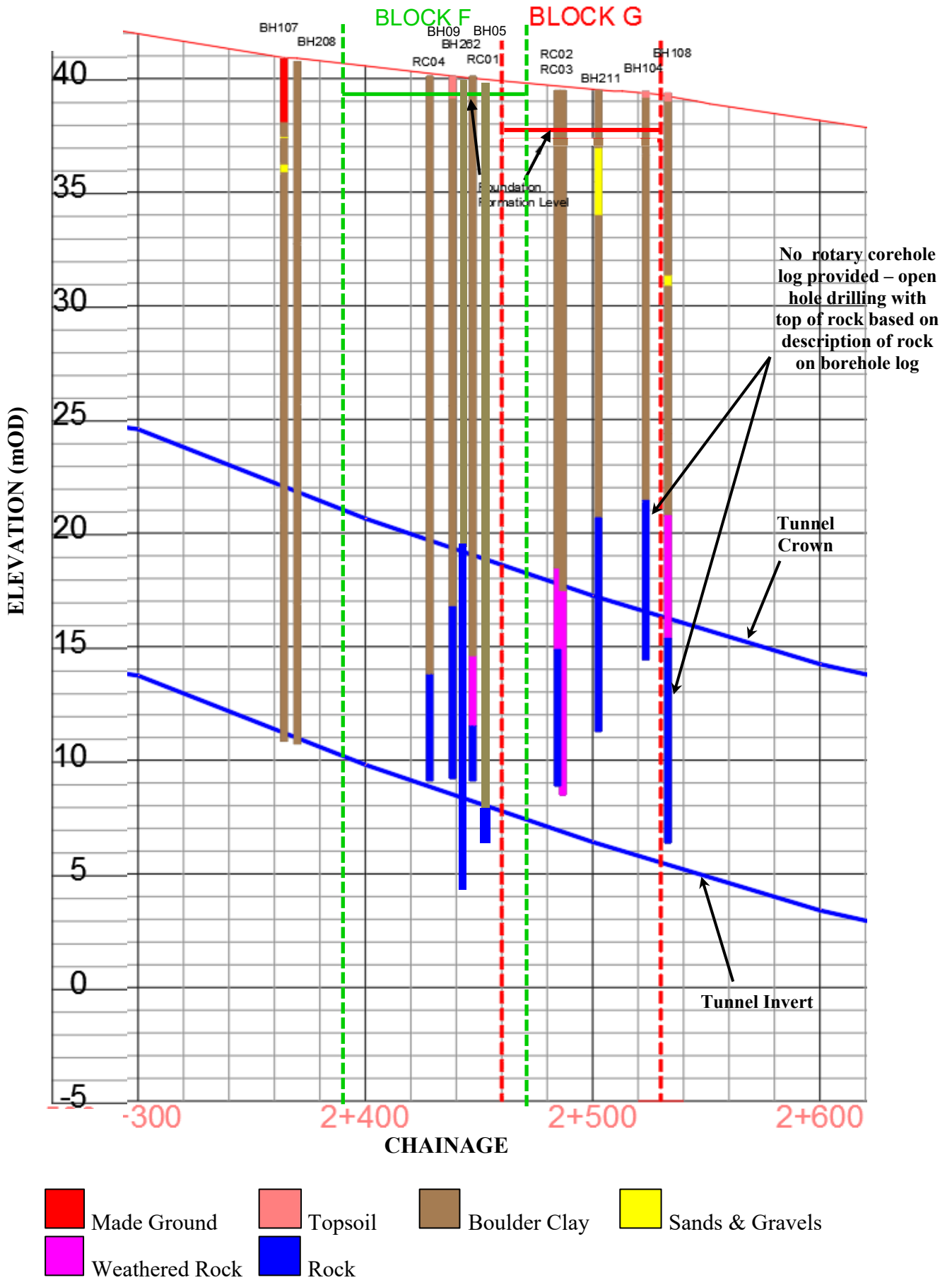


Figure 5-4: Subsurface ground profile along northbound tunnel within site

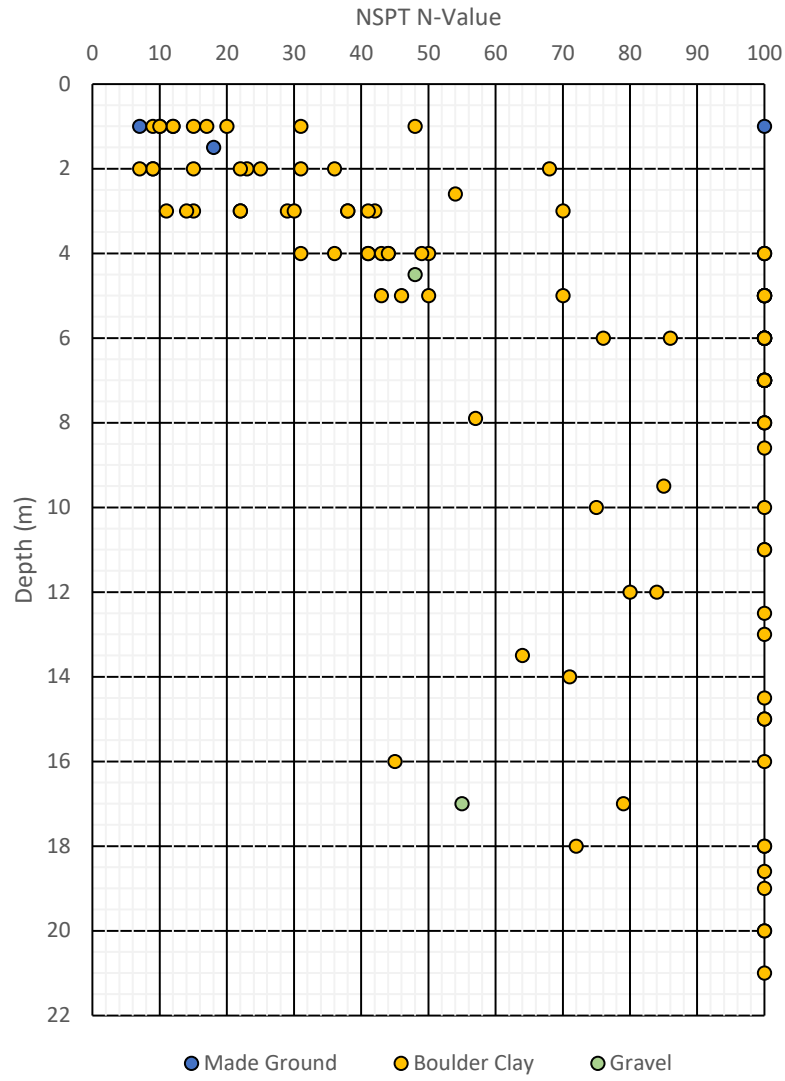


Figure 5-5: SPT N-Values vs Depth

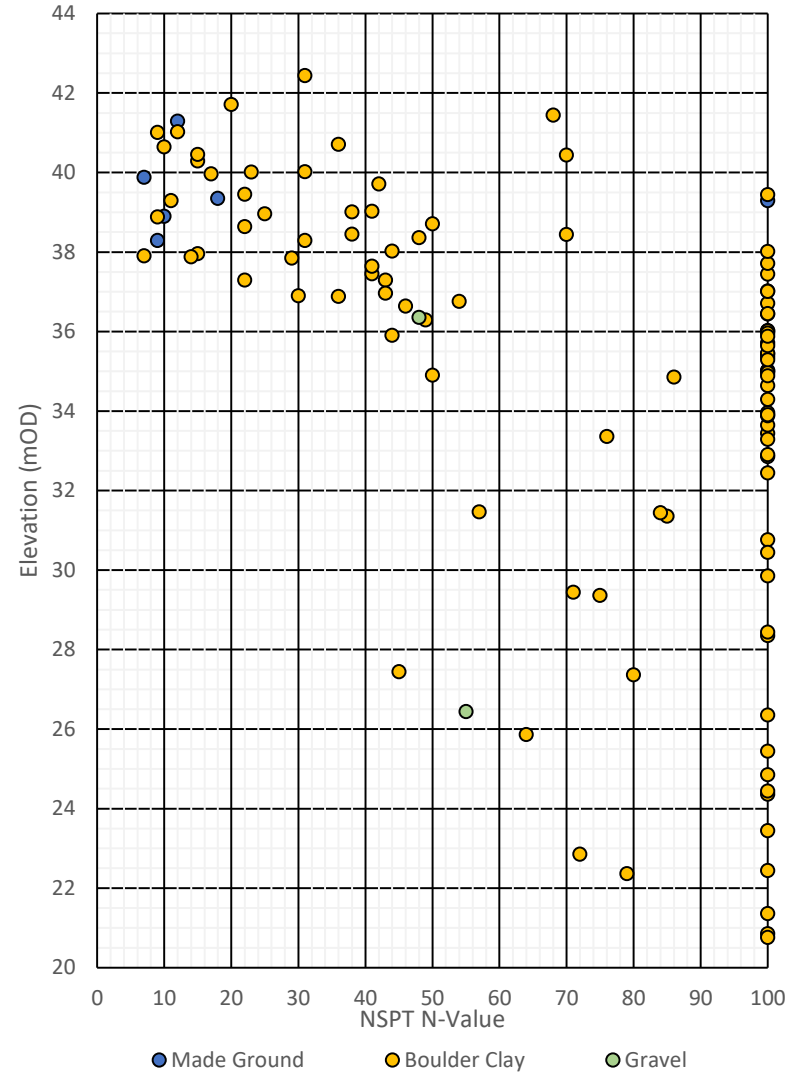


Figure 5-6: SPT N-Values vs Elevation

5.3 Ground Water Conditions

Standpipes were installed in 4 No. boreholes on the site as part of the site investigations carried out by IGSL in 1995. Readings were taken in the standpipes from October, 1995 to May 1997 typically at weekly intervals up to June, 1996, increasing to monthly intervals thereafter. A summary of the ground water levels taken from standpipes on the site is presented on Table 5-1 and a plot of the readings is shown on Figure 5-7 and Figure 5-8, against depth and elevation, respectively.

Standpipes were installed in 3 No. boreholes on the site as part of the GII 2020 site investigation and readings were taken from June to August 2020. The readings will be taken from these standpipes during and post construction at regular intervals. A summary of the ground water levels taken from standpipes on the site is presented on Table 5-2 and a plot of the readings is shown on Figure 5-9 and Figure 5-10, against depth and elevation, respectively.

The water strikes recorded in the boreholes on the site are presented on Table 5-3. It should be noted that groundwater strikes in boreholes and trial pits are not reliable indicators of the static groundwater level as the holes are typically not left open long enough for the water level to stabilise. They generally indicate where there are permeable seams below the groundwater level, or where there are perched groundwater levels over low-permeability soil or rock.

The water levels in the standpipes indicate a pattern of shallow ground water in the north and east of the site (between 1.0m and 2.0m bgl / 37.8m and 39.0mOD) and deeper ground water to the southwest and southeast (between 2.5 and 3.5 mbgl / 36.0 and 37.0mOD). There is an unusually deep depth to ground water of 6.7mbgl (32.8mOD) recorded in BH104, however, this reading is not consistent with the readings taken in the other standpipes and is considered to be an anomaly.

The first couple of standpipe readings taken in the GII 2020 site investigation in the month of July show that the water levels have not yet equilibrated, however, after approx. 14th July, it appears that the water levels are more consistent and may have equilibrated to the long term ground water levels.

The variation in the ground water levels from 1995 to 1997 over a period of approx 1.5 years show a variation in groundwater levels in each standpipe of roughly 1m, however, some larger variations occur in BH107 within the month of June where it appears to be up to 1.5m.

The depth to ground water level is taken as 1mbgl throughout the site and is hydrostatic with depth.

Table 5-1: Summary of ground water levels taken from standpipes on the site (Detailed SI 2000)

BH ID	Ground Level (mOD)	Response zone (mbgl)		Elevation (mOD)		Depth (mbgl)		Stratum Description
		Top	Base	Min	Max	Min	Max	
BH-104	39.4	17.0	25.0	32.8	38.0	1.5	6.7	Black BC (17-18mbgl), Rock (18-25mbgl)
BH-107	40.1	20.0	25.0	34.9	39.1	1.0	5.2	Hard gravelly Clay with horizons of gravel
BH-108	39.4	17.2	20.0	35.3	37.3	2.1	4.1	V. stiff/hard Brown BC (0-18.6mbgl). Broken limestone (18.6-20mbgl)

Table 5-2: Summary of ground water levels taken from standpipes on the site (GII 2020)

BH ID	Ground Level (mOD)	Response zone (mbgl)		Elevation (mOD)		Depth (m)		Stratum Description
		Top	Bottom	min	max	min	max	
BH01	42.3	1.0	5.6	40.4	40.8	1.5	1.9	Brown and Black Boulder Clay
BH06	41.6	1.0	8.0	36.4	38.0	3.7	5.2	Brown and Black Boulder Clay
BH10	39.9	1.0	7.2	38.0	38.3	1.6	2.0	Brown and Black Boulder Clay

Table 5-3: Summary of ground water strikes in the boreholes(Detailed SI 2000 & GII 2020)

SI ID	Depth of Strike (mbgl)	Elevation of Strike (mOD)	Depth rose to over time period (mbgl)	Time period (mins)
BH-107	3.4	36.65	3	30
BH-208	Dry			
BH-262	Dry			
BH-211	Dry			
BH-104	0.4	39.03	0.5	30
BH-104	18.0	21.43	16.8	30
BH-108	8.0	31.36	6.7	60
BH-105	16.5	26.94	6.1	10
BH01	3.5	38.79	3.0	-

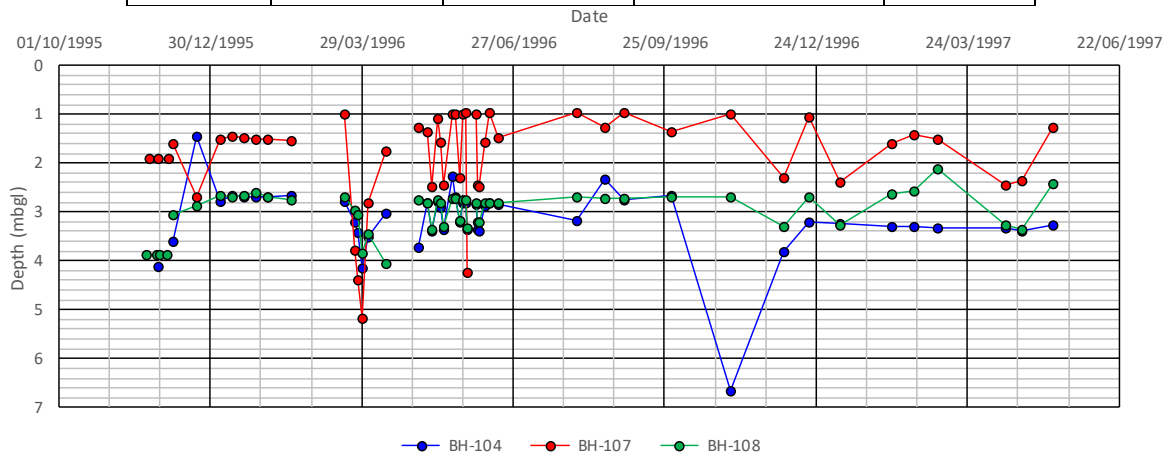


Figure 5-7: Groundwater Depth readings taken from standpipes (Oct, 1995 to May, 1997)

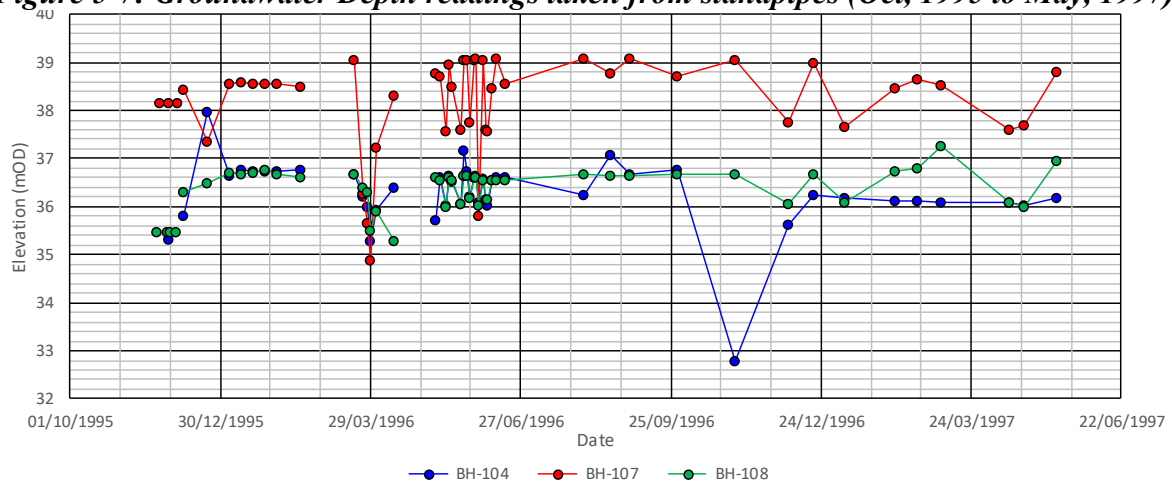


Figure 5-8: Groundwater Elevation readings taken from standpipes (Oct, 1995 to May, 1997)

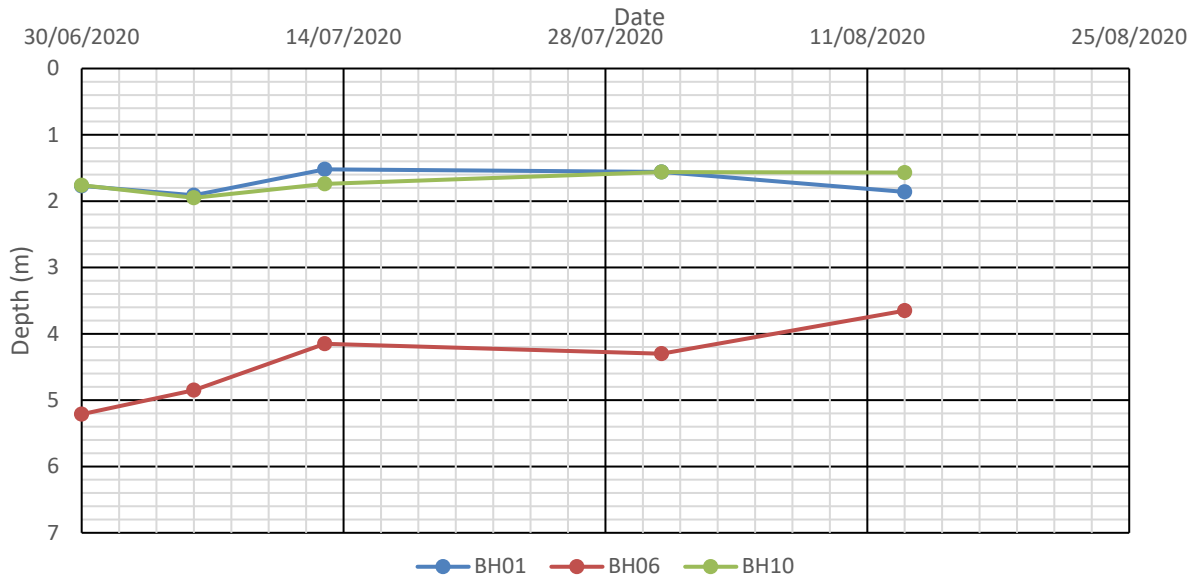


Figure 5-9: Groundwater Depth readings taken from standpipes (June to August, 2020)

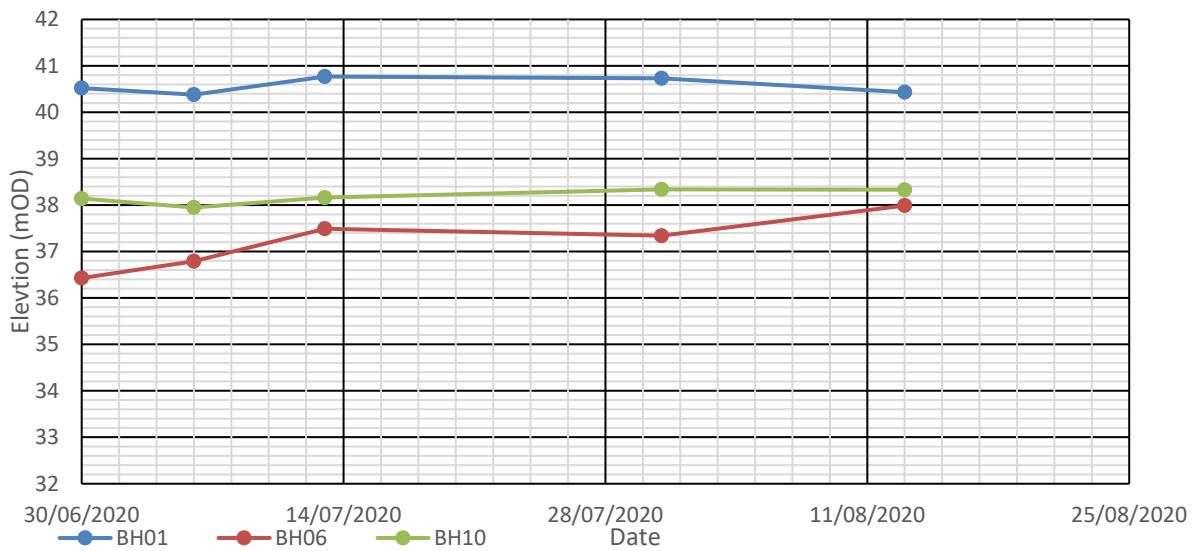


Figure 5-10: Groundwater Elevation readings taken from standpipes (June to August, 2020)

6 CHARACTERISTIC SOIL PROPERTIES

A summary of the characteristic material properties assigned to the materials and the ground model for the site are given on Table 6-1. The Dublin Boulder Clay, which is taken to comprise the very stiff to hard Upper Black, Lower Black and Lower Brown Boulder Clays, are the dominant strata within the boundaries of the site. The parameters have been presented for the Mohr Coulomb material model, as well as the more sophisticated Hardening Soil model with small-strain stiffness, which models the small strain stiffness behaviour of soils. The latter is discussed in Section 6.3.

6.1 Upper Brown Boulder Clay

The Upper Brown Dublin Boulder Clay is present beneath the Made Ground in the majority of exploratory holes and was typically described as firm/firm to stiff brown grey slightly sandy slightly gravelly to gravelly CLAY with some cobbles and occasional boulders. However, it was occasionally described as soft/soft to firm in several site investigation points.

No bulk density tests were carried out on samples of the Brown Boulder Clay. As the strength of the stratum was generally reported as firm/firm to stiff on the exploratory hole logs, the following characteristic bulk unit weight has been assigned to the stratum:

$$\gamma_b = 21.5 \text{ kN/m}^3$$

SPT N-values recorded in exploratory holes on the site ranged from 7 to 54 and undrained shear strengths inferred from these N-values ranged from 35 to 324 kPa (i.e. soft to firm, stiff to hard) using the empirical relationship $c_u = 5 \times N_{\text{SPT}}$ by Stroud (1989).

No laboratory compressibility tests were performed on samples of the Brown Boulder Clay. Therefore, the drained stiffness E' of the Brown Boulder Clay has been derived using the relationship $E' = 1500 \times N_{\text{SPT}}$. Due to the variable strength of the Upper Brown Boulder Clay which can be soft/soft to firm particularly at shallow depths (<2m) a conservative drained stiffness of $E'_k = 16,000 \text{ kPa}$ has been used in this analysis which is based on an SPT N-value of approx. 10.

$$E'_k = 16,000 \text{ kPa}$$

The Brown Boulder Clay comprises an intermediate plasticity sandy gravelly CLAY. Based on previous experience, a characteristic drained effective shearing resistance, $\phi_k' = 34^\circ$ is considered to be representative. However, due to the variable strength of the Upper Brown Boulder Clay, a conservative drained effective shearing resistance, $\phi_k' = 30^\circ$ has been used in this analysis.

6.2 Upper Black, Lower Brown and Lower Black Boulder Clay

Upper Black, Lower Brown and Lower Black Boulder Clay have similar engineering characteristics and are therefore, discussed together in this section. The stratum is described as stiff to hard with SPT N-values ranging from 40 to 86 with several refusals noted. There are no bulk density data available for the stratum. However, from experience and published data with Dublin Boulder Clay (Long et. al, 2012), the following characteristic bulk unit weight has been assumed:

$$\gamma_b = 23 \text{ kN/m}^3$$

No laboratory strength tests were performed on samples of the Boulder Clay. SPTs carried out in boreholes on the site reported N-values from 40 to 86, with several refusals reported. The Boulder Clay typically comprises a low plasticity sandy gravelly CLAY. Based on previous experience and published data (Lawlor et al, 2011), a characteristic drained effective shearing resistance, $\phi_k' = 40^\circ$ is considered to be representative.

No laboratory compressibility tests were performed on samples of the Boulder Clay.

The drained stiffness E' of the Boulder Clay has been derived using the relationship $E' = 2000 \times N_{SPT}$. Taking a characteristic SPT N-value of 45, the characteristic drained stiffness of the Boulder Clay will be:

$$E'_k = 45 \times 2000 = 90,000 \text{ kPa}$$

Conservatively, a minimum drained stiffness of 80,000kPa has been assigned to this stratum. This would be a typical value for the upper black, lower brown and lower black Boulder Clays based on field data of the settlement of a 1.5m x 1.5m pad foundation on the black boulder clay (Farrell et al., 1988).

Based on experience with Boulder Clays, the stiffness of the material increases with depth. To account for the increase in stiffness with depth, a minimum drained stiffness of 80MPa has been assigned to the material to an elevation of 34.1mOD, which corresponds to a depth of approx. 6mbgl. The stiffness is then allowed to increase with depth in accordance with the following equation which has been taken from Lawlor et al, 2011:

$$E' = 80 \times (\sigma_v'/100)^{0.5} \text{ (MPa)}$$

Where, σ_v' = effective overburden pressure.

The drained stiffness assigned to these materials is shown on Figure 6-1 and Figure 6-2 against elevation and depth, respectively.

6.3 Hardening Soil model with small-strain stiffness (HSS) material parameters

The hardening plasticity small strain stiffness (HSS) soil model available in the Plaxis program has been shown to closely model the behaviour of the very stiff Dublin Boulder Clays which are prevalent throughout Dublin City (Lawler et. al, 2011). These parameters have been published by Lawler et al. (2011) based on laboratory measurements and calibrated with field observations in finite element analysis of steep cuttings. These parameters are summarised on Table 6-2 and would be applicable to the Upper Black, Lower Brown and Lower Black Boulder Clay.

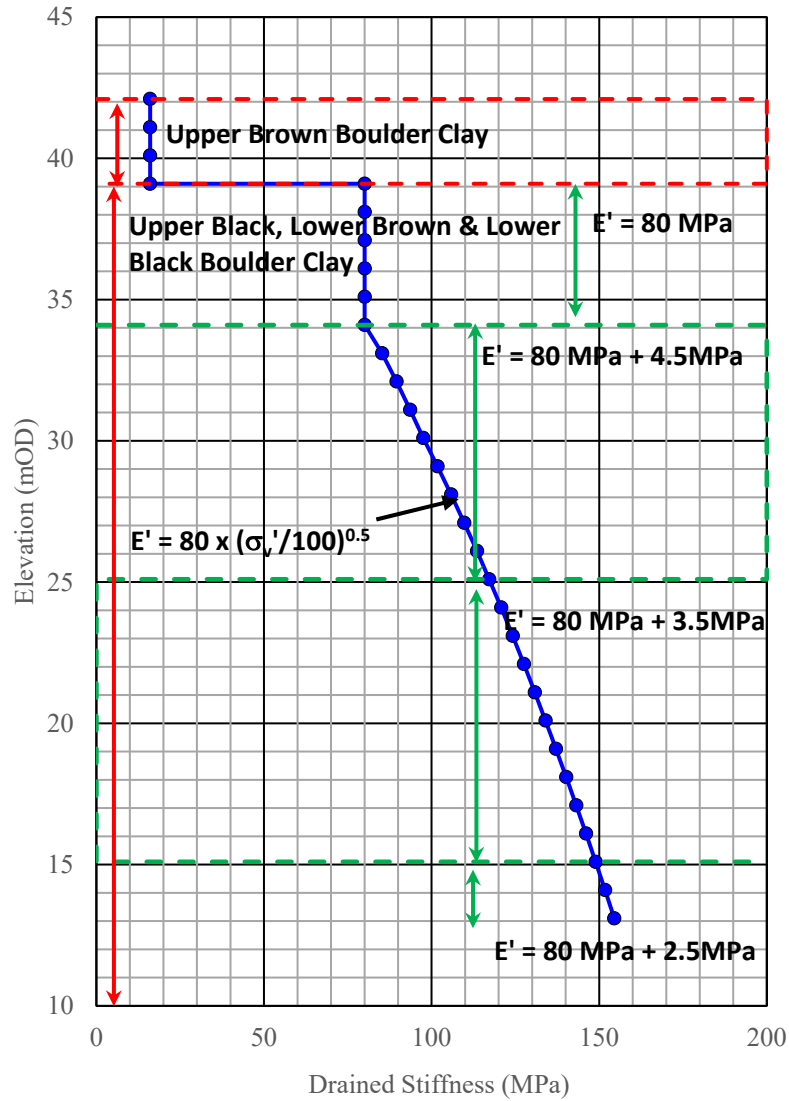


Figure 6-1: Drained stiffness of Boulder Clays showing increase with Elevation

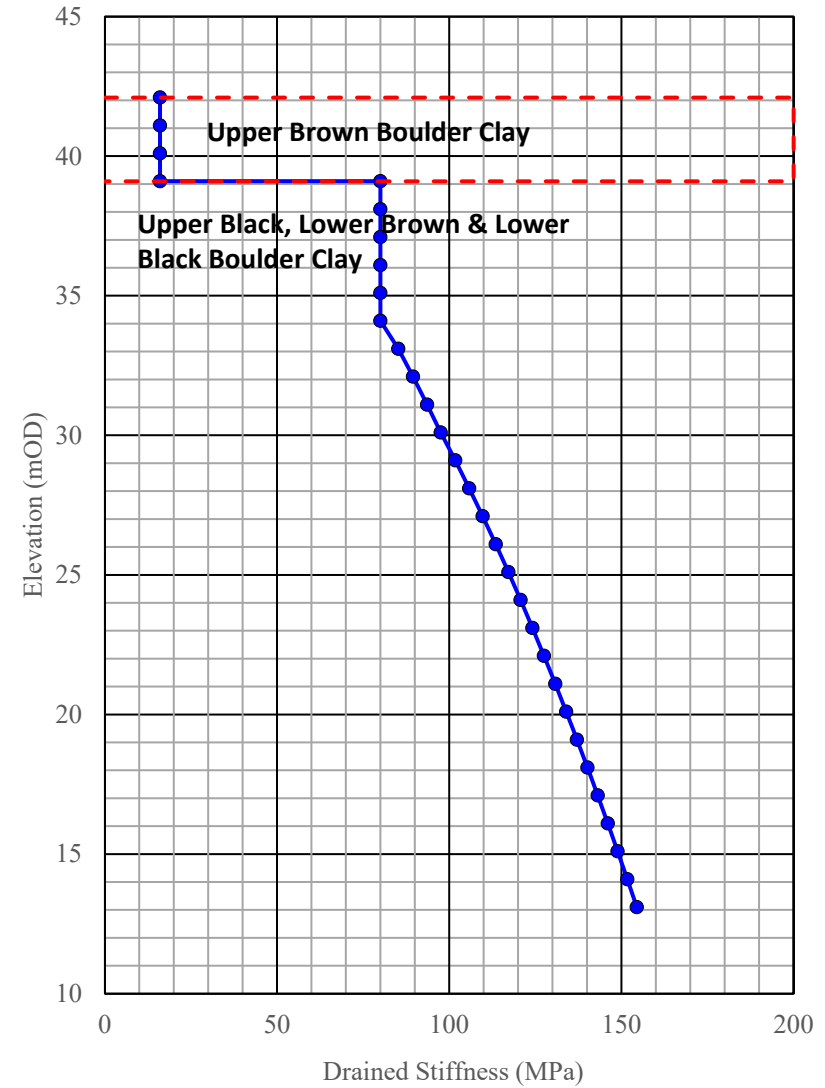


Figure 6-2: Drained stiffness of Boulder Clays showing increase with depth

Table 6-1: Summary of geotechnical design parameters & ground model for site*

Stratum	Elevation (Top of Stratum)	Stratum Thickness	Bulk Unit Weight	Young's Modulus**			K ₀	Strength				Poisson's ratio,	
	mOD			m	γ (kN/m ³)	E _u (MPa)		E' (MPa)	E' increment (MPa)	φ' (°)	ψ (°)	c' (kPa)	c _u (kPa)
*Upper Brown Boulder Clay	43.0-39.4	3.0	21.5	-	16	0	1.5	30	0	0.1	-	0.2	-
*Upper Black Boulder Clay	40.0-36.4	11.3-14.9	23	-	80	4.5MPa below 34.1mOD	1.5	40	3	0.1	-	0.2	-
*Lower Brown Boulder Clay	25.1	10.0	23	-	115	3.5MPa below 25.1mOD	1.5	40	3	0.1	-	0.2	-
*Lower Black Boulder Clay	15.1	2.1-8.0	23	-	145	2.5MPa below 15.1mOD	1.5	40	3	0.1	-	0.2	-
Limestone	13.0-7.0	> 10	26.5	-	2000	-	1.0	35	-	150	-	0.2	-

* the undrained parameters are derived within the Plaxis 3D program using the Undrained (A) option which derives strength and stiffness parameters based on the effective stress properties.

** Figure 6-1 shows the drained stiffness assigned to the soils the site

Table 6-2: Summary of geotechnical design parameters for HSS Model (after Lawler et al 2011)

Stratum	G ₀ ^{ref} (MPa)	E' ₅₀ ^{ref} (MPa)	E' _{oed} ^{ref} (MPa)	E' _{ur} ^{ref} (MPa)	γ _{0.7}	m	v _{ur}	K ₀	φ'	c' (kPa)	ψ	POP (kPa)
Black Boulder Clay	420	50	33	200	0.0001	0.5	0.2	1.5	40	0	3	1500

p'_{ref} = 100 kPa

E'₅₀^{ref} = stiffness modulus for primary loading in a drained triaxial test

E'_{oed}^{ref} = stiffness modulus for primary loading in an oedometer test

E'_{ur}^{ref} = stiffness modulus for unloading/reloading

G₀^{ref} = shear stiffness at very small strain levels

γ_{0.7} = shear strain at which G has reduced to 0.7G₀^{ref}

m = modulus exponent for stress dependency

p^{ref} = reference mean effective stress = 100 kPa

v_{ur} = Poisson's ratio for loading/unloading

c' = effective cohesion at failure

φ' = effective friction angle at failure

ψ = dilatancy angle at failure

POP = Pre-overburden pressure

7 PLAXIS 3D FINITE ELEMENT ANALYSIS

7.1 Introduction

The 3D finite element program, PLAXIS 3D, has been used to assess the impact on the Dublin Port Tunnels due to the excavation and building loads for the construction of the proposed development. The Plaxis 3D program enables structural elements as well as soils to be modelled to develop sophisticated soil/structure interaction analyses.

The assessment for the development takes into account the excavation for the basement carpark under Blocks A to E, the loads for the buildings Blocks A to G and the unloading due to construction of the attenuation tanks and the basement access ramp. Figure 7-1 shows the 3D model developed for the site. The basement access ramp and attenuation tanks are not shown on this model but can be seen on Figure 7-9.

The temporary (during construction) and permanent (post construction) condition of the site are assessed in this report.

The analyses were carried out using the ground and groundwater model discussed in Section 7.3 and 7.4 and the Design Situations presented in Section 7.8. The characteristic soil properties used in the analysis are summarised in Section 5.3 and the characteristic loads are presented in Section 7.4.

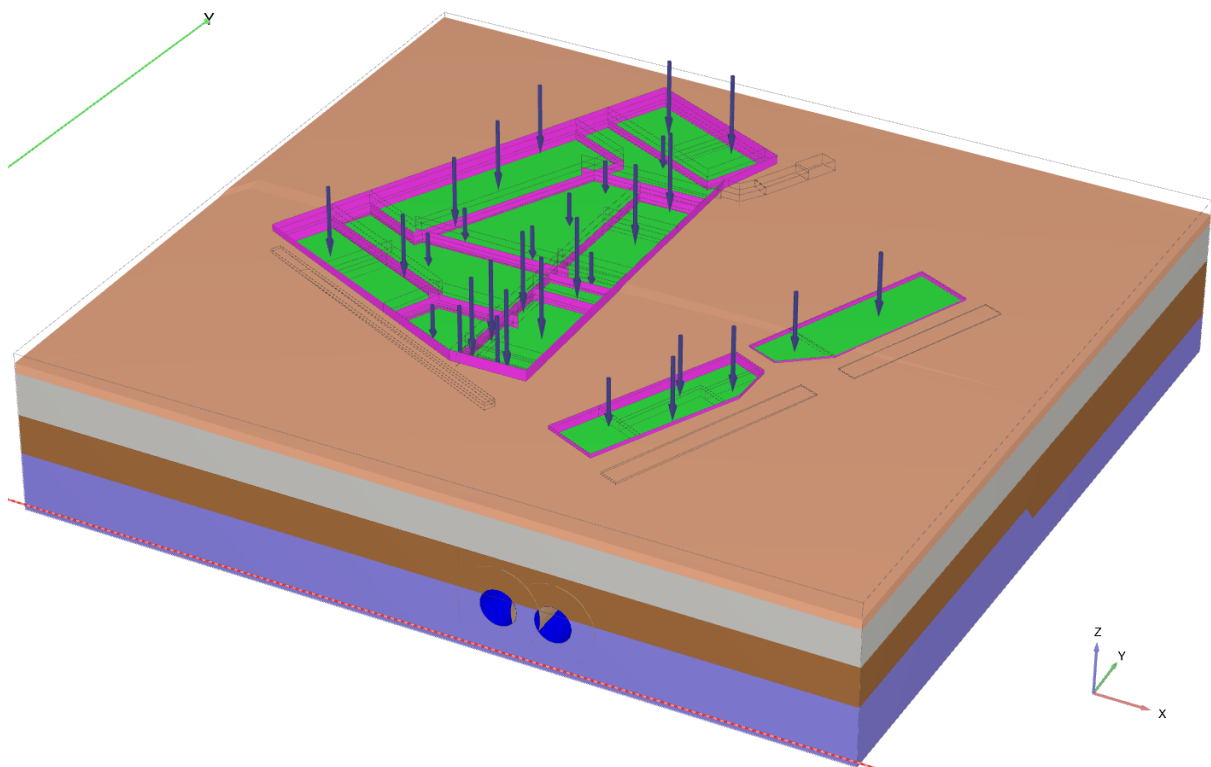


Figure 7-1: Plaxis 3D model of site (see Figure 7-9 for basement access ramp and attenuation tanks)

7.2 Design Philosophy

Section 2.2 of the *Guidance Notes for Developers, The assessment of surface and sub-surface developments in the vicinity of the Dublin Port Tunnel* states that the Dublin Port Tunnels “has

been designed to sustain surcharge loading of 22.5kNm² and remain within limits for the Serviceability Limit State (SLS).”

To ensure the SLS requirements are satisfied, the impact of the development on the Dublin Port Tunnels has been assessed using characteristic material properties and loads to determine the ground movements, tunnel deformations and increase in stress on the tunnel lining.

However, the effects of actions such as the bending moments and axial forces within the tunnel lining, are assessed in accordance with Design Approach 1 Combination 1 (DA1.C1) of Eurocode 7 (IS EN 1997-1: 2005) which applies partial factors of 1.35 and 1.5 to permanent and variable unfavourable loads, respectively. Conservatively, it has been assumed in this analysis that all loads applied are variable unfavourable loads, therefore, the most onerous partial factor of 1.5 has been applied to bending moments, axial forces and shear forces, where appropriate.

The drained (long-term) and undrained (short-term) conditions have been assessed.

7.3 Plaxis Ground Model

The ground conditions vary across the site, particularly from north to south where the tunnel extends from fully within boulder clay at the north of the site, to within rock at the tunnel invert from approx. Ch. 2+400. The stratigraphy used to develop the plaxis ground model is shown on Table 6-1. The ground profiles, GP-A, GP-B and GP-C were used to model the varying ground conditions and ground levels across the site and these are summarised on Table 7-1. The position of the ground profiles are shown on Figure 7-2. The ground profiles are assigned different ground levels to model the varying ground elevations on the site.

Cross section profiles showing the ground profiles, GP-A and GP-B and GP-C are shown on Figure 7-3 and Figure 7-4, respectively. Due to the uncertainty in the top of competent rock on the site, the top of rock has been conservatively estimated to rise from 9mOD at the north and centre of the site (which is below the tunnel invert level) to 13mOD at the centre to south of the site (which is above the tunnel invert and below the tunnel crown).

Profiles showing the transition of the tunnels into rock from the north to the south of the model are shown for the northbound and southbound tunnels on Figure 7-5 and Figure 7-6.

Table 7-1: Summary of Ground Models GM-A to GM-C

Ground Model	GM-A		GM-B		GM-C	
	Top Elevation (mOD)	Stratum Thickness (m)	Top Elevation (mOD)	Stratum Thickness (m)	Top Elevation (mOD)	Stratum Thickness (m)
Upper Brown Boulder Clay	43.0-40.0*	3.0	42.5-40.0*	3.0	41.4-39.4*	3.0
Upper Black Boulder Clay	40.0-37.0	11.9-14.9	39.5-37.0	11.9-14.4	38.4-36.4	11.3-13.3
Lower Brown Boulder Clay	25.1	18.1	25.1	12.1	25.1	12.1
Limestone	7.0	> 10	13.0	>10	13.0	>10

*Ground levels reduce from west to east

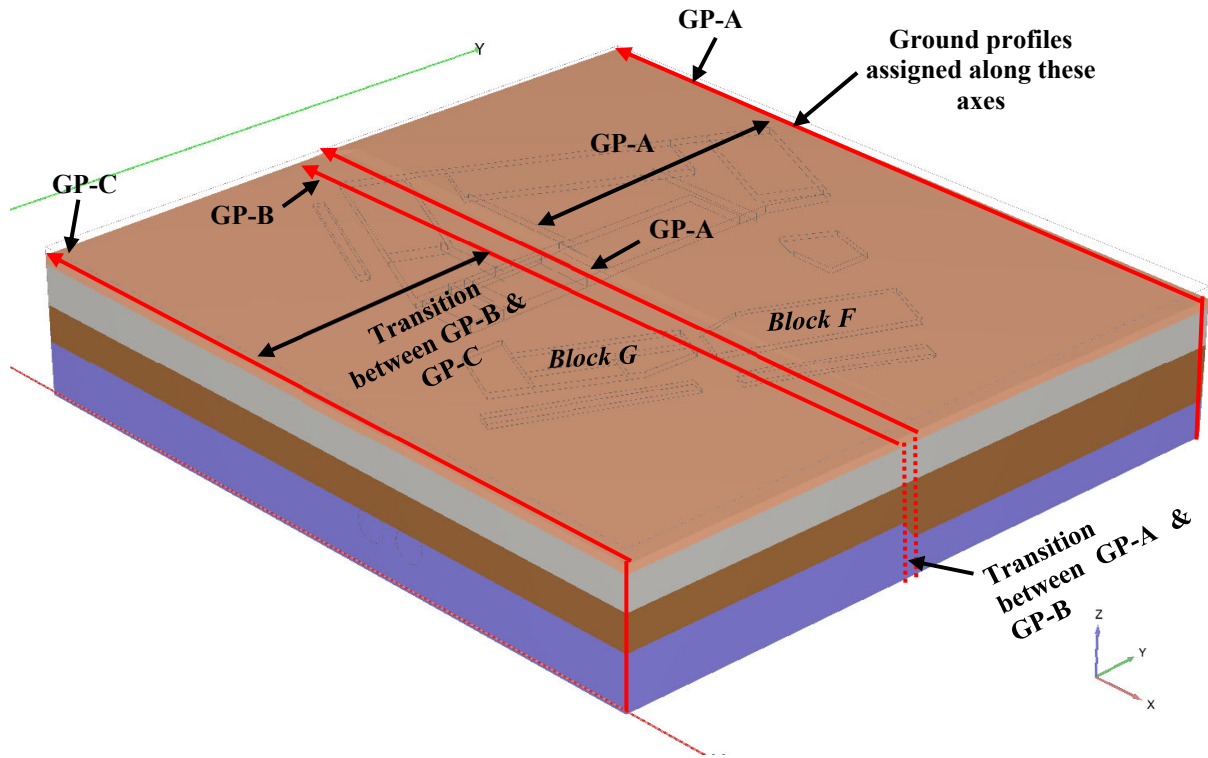


Figure 7-2: 3D Ground Model with locations of GP-A to GP-C

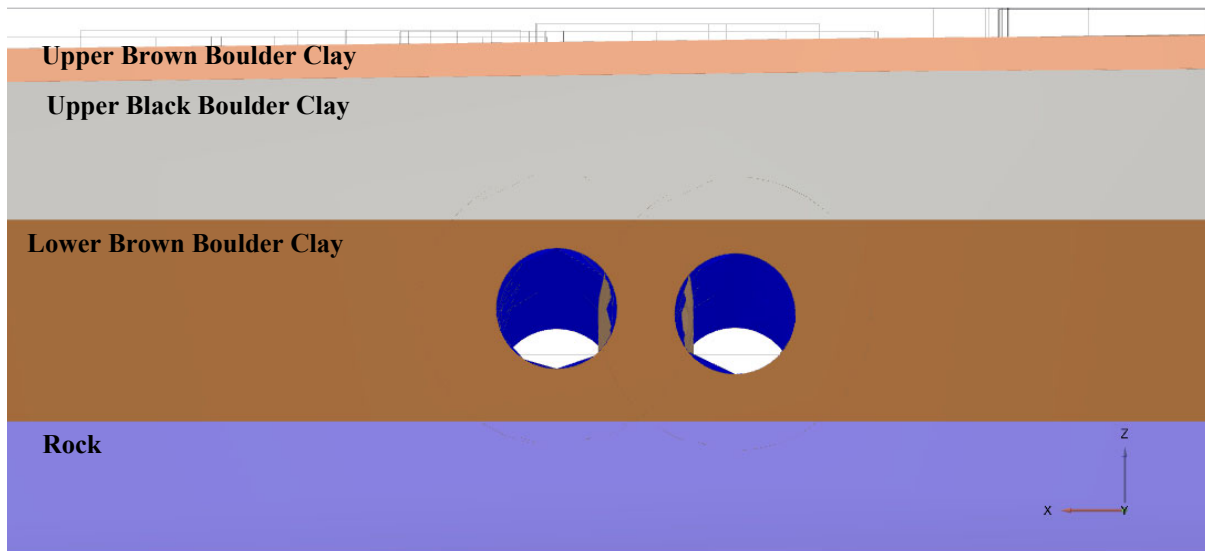


Figure 7-3: Ground Profile GP-A (level of tunnel varies)

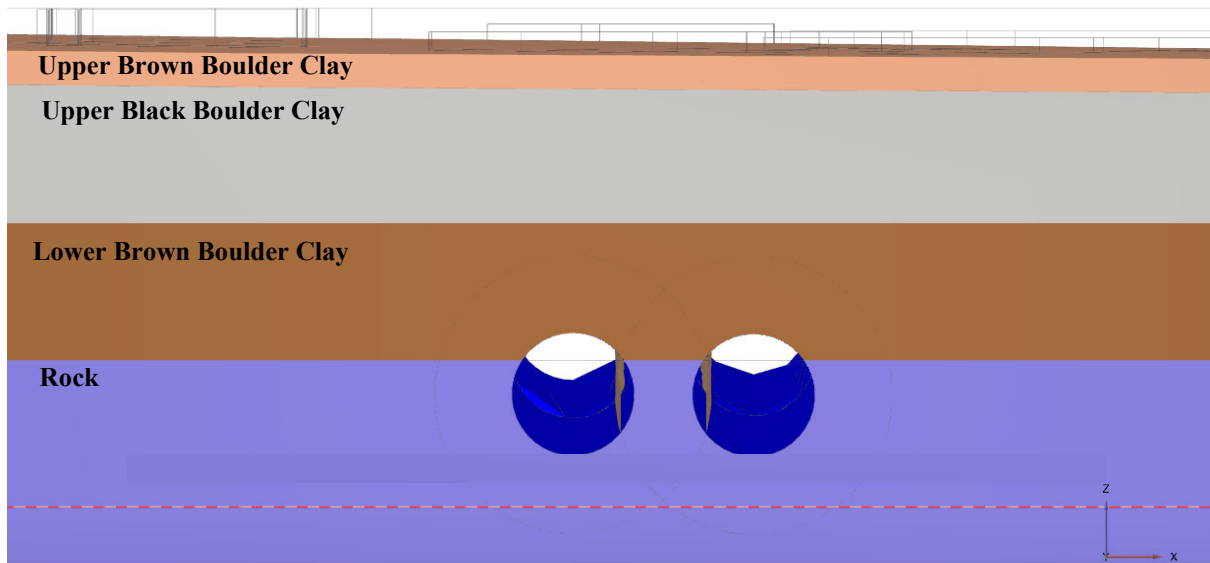


Figure 7-4: Ground Profile GP-B & GP-C (level of tunnel varies)

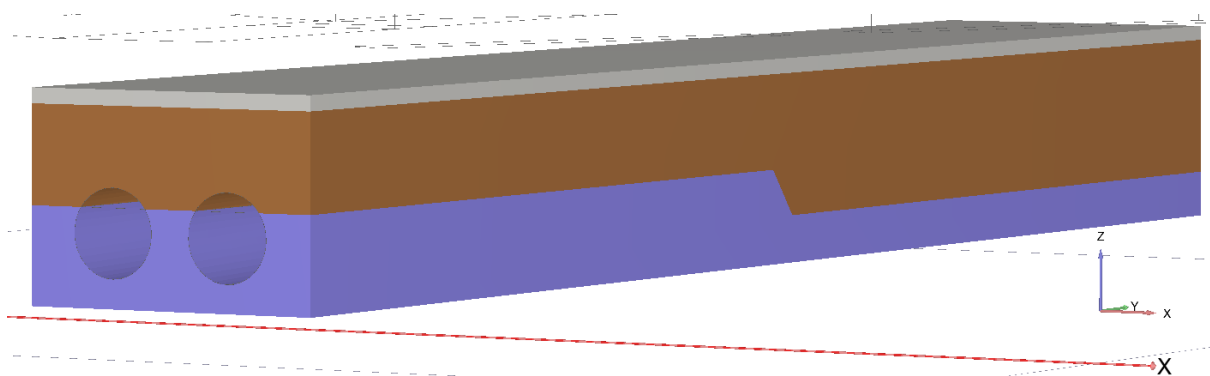


Figure 7-5: Profile showing transition of tunnel into rock along the northbound and southbound tunnels

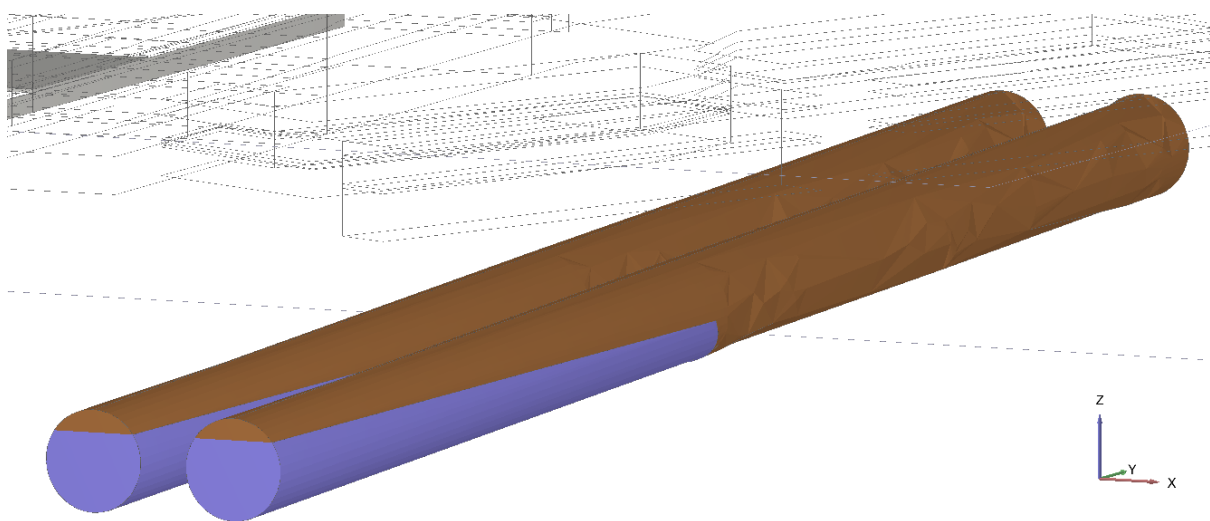


Figure 7-6: Profile showing transition of tunnel into rock along the northbound and southbound tunnels

7.4 Ground Water Model

The depth to ground water level is taken as 1mbgl throughout the site and is hydrostatic with depth. This is referred to as the Global Groundwater Level in this report and is shown on Figure 7-8. This is a conservative estimate based on the water level readings in the vicinity of the site as presented in Section 5.3.

Within the excavations, the groundwater is lowered to the base of the excavation. The groundwater level below the excavation is interpolated to the global groundwater level over a depth of approx. 5m below excavation level as shown on Figure 7-7.

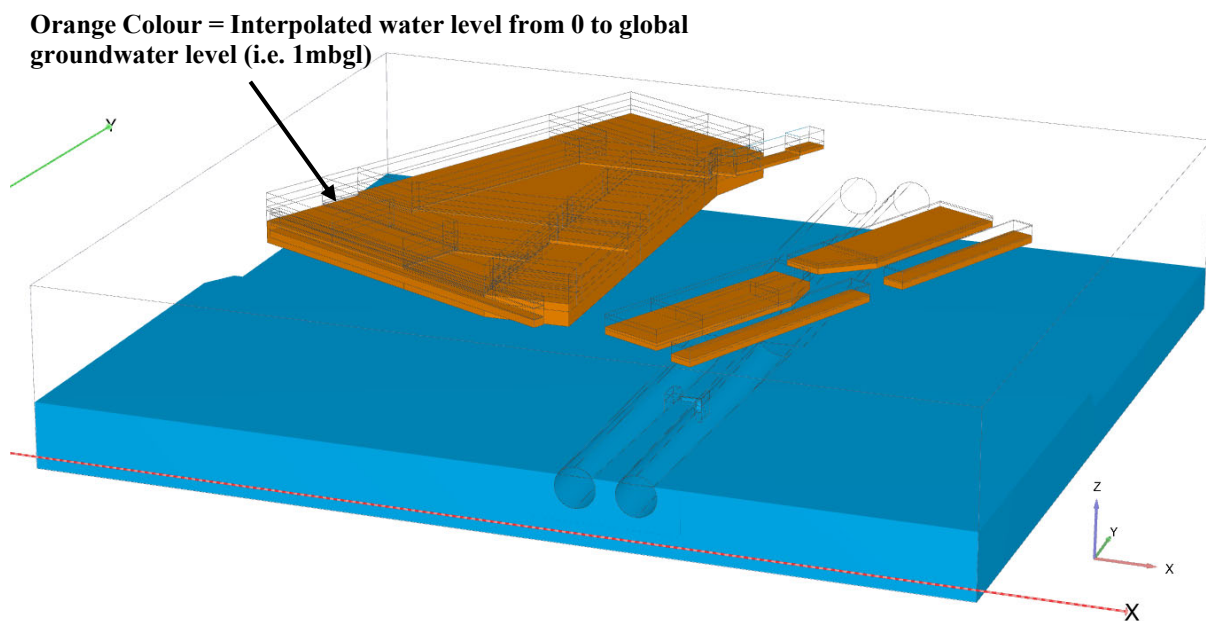


Figure 7-7: Interpolated Ground water level below excavations (i.e. Blocks F and G, underground carpark and attenuation tanks)

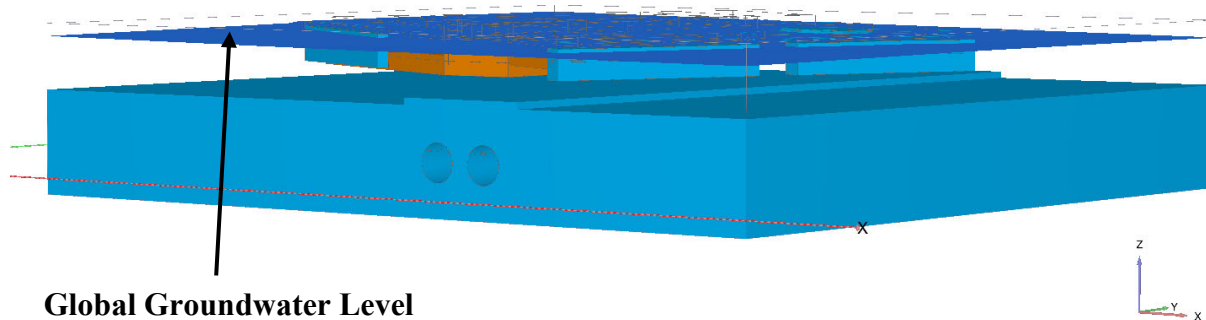


Figure 7-8: Global Ground Water Level

7.5 Site Model

The development has been modelled on the Plaxis Program using plate elements as boundary and internal walls. The position of the buildings and tunnels etc have been input into the model

using an AutoCAD drawing set to ITM coordinates. Therefore, the site layout represents the proposed position of the final development.

The ground within the walls of the basement is excavated to the base of the foundation for the building/basement and the bearing pressures are applied at that level. The excavation levels for each block, the basement carpark are summarised on Table 2-1 and Table 2-2. The excavation levels for the attenuation tanks are summarised on Table 2-3 and the excavation levels for the access ramp are discussed in Section 2.4.

To model the reduction in the finished floor levels for the basement, the basement excavation levels have been lowered in a series of steps from north to south. The final excavation levels for Blocks F and G, the basement, the attenuation tanks and the basement access ramp modelled in the Plaxis program are shown on Figure 7-9. This model shows the small steps within the basement to model the reduction in ground levels. The model includes a plate at these steps to prevent local slope failures in the program.

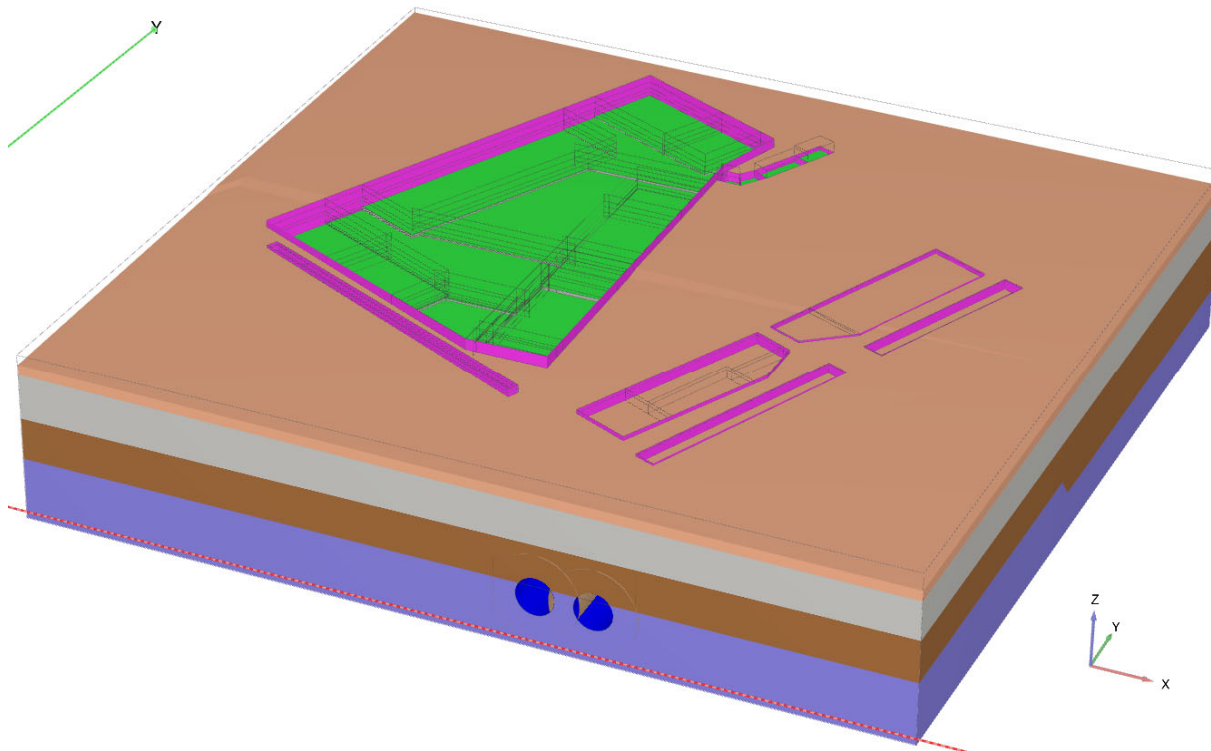


Figure 7-9: Final excavation levels for Blocks F and G, the basement, the attenuation tanks and the access ramp in the Plaxis program

7.6 Characteristic Loads

The bearing pressures applied to the model are discussed in detail in Section 2.4 and is shown on Figure 2-6.

Attenuation Tank Loads

The permanent construction of the attenuation tanks has a net unloading effect, as outlined in Section 2.4. However, the unloading effect is greatest in the temporary condition when excavating to formation level for the attenuation tanks (i.e. prior to their construction) due to the removal of soil above.

As discussed in Section 7.8, Design Stage DS-4 assesses the most onerous unloading condition during construction. This design situation includes the excavation to formation level for the attenuation tanks, the basement and access ramp, Blocks F and G. No loads are applied in this design situation.

Design Stage DS-5 models the permanent loading on the site due to the construction of the development i.e. Blocks A to G, the basement, to assess the potential largest stresses and deformations on the tunnel. The attenuation tanks have not been included in this design situation as it has a net unloading effect which would give a less conservative assessment when analysing the effect of the development on the tunnels.

Basement Access Ramp

The excavation for the basement access ramp has been included in Design Stage DS-4 which assesses the most onerous unloading condition during construction. The excavation levels are determined as the finished road levels shown on Figure 2-8 minus the road build up i.e. road pavement and road pavement foundation. The road build-up is taken as a 0.2m thick road pavement with 150mm thick layer of Clause 804 and 600mm thick capping layer.

The basement access ramp has not been included in design situation DS-5 as it has an unloading effect which would give a less conservative assessment when analysing the effect of the development on the tunnels.

7.7 Tunnel Details & Material Properties

The details of the tunnel used in the Plaxis analysis are presented on Table 7-2. A profile and 3D view of the tunnels showing Pedestrian Cross Passage are shown on Figure 7-10 and Figure 7-11, respectively. The tunnel crown levels were taken from the as-built drawings provided by TII (drawings No. DR-CB-PRO-C1-70041-11-X and DR/HA/BT/C11/41121/05/X). The Pedestrian Cross Passage details and material properties are also summarised on Table 7-2.

Table 7-2: Summary of Tunnel Details in 3D Plaxis Model

Tunnel	Northbound	Southbound	**Pedestrian Cross Passage
Tunnel Chainage	2+360 to 2+540	2+360 to 2+540	2+515 NB 2+517 SB
Ground Level (mOD)	41.7 to 39.5	41.4 to 39.5	40.0
Tunnel Crown *Level (mOD)	22.2 to 16.0	22.63 to 15.9	13.2
Internal Tunnel Diameter (m)	10.84	10.84	2.5***
Primary Tunnel Lining Thickness (mm)	350	350	350 (secondary lining thickness)
Thickness of Overburden above Tunnels (m)*	19.5 to 23.5	18.7 to 23.6	26.8

* the tunnels are inclined and fall from north to south as can be seen on Figure 7-10 and on the ground profile on Figure 5-4.

**relates to cross passage levels

***For modelling purposes for numerical convergence, the cross passage is assumed to be circular with an equivalent diameter. This assumption does not affect the results.

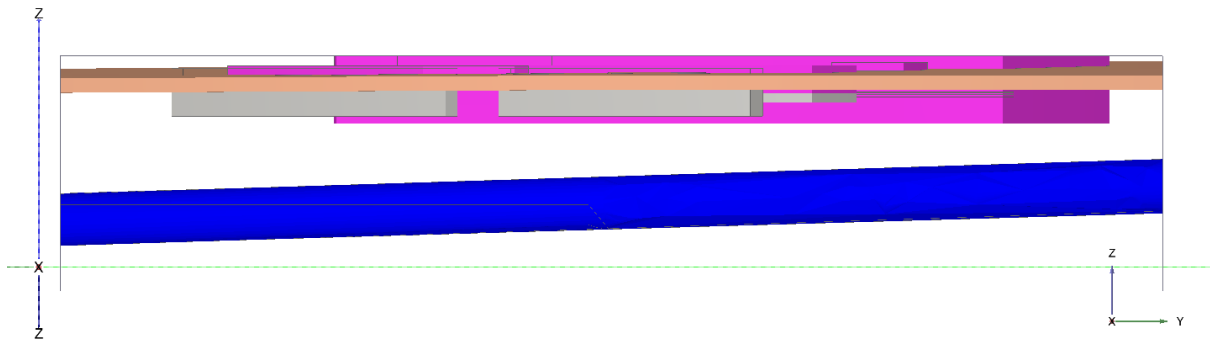


Figure 7-10: Profile view of tunnels (facing west) showing drop of tunnel from north to south

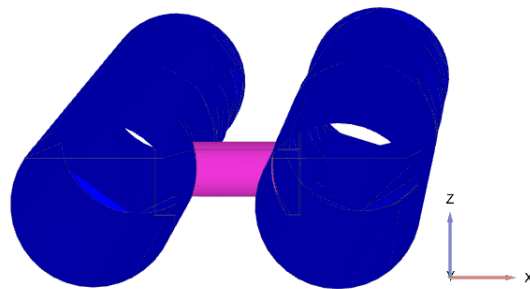


Figure 7-11: 3D view of tunnels showing Pedestrian Cross Passage

The tunnel and cross passage are modelled in the Plaxis program as a continuous plate element with the material properties given on Table 7-3.

Table 7-3: Material properties of the DPT tunnel lining & cross passage

Material type	Elastic
Isotropic	Yes
*E (kN/m)	1.5E+07
d (m)	0.35
w (kN/m/m)	2.0
v	0.2

*long term Youngs Modulus for Concrete, $E = 0.5 * 30\text{GPa}$

7.8 Design Situations

The design situations DS-1 to DS-5 have been assessed to account for the different excavation depths and loading combinations for the development that would have an impact on the Dublin Port Tunnels.

The design situations analysed in this report are presented on Table 7-4 and the excavation levels and loads for each Design Situation are presented on Table 7-5. The following is an outline of the design situations:

- DS-1 to DS-2 model the excavation and loading, respectively, of Block F and G. There is no basement excavation included in these design situations. DS-1 and DS-2 are shown on Figure 7-12 and Figure 7-13, respectively.
- DS-3 and DS-5 model the excavation and loading for Blocks A to E, respectively, with the loads applied to Block F and G. The basement excavation is included in these design situations. DS-3 and DS-5 are shown on Figure 7-14 and Figure 7-16, respectively.
- DS-4 models the excavation for Blocks G, F, the basement excavation, the access ramp and the attenuation tanks. No loads are applied in this design situation. Therefore, this design situation models the temporary unloading condition. DS-4 is shown on Figure 7-15

The Dublin Port Tunnels modelled in the Plaxis Program are shown on Figure 7-17

Table 7-4: Design Situations for Plaxis 3D analysis

Design Situations	Block G		Block F		Basement Excavation		Attenuation Tanks		Access Ramp	
	Exc	L	Exc	L	Exc	L	Exc	L	Exc	L
DS-1	Y	N	Y	N	N	N	N	N	N	N
DS-2	Y	Y	Y	Y	N	N	N	N	N	N
DS-3	Y	Y	Y	Y	Y	N	N	N	N	N
DS-4	Y	N	Y	N	Y	N	Y	N	Y	N
DS-5	Y	Y	Y	Y	Y	Y	N	N	N	N

Exc = Excavation; L = Load applied

Table 7-5: Excavation Levels and Loads for Design Situations DS-1 to DS-5

Design Situations		Block G	Block F	Blocks A to E & Basement Excavation	Attenuation Tanks
DS-1	Excavation Level (mOD)	37.85	39.45	-	-
	Load (kPa)	0	0		
DS-2	Excavation Level (mOD)	37.85	39.45	-	-
	Load (kPa)**	70-95	88-95		
DS-3	Excavation Level (mOD)	37.85	39.45	Varies*	-
	Load (kPa)**	70-95	88-95	Varies	
DS-4	Excavation Level (mOD)	37.85	39.45	Varies*	36.9-37.4
	Load (kPa)**	0	0	Varies*	0
DS-5	Excavation Level (mOD)	37.85	39.45	Varies*	-
	Load (kPa)**	70-95	88-95	Varies*	

*See Section for excavation levels in basement area for carpark and Blocks A to E.

**See section 7.6 for characteristic bearing pressures

- indicates this element was not modelled

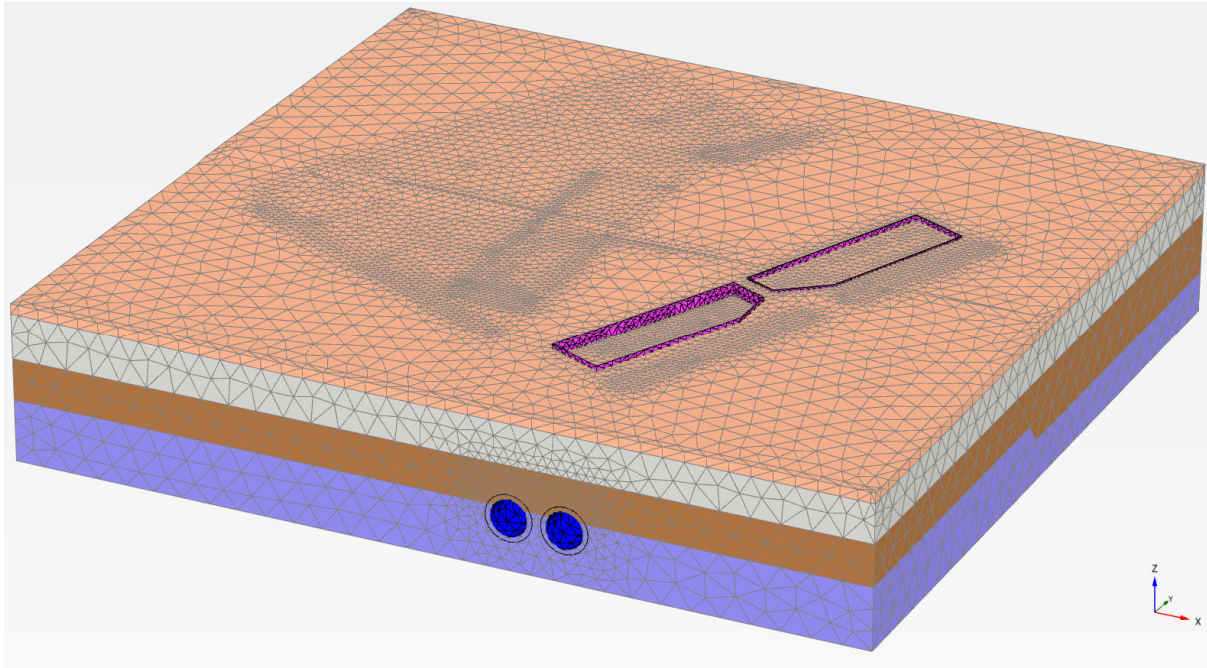


Figure 7-12: 3D Plaxis Model showing Design Situation DS-1

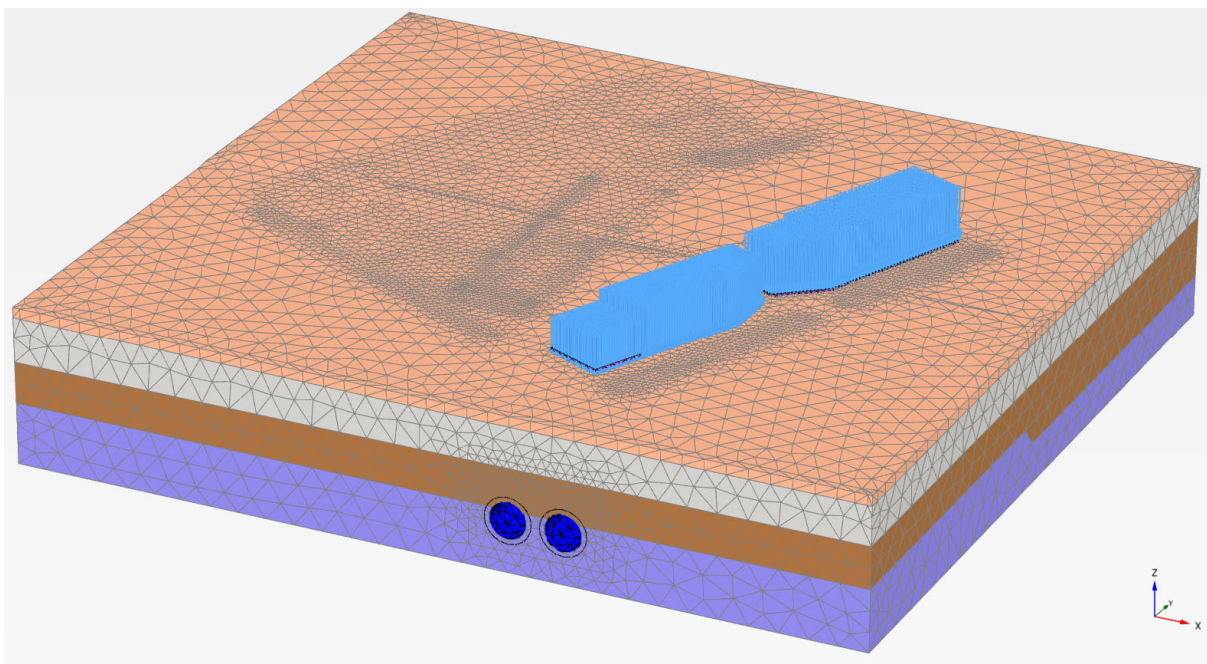


Figure 7-13: 3D Plaxis Model showing Design Situation DS-2

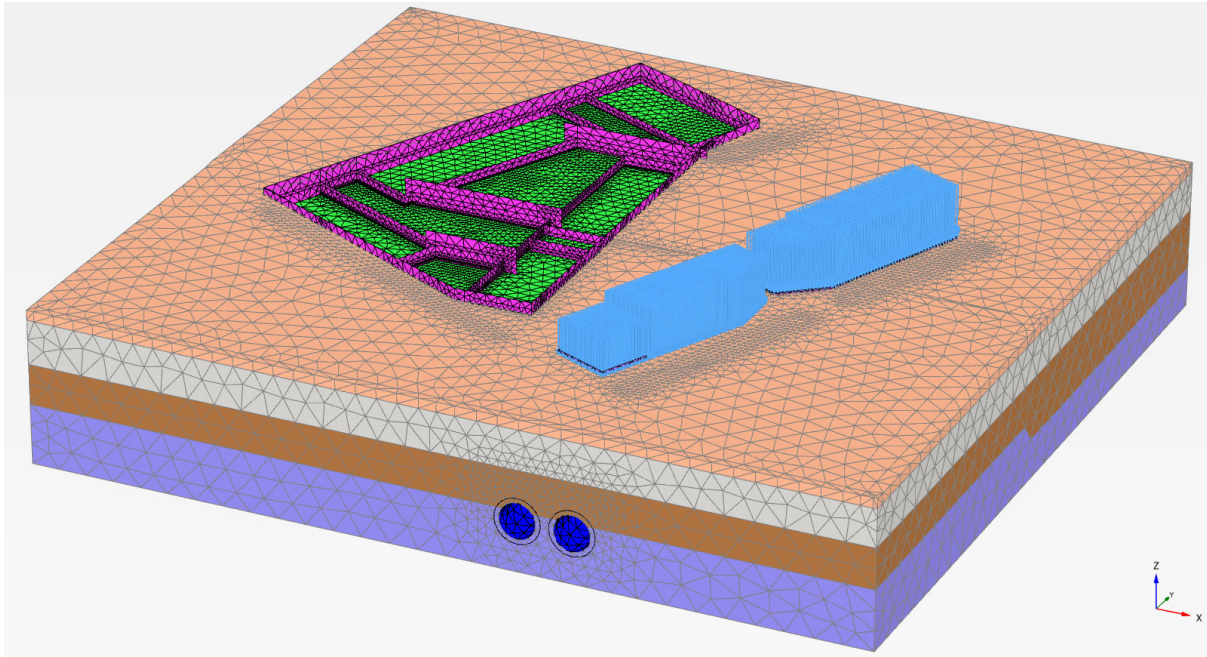


Figure 7-14: 3D Plaxis Model showing Design Situation DS-3

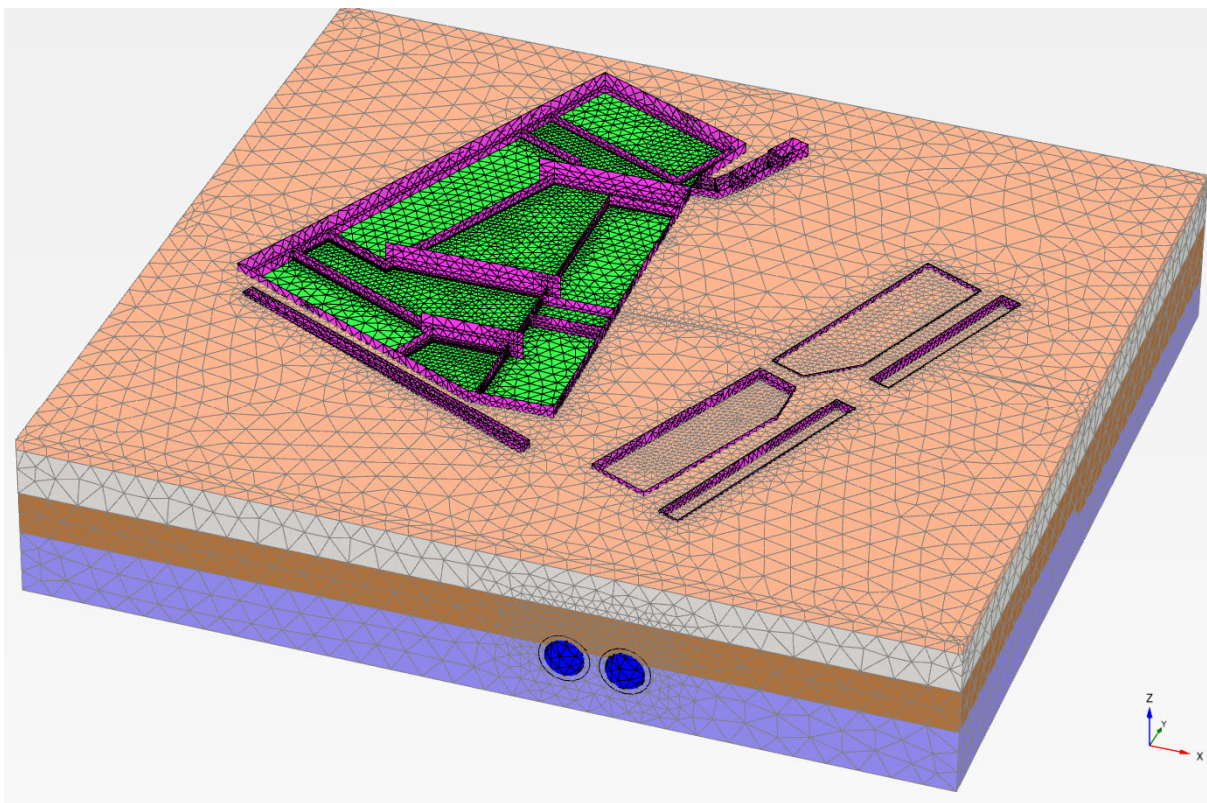


Figure 7-15: 3D Plaxis Model showing Design Situation DS-4

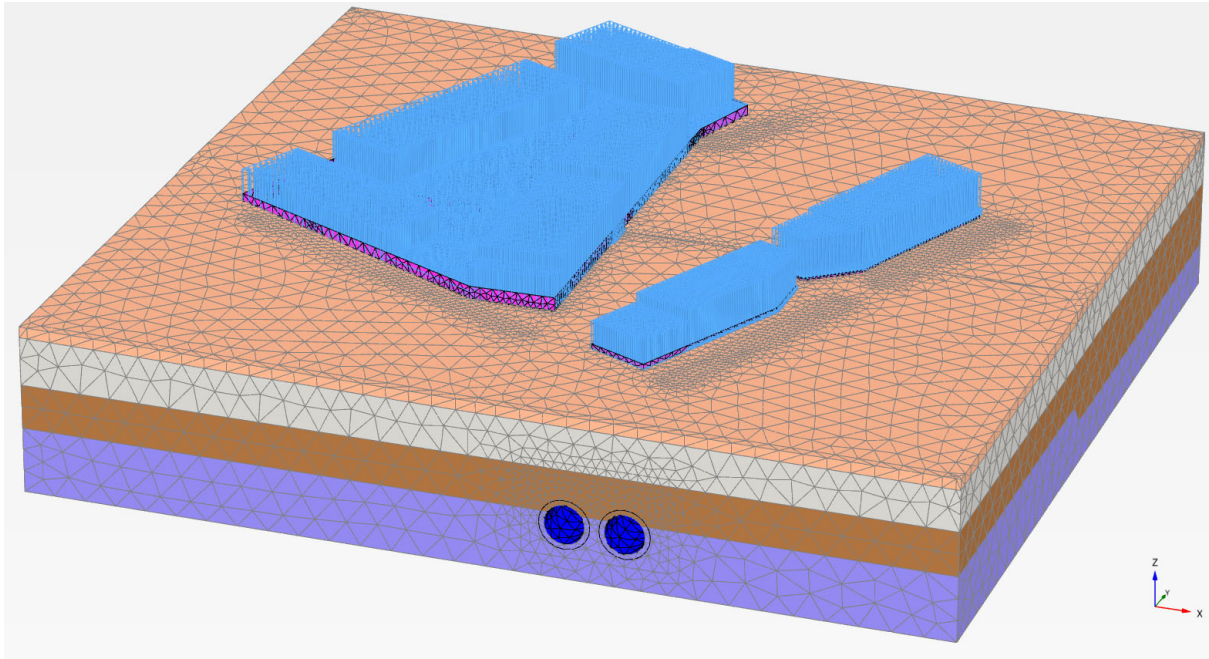


Figure 7-16: 3D Plaxis Model showing Design Situation DS-5

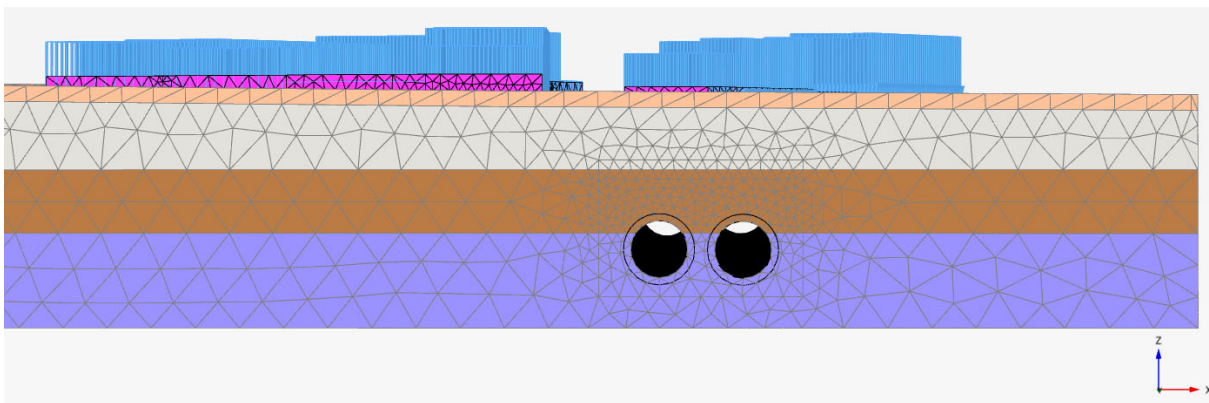


Figure 7-17: 3D Plaxis Model showing the Dublin Port Tunnels model (southern side of site)

7.9 Plaxis 3D Results

This section of the report presents the results of the Plaxis 3D analysis which includes the increase in total stress on the tunnel, tunnel distortion such as ovalisation/squatting (i.e. the increase (ovalisation) or decrease (squatting) of the tunnel lining diameter from its original state) and the axial forces, shear forces and bending moments in the transverse and longitudinal direction.

The results of the Plaxis 3D analysis are presented in this section for Design Situations DS-1 to DS-5 for both the Hardening Soil model with small-strain stiffness (HSS) and Mohr Coulomb (MC) material models. These design situations cover the worst combination of excavation and loading for the entire development. The results presented in this section represent the worst possible effect on the tunnels for these design situations.

A sensitivity analysis of the model was carried out for undrained conditions and for a reduced global water level of 5mbgl. The results indicated that the more conservative results were determined using the drained condition with a shallow water level (i.e. 1mbgl). These more conservative results are presented and discussed in this report.

Individual plots of the Plaxis 3D results (i.e. axial forces, shear forces and bending moments and displacements) are included in Appendix C for both the HSS and MC models. A comparison of the HSS and MC models is included in Appendix D.

The structural forces and bending moments at the connection of the TBM tunnels with the Pedestrian Cross Passage (PCP) have been extracted from the results when assessing the forces/bending moments in the lining of the TBM tunnels. This is because the joint at this connection is designed to take the forces and bending moments at this location, as can be seen on Figure 4-5 which shows the steel I-beam Section at the connection to the primary lining of the TBM tunnel sections. Therefore, the results at the connection would not be representative of those occurring within the lining of the TBM section. For this reason, the maximum/minimum values shown on the figures extracted from the model may not always reflect the values in the summary tables given in this section of the report.

The following is a summary of the output results from the Plaxis 3D program that are presented in this report:

1. Change in total stress on the tunnel lining crown and invert are presented on Table 7-6 to Table 7-9, for the northbound and southbound tunnels, respectively and for the MC & HSS material models. The change in total stress along the crown and invert of the north and southbound tunnels are plotted in Appendix C on Figure C1 to C4 for the MC & Figure C19 & C22 for the HSS material models.
2. The change in total stress on the crown of the Pedestrian Cross Passage is summarised on Table 7-10 for the MC & HSS material models.
3. A summary of the characteristic bending moments and axial forces on the tunnels is presented on Table 7-11 to Table 7-14 for the MC & HSS material models. Plots of the axial forces and bending moments along the length of the tunnels are plotted in Appendix C on Figure C13 to C16 for the MC & Figure C31 to C34 for the HSS material models. The orientation of the principal axes is shown on Figure 7-18.
4. A summary of the characteristic shear forces on the tunnels is presented on Table 7-11 to Table 7-14 for the MC & HSS material models. Plots of the shear forces along the length of the tunnels are plotted in Appendix C on Figure C17 to C18 for the MC & and Figure C31 to C34 for the HSS material models. The orientation of the principal axes is shown on Figure 7-18.

A summary of the horizontal and vertical deformations of the tunnels are presented on Table 7-15 to Table 7-18 for the northbound and southbound tunnels, respectively. The horizontal and vertical deformations along the tunnel crown and along the eastern and western edges of the tunnels are plotted in Appendix C on Figure C5 to C12 for the MC and on Figure C35 to C36 for the HSS material model.

The most onerous results shown on these tables are **highlighted in red**. The orientation of the principal axes along tunnel plate are shown on Figure 7-18.

Note: The horizontal and vertical displacements at the tunnel invert were < 0.3mm which are negligible, therefore, these results were not plotted in the report.

Results from the model have been extracted and are shown on Figure 7-22 to Figure 7-31. The most onerous results are typically shown, however, some other results are also shown for information. The following is a summary of the figures showing the results presented in this section:

- Figure 7-23: Max Axial Force on DPTs (N1 i.e. Longitudinal Force) - DS-2 NB -MC
- Figure 7-24: Max Axial Force on DPTs (N2 i.e. Hoop Force)
- Figure 7-25: Max Bending Moment on DPTs (M11 i.e. Longitudinally along tunnel)
- Figure 7-26: Max Bending Moment on DPTs (M22 i.e. transversely across tunnel)
- Figure 7-27: Max Shear Force on DPTs (Q23 i.e. Transversely across tunnel)
- Figure 7-28: Max Shear Force on DPTs (Q13 i.e. Longitudinally along tunnel)
- Figure 7-19: Min. Vertical Tunnel Displacements (settlement)
- Figure 7-20: Max. Vertical Tunnel Displacements (heave)
- Figure 7-21: Min. Horizontal Tunnel Displacements
- Figure 7-22: Max. Horizontal Tunnel Displacements
- Figure 7-29: Vertical Total Stress (Initial conditions with Tunnels installed, at $y = 71$ i.e. max increase in stress on tunnels)
- Figure 7-30: Vertical Total Stress @ max change in total stress on tunnel lining i.e. at $y=71$ (DS-2 SB MC)
- Figure 7-31: Location of max change in total stress on tunnel lining i.e. $y = 71.0$ (DS-2 SB MC) – Section A-A

Table 7-6: Change in Total Stress on the tunnel lining crown & invert (NB MC)

Design Situations	Total Overburden Pressure on Tunnels pre-construction (kPa)		Total Overburden Pressure Post Construction (kPa)		Change in Total Stress (kPa) Note 1		Change in Stress as a % of Total Overburden Pressure Pre-Construction	
	Crown	Invert	Crown	Invert	Crown	Invert	Crown	Invert
DS-1	555	417	540	424	-15.0	-6.1	-2.7%	-1.5%
DS-2	553	418	566	431	12.7	13.8	2.3%	3.3%
DS-3	555	418	564	428	8.4	10.8	1.5%	2.6%
DS-4	553	524	534	510	-18.6	-14.1	-3.4%	-2.7%
DS-5	553	418	565	432	12.4	14.6	2.2%	3.5%

Notes

1 + indicates an increase in stress

2 ie current stress on DPTs

Table 7-7: Change in Total Stress on the tunnel lining crown & invert (NB HSS)

Design Situations	Total Overburden Pressure on Tunnels pre-construction (kPa)		Total Overburden Pressure Post Construction (kPa)		Change in Total Stress (kPa) Note 1		Change in Stress as a % of Total Overburden Pressure Pre-Construction	
	Crown	Invert	Crown	Invert	Crown	Invert	Crown	Invert
DS-1	452	404	448	398	-3.5	-1.9	-0.8%	-0.5%
DS-2	445	404	450	379	5.0	11.3	1.1%	2.8%
DS-3	491	404	487	376	1.9	8.0	0.4%	2.0%
DS-4	472	404	465	375	-6.7	-8.1	-1.4%	-2.0%
DS-5	445	404	449	378	4.6	10.3	1.0%	2.5%

Notes

1 + indicates an increase in stress

2 ie current stress on DPTs

Table 7-8: Change in Total Stress on the tunnel lining crown & invert (SB MC)

Design Situations	Total Overburden Pressure on Tunnels pre-construction (kPa)		Total Overburden Pressure Post Construction (kPa)		Change in Total Stress (kPa) Note 1		Change in Stress as a % of Total Overburden Pressure Pre-Construction	
	Crown	Invert	Crown	Invert	Crown	Invert	Crown	Invert
DS-1	555	429	536	436	-19.2	-3.6	-3.5%	-0.8%
DS-2	555	413	574	422	19.3	8.9	3.5%	2.2%
DS-3	555	413	570	420	15.3	7.0	2.8%	1.7%
DS-4	555	403	531	411	-23.5	-6.9	-4.2%	-1.7%
DS-5	555	413	574	422	19.1	9.0	3.4%	2.2%

Notes

1 + indicates an increase in stress

2 ie current stress on DPTs

Table 7-9: Change in Total Stress on the tunnel lining crown & invert (SB HSS)

Design Situations	Total Overburden Pressure on Tunnels pre-construction (kPa)		Total Overburden Pressure Post Construction (kPa)		Change in Total Stress (kPa) Note 1		Change in Stress as a % of Total Overburden Pressure Pre-Construction	
	Crown	Invert	Crown	Invert	Crown	Invert	Crown	Invert
DS-1	446	383	442	394	-3.7	-1.8	-0.8%	-0.5%
DS-2	448	383	454	394	6.0	11.1	1.3%	2.9%
DS-3	498	383	495	391	2.7	8.4	0.5%	2.2%
DS-4	445	383	440	393	-5.6	-4.8	-1.3%	-1.3%
DS-5	448	383	454	394	5.4	10.4	1.2%	2.7%

Notes

1 + indicates an increase in stress

2 ie current stress on DPTs

Table 7-10: Change in Total Stress on the crown of the Pedestrian Cross Passage (MC & HSS)

Design Situation	Mohr Coulomb (MC)	HSS
DS-1	-17.3	-2.6
DS-2	16.0	11.3
DS-3	14.0	6.9
DS-4	-18.0	-4.0
DS-5	16.0	11.1

Notes
1 + indicates an increase in stress

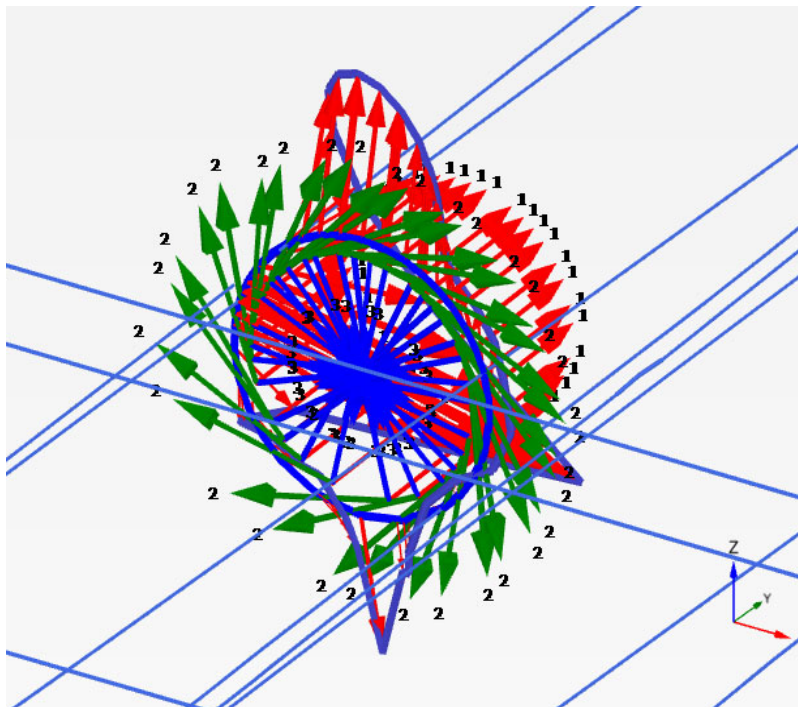


Figure 7-18: Orientation of axes along tunnel plate

Table 7-11: Summary of the characteristic bending moments and axial and shear forces on the tunnels (NB MC)

Design Situations		N_1[kN/m]	N_2[kN/m]	M_11[kNm/m]	M_22[kNm/m]	Q_23[kN/m]	Q_13[kN/m]	Q_12[kN/m]
Tunnels Constructed	min	53	1052	-70	-138	-189	-94	-534
	max	678	2651	50	172	225	143	557
DS-1	min	53	1094	-70	-141	-198	-94	-538
	max	679	2648	50	173	240	143	550
DS-2	min	54	1133	-69	-136	-180	-93	-526
	max	678	2656	49	173	222	143	555
DS-3	min	57	1132	-68	-126	-187	-87	-542
	max	677	2635	48	170	221	138	567
DS-4	min	55	1128	-69	-132	-201	-87	-544
	max	677	2626	49	170	237	138	557
DS-5	min	58	1138	-69	-135	-181	-93	-530
	max	677	2655	49	172	221	141	549
	min	53	1052	-70	-141	-201	-94	-544
	max	679	2656	50	173	240	143	567

Note: bending moments and axial forces taken along the full length of the tunnel shown on the model

'+ ive is compression

Table 7-12: Summary of the characteristic bending moments and axial and shear forces on the tunnels (NB HSS)

Design Situations		N_1[kN/m]	N_2[kN/m]	M_11[kNm/m]	M_22[kNm/m]	Q_23[kN/m]	Q_13[kN/m]	Q_12[kN/m]
Tunnels Constructed	min	171	1065	-42	-68	-117	-39	-204
	max	442	2075	27	61	116	72	233
DS-1	min	158	1059	-42	-68	-117	-39	-202
	max	435	2072	27	61	114	72	229
DS-2	min	156	1078	-41	-68	-117	-40	-204
	max	441	2079	27	61	114	72	227
DS-3	min	154	1074	-41	-68	-118	-38	-207
	max	439	2066	27	61	115	70	220
DS-4	min	159	1055	-41	-69	-117	-39	-203
	max	435	2059	27	61	114	70	224
DS-5	min	155	1078	-41	-68	-117	-39	-206
	max	441	2077	27	61	114	72	226
	min	154	1055	-42	-69	-118	-40	-207
	max	442	2079	27	61	116	72	233

Note: bending moments and axial forces taken along the full length of the tunnel shown on the model

'+ ive is compression

Table 7-13: Summary of the characteristic bending moments and axial and shear forces on the tunnels (SB MC)

Design Situations		N_1[kN/m]	N_2[kN/m]	M_11[kNm/m]	M_22[kNm/m]	Q_23[kN/m]	Q_13[kN/m]	Q_12[kN/m]
Tunnels Constructed	min	31	1037	-71	-130	-218	-80	-580
	max	669	2624	47	175	232	140	514
DS-1	min	28	1128	-71	-135	-221	-79	-588
	max	674	2617	47	180	250	139	515
DS-2	min	32	1150	-70	-120	-212	-87	-547
	max	661	2643	48	165	215	140	501
DS-3	min	23	1151	-71	-119	-212	-87	-558
	max	659	2640	49	164	211	140	498
DS-4	min	23	1145	-71	-133	-222	-79	-597
	max	672	2612	48	178	248	139	507
DS-5	min	32	1150	-70	-119	-209	-85	-545
	max	661	2643	48	163	213	138	496
	min	23	1037	-71	-135	-222	-87	-597
	max	674	2643	49	180	250	140	515

Note: bending moments and axial forces taken along the full length of the tunnel shown on the model

'+ ive is compression

Table 7-14: Summary of the characteristic bending moments and axial and shear forces on the tunnels (SB HSS)

Design Situations		N_1[kin/m]	N_2[kN/m]	M_11[kNm/m]	M_22[kNm/m]	Q_23[kN/m]	Q_13[kN/m]	Q_12[kN/m]
Tunnels Constructed	min	159	1031	-39	-75	-114	-37	-225
	max	439	2056	27	63	127	71	199
DS-1	min	149	1096	-39	-76	-113	-37	-223
	max	433	2052	27	63	127	70	197
DS-2	min	145	1118	-39	-74	-113	-37	-223
	max	439	2063	27	63	127	71	196
DS-3	min	143	1106	-39	-74	-114	-38	-227
	max	437	2058	27	63	127	72	196
DS-4	min	149	1093	-39	-76	-113	-37	-223
	max	432	2046	27	63	126	69	195
DS-5	min	145	1114	-39	-74	-113	-37	-224
	max	439	2062	27	63	127	71	196
	min	143	1031	-39	-76	-114	-38	-227
	max	439	2063	27	63	127	72	199

Note: bending moments and axial forces taken along the full length of the tunnel shown on the model

'+ ive is compression

Table 7-15: Change in horizontal and vertical deformations on the tunnels (NB MC)*

Design Situations	Vertical Displacement (mm)		Horizontal Displacement (mm)		Max Ovalisation Strain (%)
	min	max	min	max	
DS-1	0.0	0.9	0.0	0.3	0.008%
DS-2	-1.0	0.2	-0.6	0.1	0.009%
DS-3	-0.9	0.4	-2.3	0.0	0.021%
DS-4	0.0	1.0	-2.0	0.2	0.019%
DS-5	-1.0	0.2	-0.8	0.1	0.009%
	-1.0	1.0	-2.3	0.3	0.021%

Note: deformations taken along the full length of the tunnel shown on the model

*Calculated as change in displacements between crown and invert (vertical displacement) or edges of tunnel (horizontal displacement)

Table 7-16: Change in horizontal and vertical deformations on the tunnels (NB HSS)*

Design Situations	Vertical Displacement (mm)		Horizontal Displacement (mm)		Max Ovalisation Strain (%)
	min	max	min	max	
DS-1	0.0	0.2	0.0	0.2	0.002%
DS-2	-0.4	0.0	-0.1	0.1	0.003%
DS-3	-0.2	0.1	-0.3	0.1	0.003%
DS-4	0.0	0.3	-0.3	0.2	0.003%
DS-5	-0.3	0.0	-0.1	0.1	0.003%
	-0.4	0.3	-0.3	0.2	0.003%

Note: deformations taken along the full length of the tunnel shown on the model

*Calculated as change in displacements between crown and invert (vertical displacement) or edges of tunnel (horizontal displacement)

Table 7-17: Change in horizontal and vertical deformations on the tunnels (SB MC)*

Design Situations	Vertical Displacement (mm)		Horizontal Displacement (mm)		Max Ovalisation Strain (%)
	min	max	min	max	
DS-1	0.0	1.5	-0.2	0.4	0.014%
DS-2	-1.6	0.0	-0.9	0.1	0.015%
DS-3	-1.6	0.1	-2.1	0.1	0.019%
DS-4	-0.5	1.6	-1.4	0.1	0.014%
DS-5	-1.6	0.0	-1.1	0.1	0.015%
	-1.6	1.6	-2.1	0.4	0.019%

Note: deformations taken along the full length of the tunnel shown on the model

*Calculated as change in displacements between crown and invert (vertical displacement) or edges of tunnel (horizontal displacement)

Table 7-18: Change in horizontal and vertical deformations on the tunnels (SB HSS)*

Design Situations	Vertical Displacement (mm)		Horizontal Displacement (mm)		Max Ovalisation Strain (%)
	min	max	min	max	
DS-1	0.0	0.3	-0.1	0.0	0.003%
DS-2	-0.5	0.0	-0.1	0.1	0.005%
DS-3	-0.4	0.0	-0.1	0.0	0.004%
DS-4	0.0	0.4	-0.1	0.0	0.004%
DS-5	-0.5	0.0	-0.1	0.0	0.005%
	-0.5	0.4	-0.1	0.1	0.005%

Note: deformations taken along the full length of the tunnel shown on the model

*Calculated as change in displacements between crown and invert (vertical displacement) or edges of tunnel (horizontal displacement)

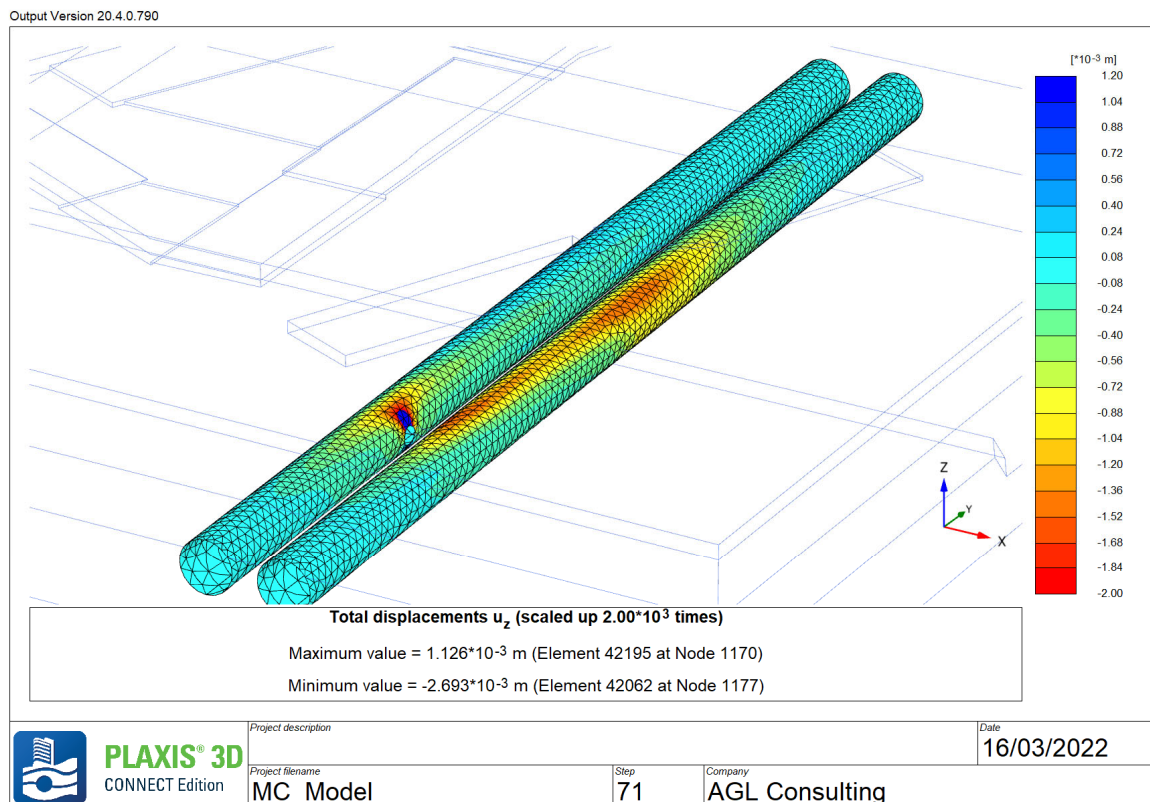


Figure 7-19: Min. Vertical Tunnel Displacements (settlement) (DS-5 SB MC)

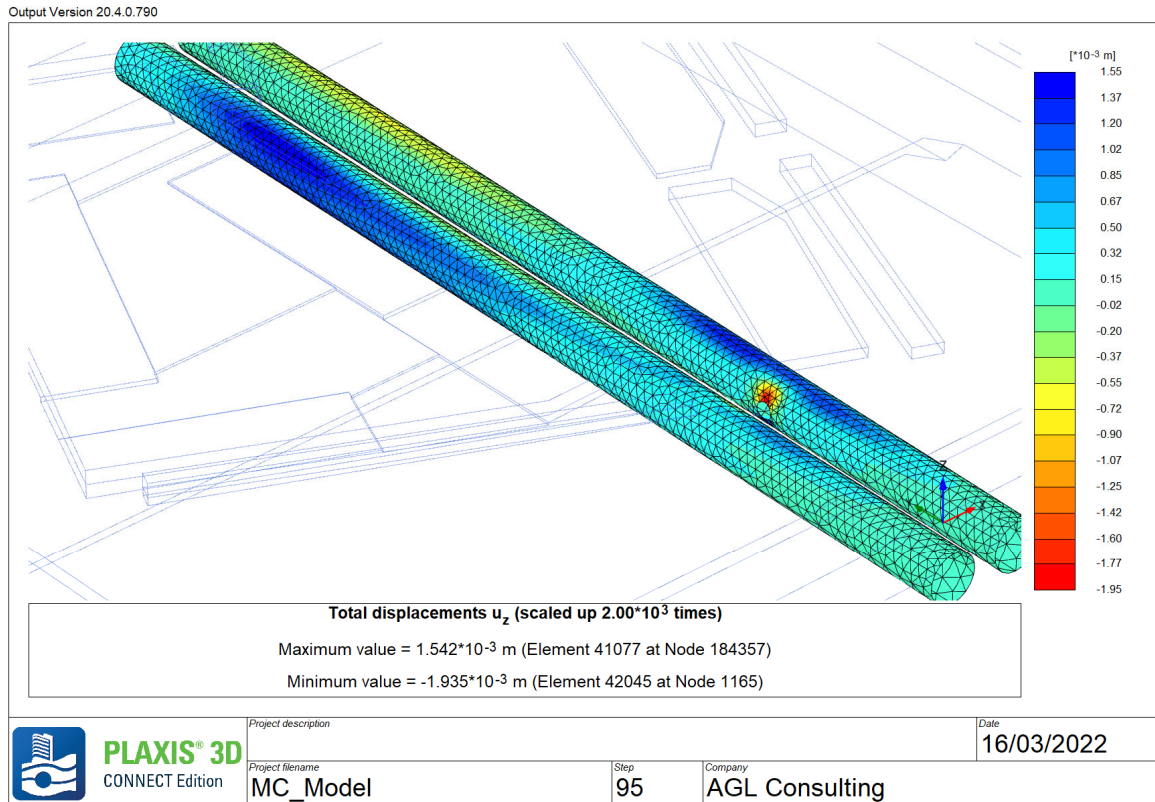


Figure 7-20: Max. Vertical Tunnel Displacements (heave) (DS-4 SB MC)

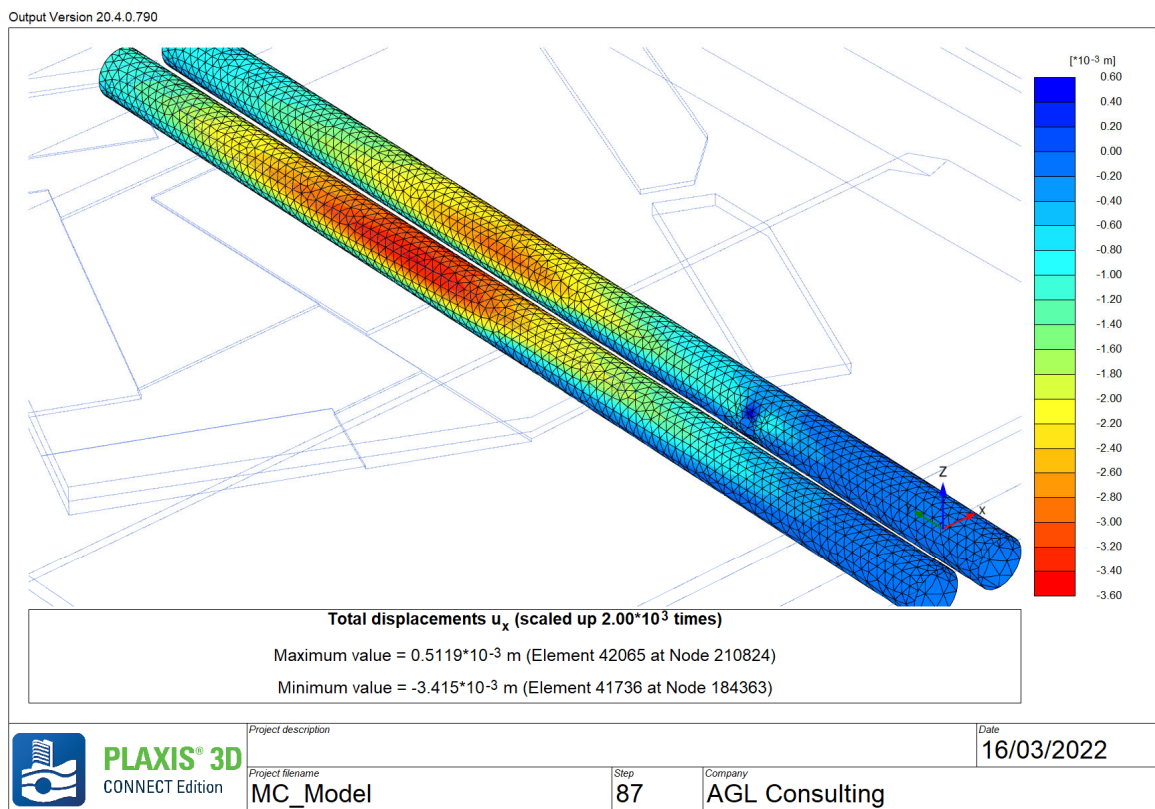


Figure 7-21: Min. Horizontal Tunnel Displacements (DS-3 NB MC)

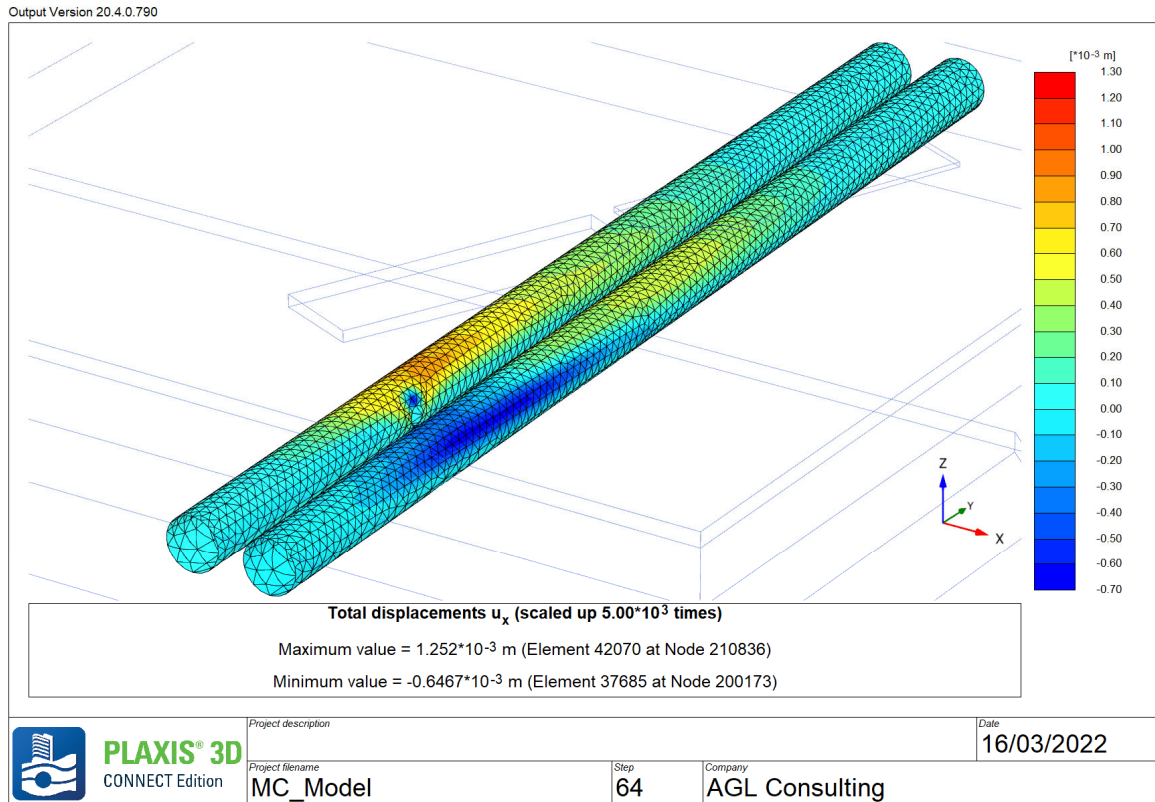


Figure 7-22: Max. Horizontal Tunnel Displacements (DS-1 SB MC)

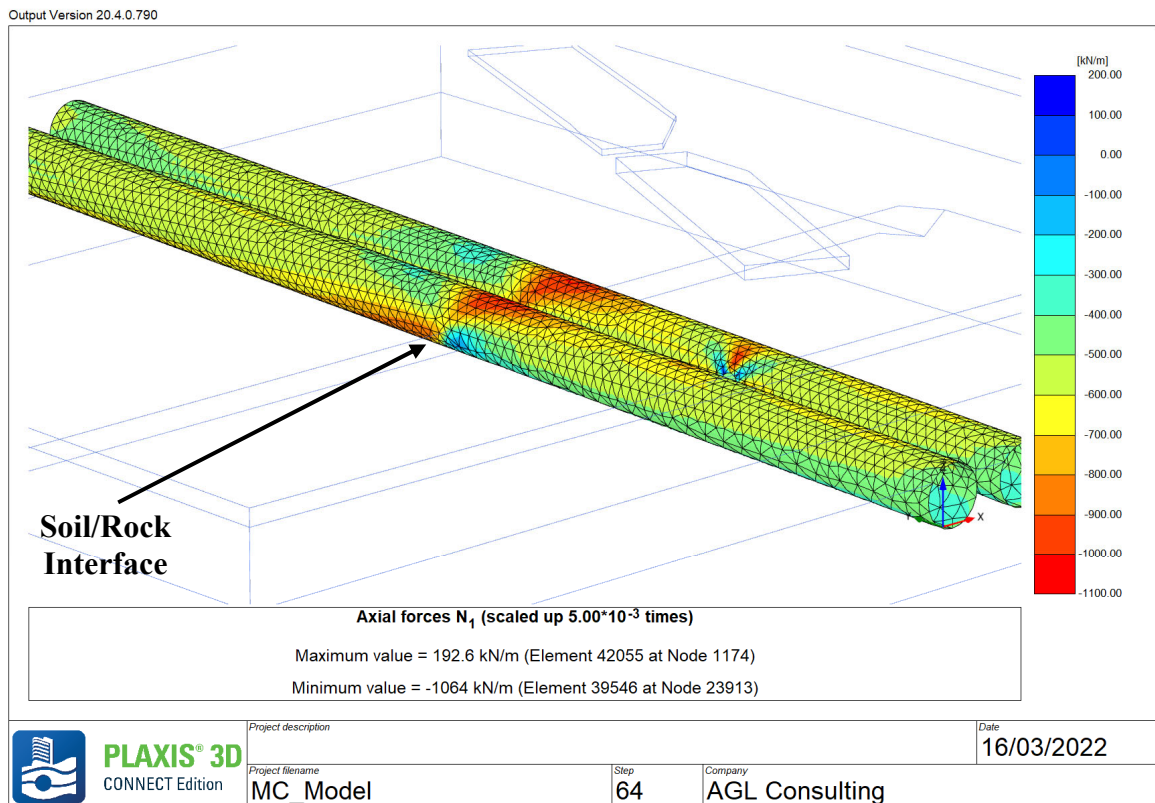


Figure 7-23: Max Axial Force on DPTs (N_1 i.e. Longitudinal Force) (DS-1 NB MC)

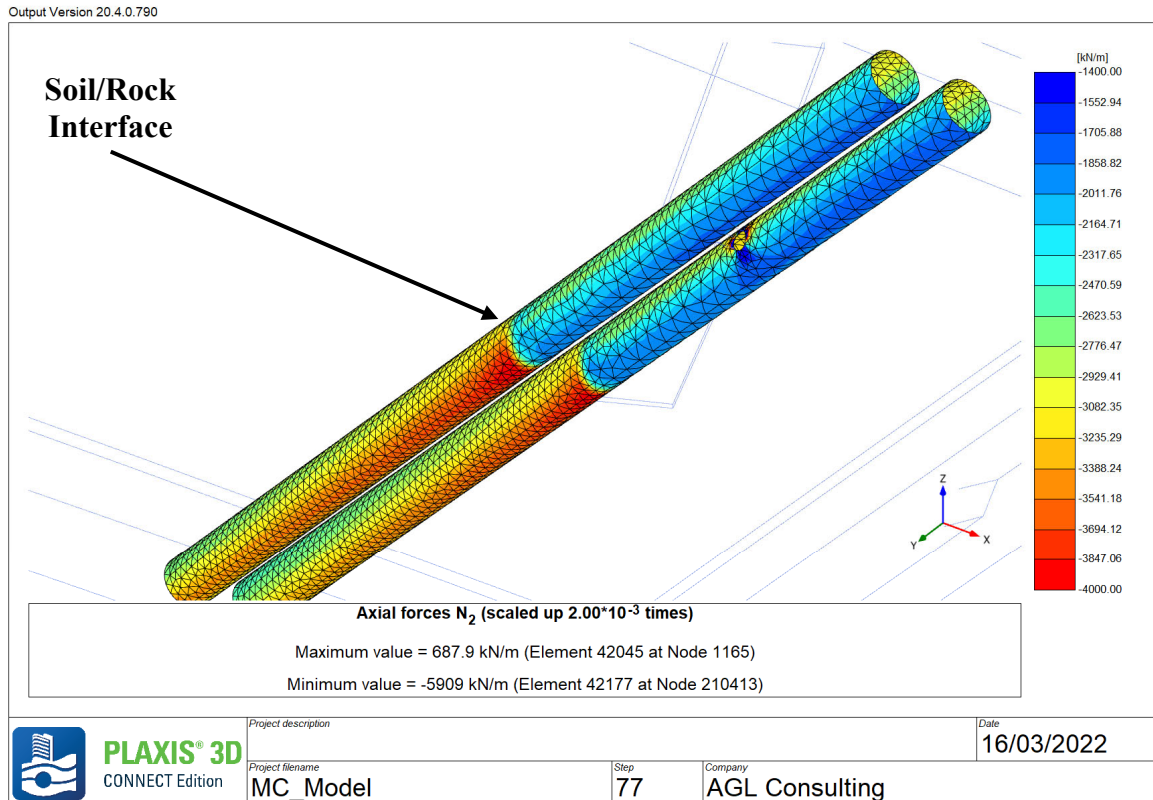


Figure 7-24: Max Axial Force on DPTs (N_2 i.e. Hoop Force) (DS-2 NB MC)

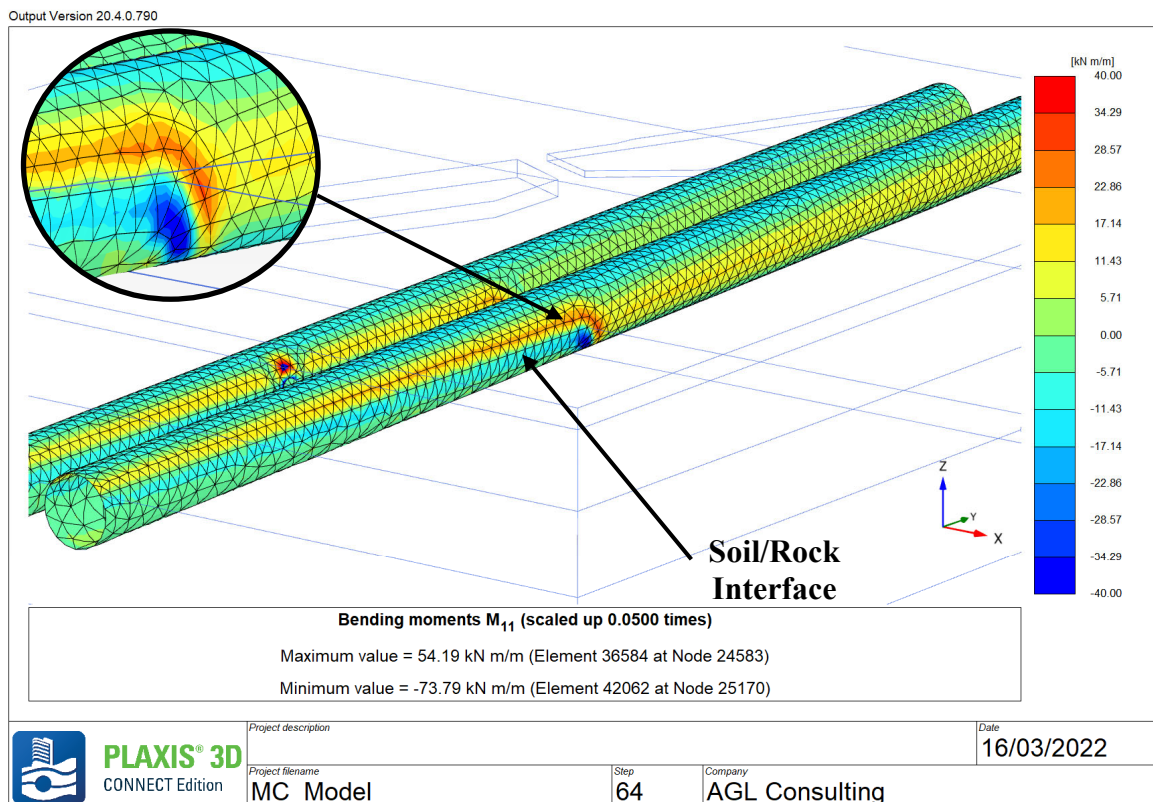


Figure 7-25: Max Bending Moment on DPTs (M_{11} i.e. Longitudinally along tunnel) (DS-1 SB MC)

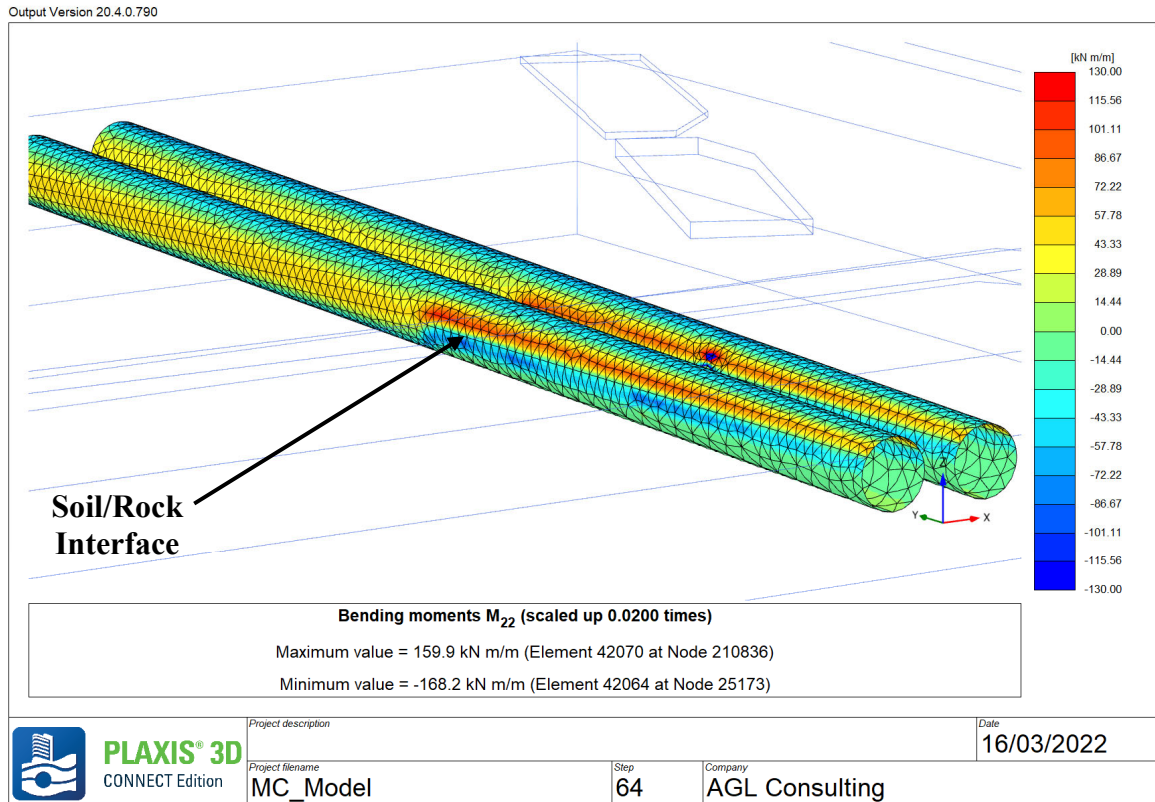


Figure 7-26: Max Bending Moment on DPTs (M_{22} i.e. transversely across tunnel) (DS-1 SB MC)

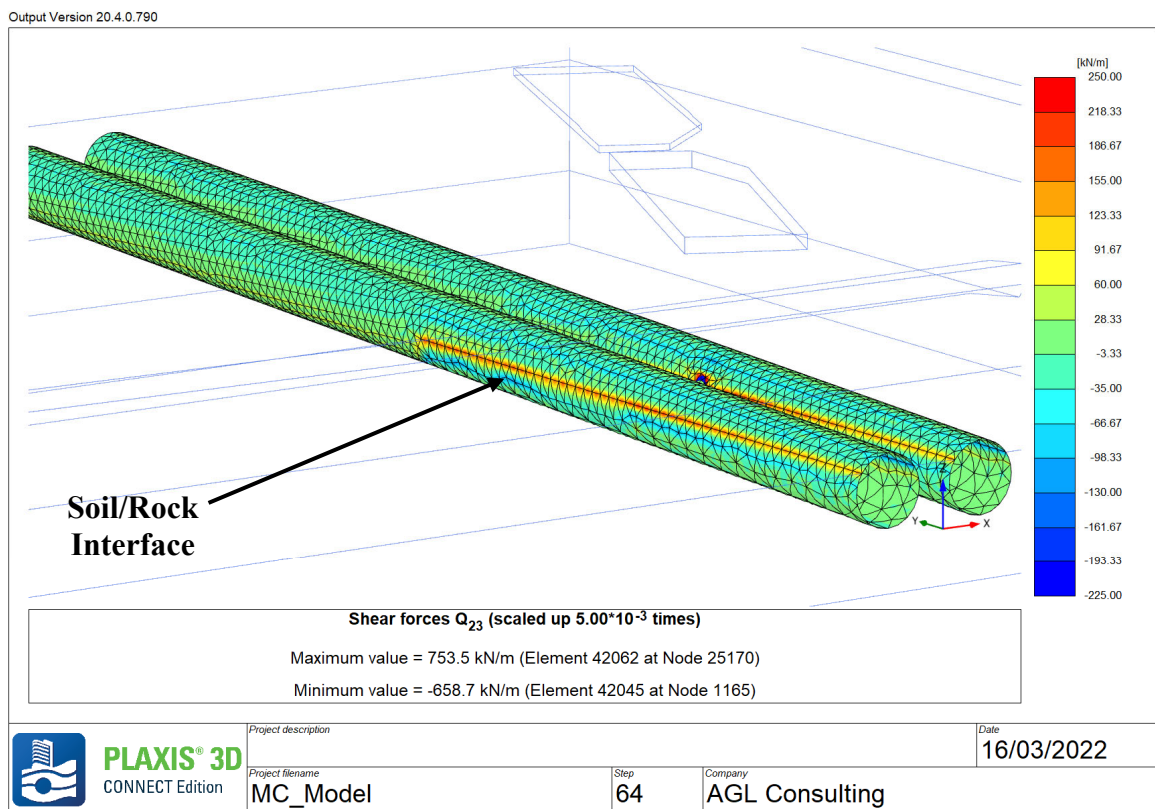


Figure 7-27: Max Shear Force on DPTs (Q_{23} i.e. Transversely across tunnel) (DS-1 SB - MC)

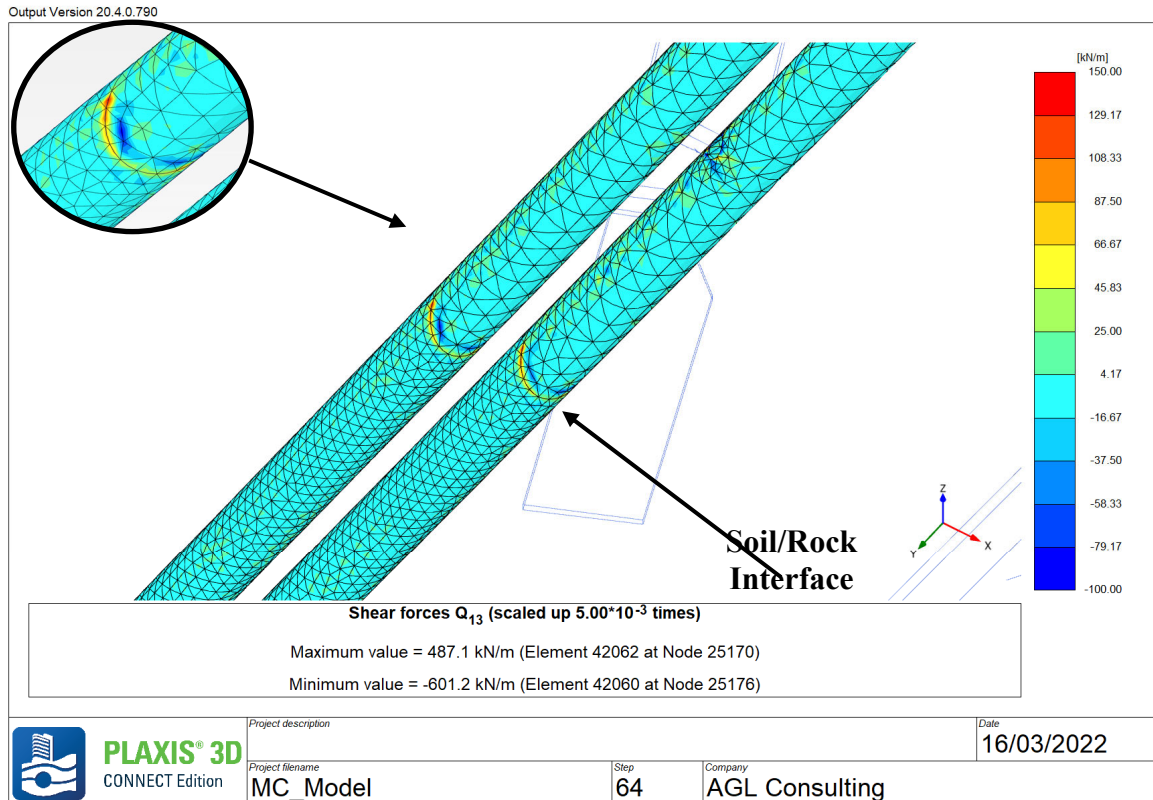


Figure 7-28: Max Shear Force on DPTs (Q_{13} i.e. Longitudinally along tunnel) (DS-1 NB MC)

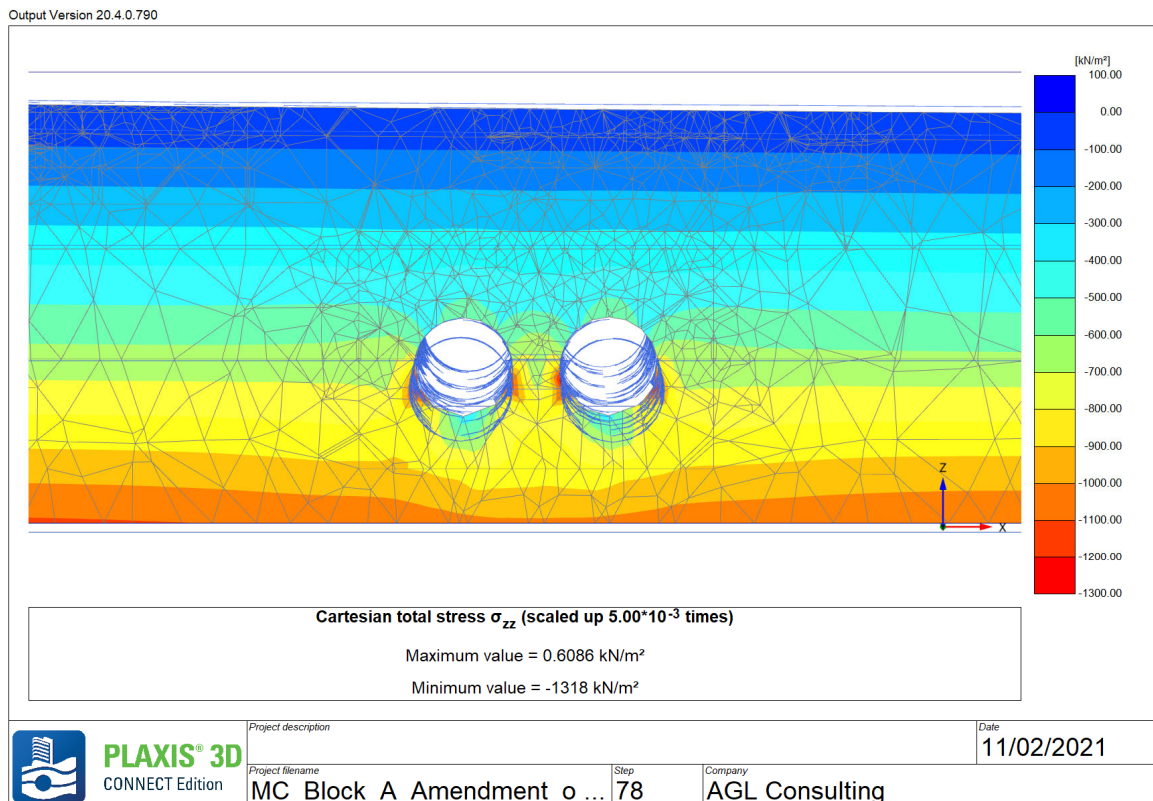


Figure 7-29: Vertical Total Stress (Initial conditions with Tunnels installed, at $y = 71$ i.e. max increase in stress on tunnels)

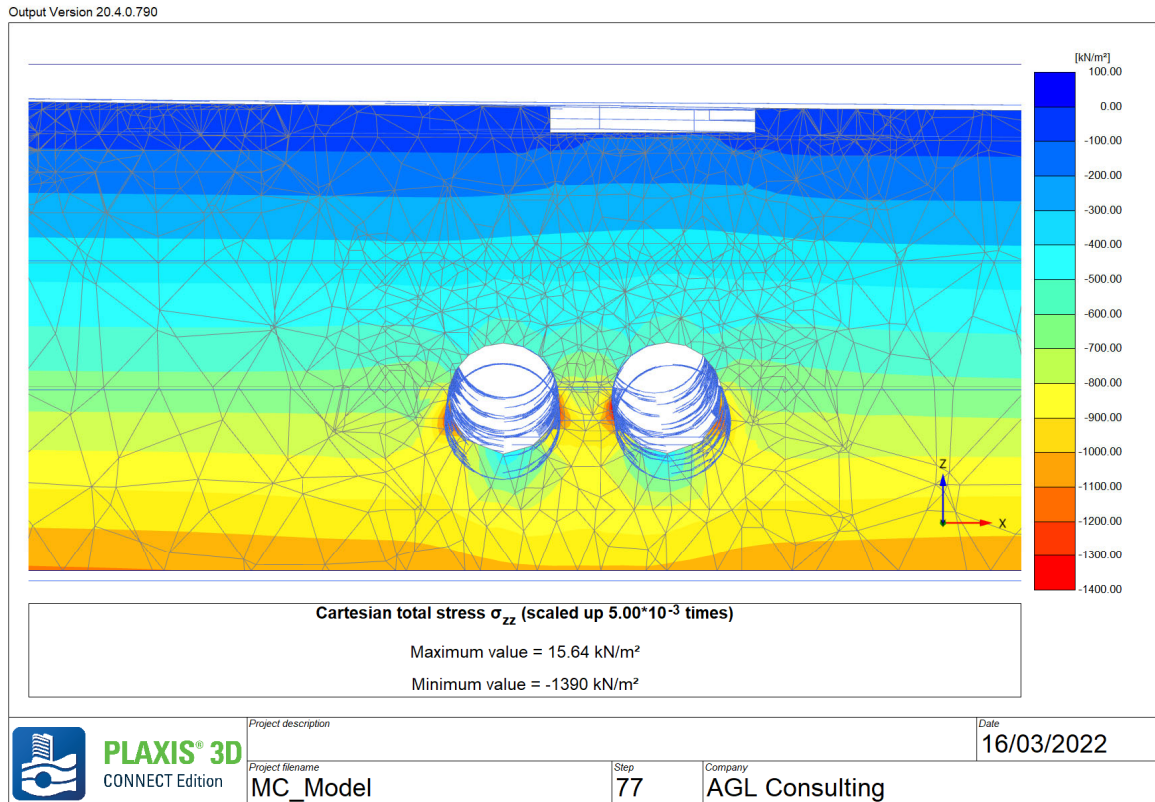


Figure 7-30: Vertical Total Stress @ max change in total stress on tunnel lining i.e. at $y=71$ (DS-2 SB MC)

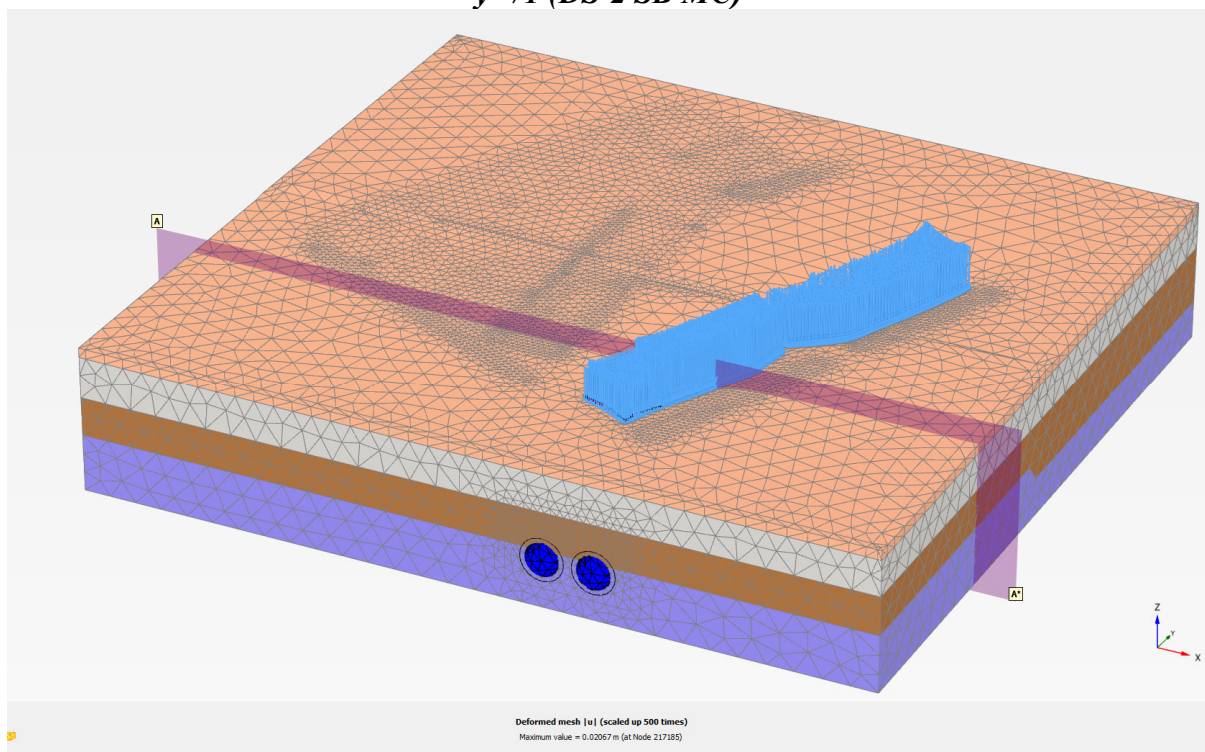


Figure 7-31: Location of max change in total stress on tunnel lining i.e. $y = 71.0$ (DS-2 SB MC) – Section A-A

7.10 Discussion

The results from the Plaxis 3D model are discussed in this section and a general discussion of the results is carried out. The structural assessment of the tunnel is given in Section 8.

- The impact of the development has been assessed using the Plaxis 3D software to enable the combined effect of the development on the Dublin Port Tunnels (DPTs) to be analysed.
- The Hardening Soil model with small-strain stiffness (HSS) and the Mohr Coulomb (MC) material models have been used to model the behaviour of the Boulder Clays.
- The HSS soil model available in the Plaxis program has been shown to correlate well with field measurements taken in the very stiff Dublin Boulder Clays which are prevalent throughout Dublin City (Lawler et. al, 2011). The material model allows for the small strain stiffness of the material to be modelled.
- A more conservative assessment of the impact of the development has also been carried out using Mohr Coulomb (MC) parameters. This material model assumes lower stiffness values for the Boulder Clays and does not have a function to model the small strain stiffness which is characteristic of Dublin Boulder Clays.
- The MC model is more onerous than the HSS model in all respects, i.e. axial force, bending moments, shear forces and vertical and horizontal displacements. This is considered to be due to the greater stiffness and the inclusion of the dilation parameter (3 degrees) in the HSS model.
- The HSS model indicates that there would be a significantly lower increase in stress on the tunnel crown (approx 6.0kPa for DS-2 SB) in comparison to the MC model (approx. 19.3kPa for DS-2 SB). As discussed in Appendix C, this is considered to be due to the arching effect being modelled in the HSS model which is re-distributing the vertical stresses around the tunnel. This is slightly more significant where the tunnel is partially within rock than when it is fully within Boulder Clay.
- The displacements in the MC model were consistently higher than those recorded in the HSS model. The maximum horizontal and vertical deformations in the MC model were 2.1mm (DS-3 SB), while those in the HSS model was 0.5mm (DS-5 SB).
- The axial forces, shear forces and bending moments on the tunnel are quite similar between the tunnel installation stage and the design situations DS-1 to DS-5 for both the HSS and MC material models. For example, the maximum increase in the axial force due to the development, was 9.9% in the longitudinal direction (N1) and approx. 1% in the transverse direction (N2) which corresponded to only 19kN/m. The maximum increase in the bending moment was 4.0% (M22) and in the shear force was 7.5% (Q23). These increases occurred predominantly in the MC material model.
- The transition of the tunnel into rock both in the longitudinal and transverse direction is evident from the forces and displacements shown on the Plaxis results on Figure 7-19 to Figure 7-22. The higher stiffness of the rock relative to the surrounding Boulder Clay, which gives rise to relatively higher displacements at these points, causes higher shear forces, axial forces and bending moments to occur at these transition points. As would be expected, this shear force is considerably reduced in the HSS model, due to the stiffer Young's modulus in the boulder clay giving lower ground movements. While these forces, bending moments and displacements are relatively higher, the impact of these have been assessed in Section 8 and are found to lie within the tunnel design limits for both the MC and HSS models.
- As mentioned in Section 7.9, the structural forces and bending moments at the connection of the TBM tunnels with the Pedestrian Cross Passage (PCP) have been extracted from the

results when assessing the forces/bending moments in the lining of the TBM tunnels. This is due to the different lining details provided at the connection, which as can be seen on Figure 4-5 and Figure 4-7 includes a steel I-beam around the opening of primary lining of the TBM tunnel. Therefore, the forces/bending moments at the opening are not relevant to the standard section details of the tunnel lining.

- The maximum increase in the vertical stress on the Pedestrian Cross Passage is 16.0kPa for the Mohr-Coulomb model and 8.3kPa for the HSS model.

8 STRUCTURAL ASSESSMENT ON TUNNEL LINING

8.1 Change in Vertical Total Stress on the Tunnel Lining

Section 2.2 of the TII document *Guidance Notes for Developers, The assessment of surface and sub-surface developments in the vicinity of the Dublin Port Tunnel* states the following:

- *“Surcharge Loading: The NRA requires the developer to demonstrate that a development does not incur a surcharge loading on the tunnel in excess of 22.5kNm² either during construction or at completion. Cognisance must be taken of any surcharge loading at depth due to anchors or piles.*
- *Unloading: The NRA requires the developer to demonstrate that the method and sequencing of construction of the development minimises or eliminates the potential for tunnel deformation”*

The change in the vertical total stress on the tunnel lining was determined using the 3D Plaxis finite element analysis program and the results are presented on Table 7-6 and Table 7-9, for the northbound and southbound tunnels, respectively. The results indicate that the surcharge loading on the tunnel does not exceed 22.5kPa and is therefore, within the tunnel design limits.

The maximum increase in stress on the tunnel lining is calculated to be 19.3kPa for Design Situation, DS-2 for the Mohr Coulomb (MC) material model, and the location of this stress is below the centre of Block G on the southbound tunnel. The total overburden pressure on the tunnels prior to construction on the site is calculated by the 3D Plaxis program to be 555kPa, therefore, the maximum change in stress due to the construction of the development as a percentage of the pre-construction total stress currently on the tunnels is 3.5%. This is a relatively low percentage increase in the stress on the tunnel lining, particularly considering the magnitude of the total stress currently on the tunnel.

The maximum increase in vertical total stress on the tunnel lining from the HSS model was 6.0kPa (DS-2 SB) which is significantly lower than that recorded by the MC material model. As discussed in Appendix C, this is considered to be due to the arching effect being modelled in the HSS model which is re-distributing the applied vertical stresses around the tunnel. The MC material model is a conservative assessment of the behaviour of the boulder clay due to the applied load, however, the HSS model has been shown in publications (eg. Lawlor et al., 2011) to closely model the behaviour of the boulder clays, therefore, this may provide a more accurate model of the behaviour of the boulder clay due to the development.

8.2 Tunnel Lining Bending Moments and Axial forces

8.2.1 Transverse Joints

The design bending moments (M_{22}) and axial forces (N_2) calculated in the Plaxis 3D program are shown on Figure 8-1 to Figure 8-4 for Design Situations DS-1 to DS-5 along with the design envelope for the primary lining along the transverse direction. Conservatively and for simplicity, it has been assumed in this analysis that the bending moments are due to variable unfavourable loads with a partial factor of 1.5 applied. A partial factor of 1 has been assigned to the axial forces as these are favourable. The results indicate that the combined design axial forces and bending moments plot within the N-M plot, and are therefore, acceptable. The N-M interaction plot along the transverse direction was extracted from the calculations provided by Haswell Consulting Engineers (document No. CA_HA_BT_C11_54026_02_O_BORED_LINING_CALC).

The results shown on Figure 8-1 to Figure 8-4 and summarised on Table 7-10 to Table 7-13 show that the change in the axial forces and bending moments from the current tunnel

conditions is relatively low. The max. change in the axial forces represents 9.9% increase from the current loads on the tunnels. Similarly, the maximum change in the bending moments represents a 4.0% increase. Both of these occur in the MC material model. These are considered quite low relative to the current loads and bending moments on the tunnels.

The tunnel lining remains in compression in all of the design situations, therefore, there are no tension forces on the tunnel lining in the transverse direction.

As can be seen from the results, the axial forces and bending moments on the tunnel lining from the HSS model were significantly lower than that recorded by the MC material model. As discussed in Appendix C, this is considered to be due to the arching effect being modelled in the HSS model which is re-distributing the vertical stresses around the tunnel.

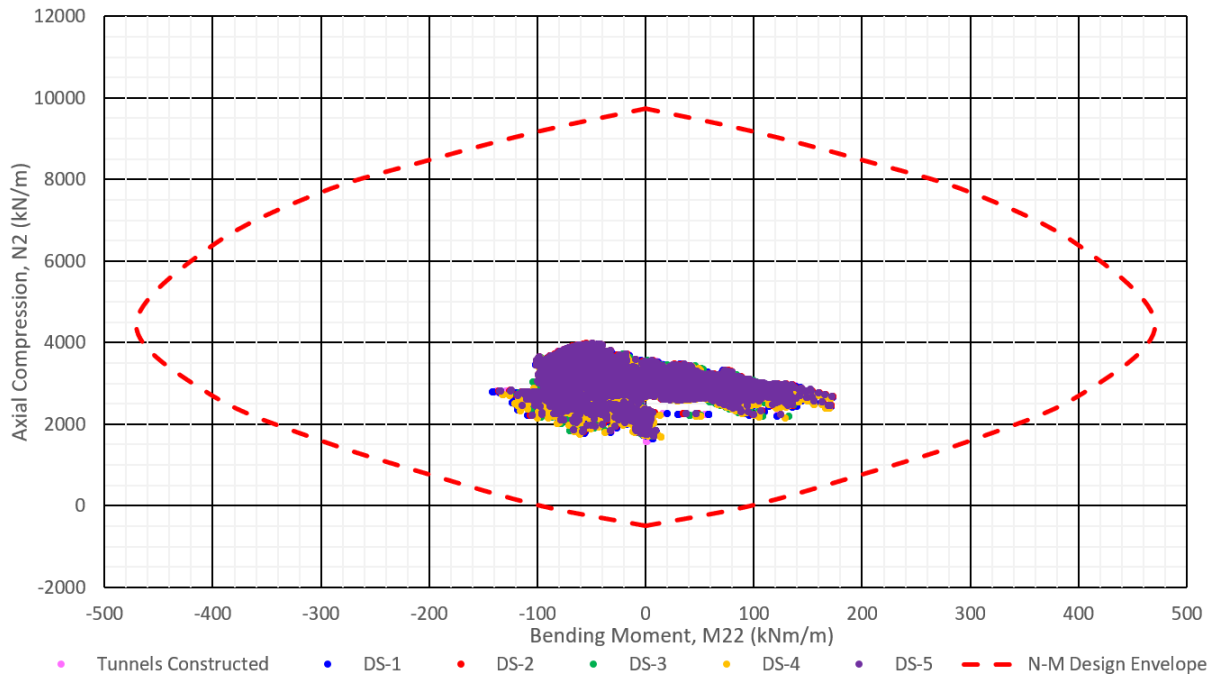


Figure 8-1: Design N-M Interaction Chart for tunnel lining along transverse direction with Plaxis 3D results plotted - MC NB

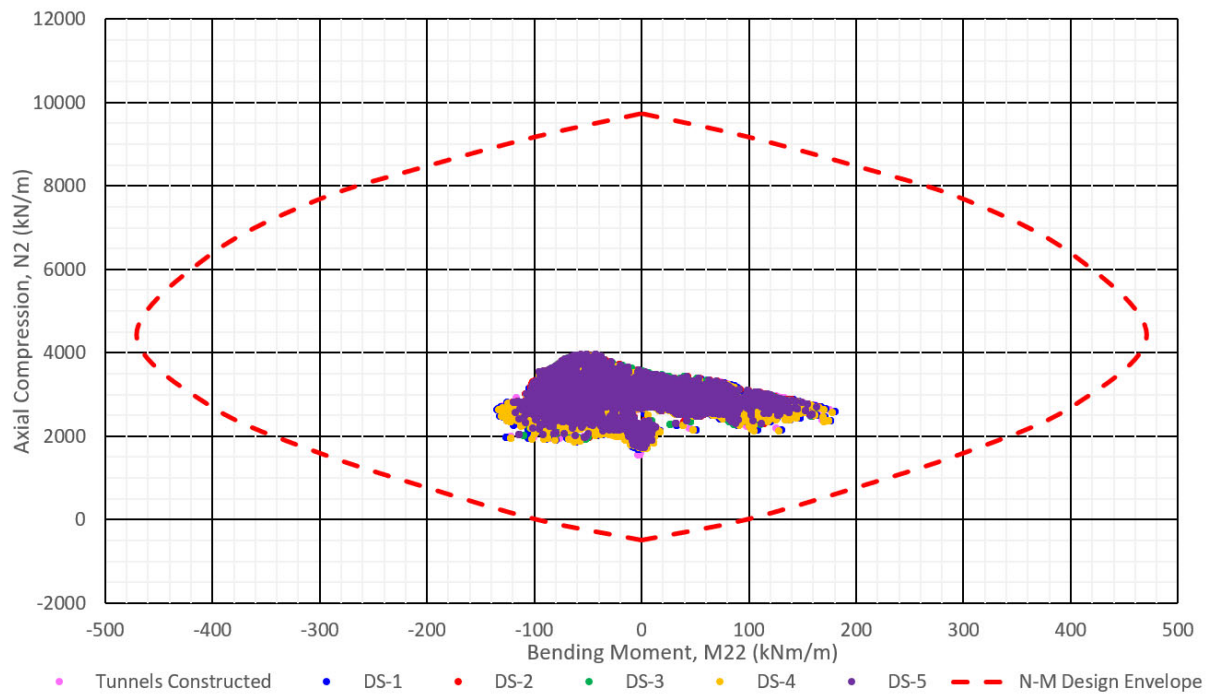


Figure 8-2: Design N-M Interaction Chart for tunnel lining along transverse direction with Plaxis 3D results plotted - MC SB

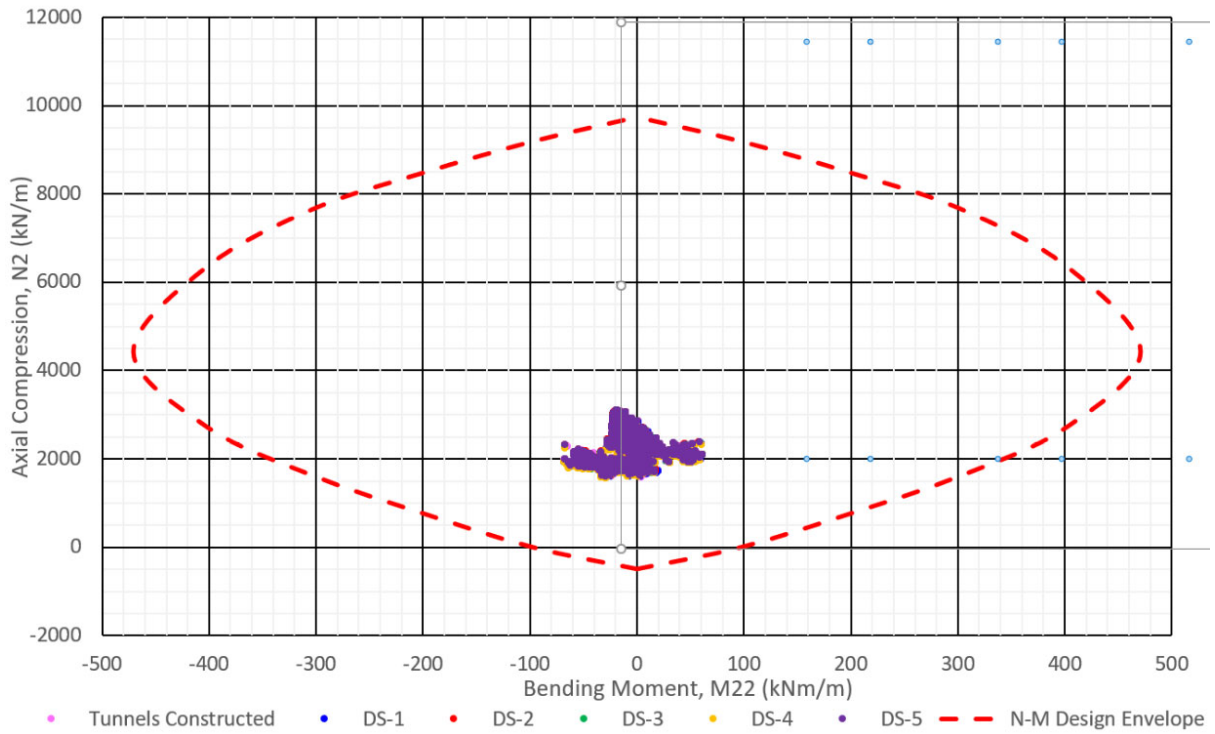


Figure 8-3: Design N-M Interaction Chart for tunnel lining along transverse direction with Plaxis 3D results plotted - HSS NB

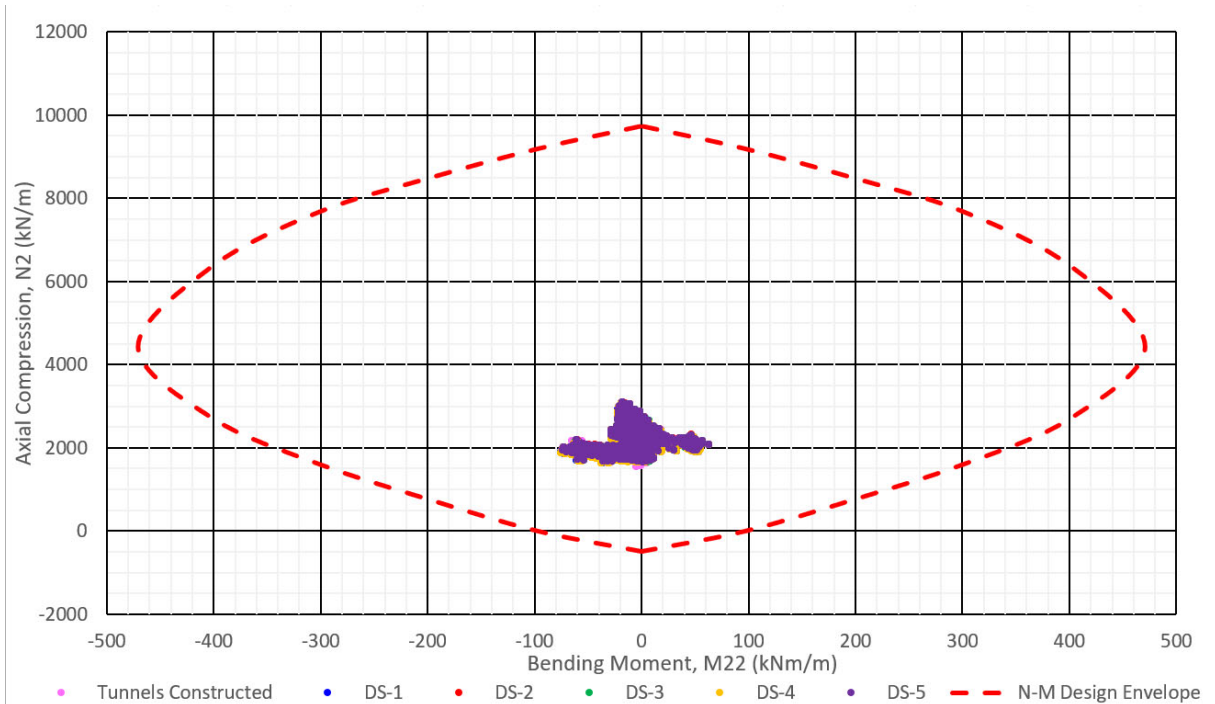


Figure 8-4: Design N-M Interaction Chart for tunnel lining along transverse direction with Plaxis 3D results plotted - HSS SB

8.2.2 Longitudinal Joints

The design bending moments (M_{11}) and axial forces (N_1) calculated in the Plaxis 3D program are shown on Figure 8-5 to Figure 8-8 for Design Situations DS-1 to DS-5 along with the design envelope for the primary lining along the longitudinal direction. Conservatively and for simplicity, it has been assumed in this analysis that the bending moments are due to variable unfavourable loads with a partial factor of 1.5 applied. A partial factor of 1 has been assigned to the axial forces as these are favourable. The results indicate that the combined design axial forces and bending moments plot within the N-M plot, and are therefore, acceptable.

The N-M interaction plot along the longitudinal direction was determined by AGL using the Adsec software using the reinforcement arrangement in the longitudinal direction shown on the as built tunnel drawing No. DR/HA/BT/C11/41013/08/X provided by TII. The longitudinal reinforcement comprises 2 No. rows of 10mm diameter U-bars with cover of 35mm and spacing of 200mm over the 350mm thick primary tunnel lining.

The results shown on Figure 8-5 to Figure 8-8 and summarised on Table 7-11 to Table 7-14 show that the change in the axial forces and bending moments is relatively low. The max. change in the axial forces represents 1.0% increase from the current loads on the tunnels. Similarly, the maximum change in the bending moments represents a 1.0% increase. These are considered quite low relative to the current loads and bending moments on the tunnels.

The tunnel lining remains in compression in all of the design situations, therefore, there are no tension forces on the tunnel lining and connection bolts in the longitudinal direction.

As can be seen from the results, the axial forces and bending moments on the tunnel lining from the HSS model were lower than that recorded by the MC material model. As discussed in Appendix C, this is considered to be due to the arching effect being modelled in the HSS model which is re-distributing the vertical stresses around the tunnel.

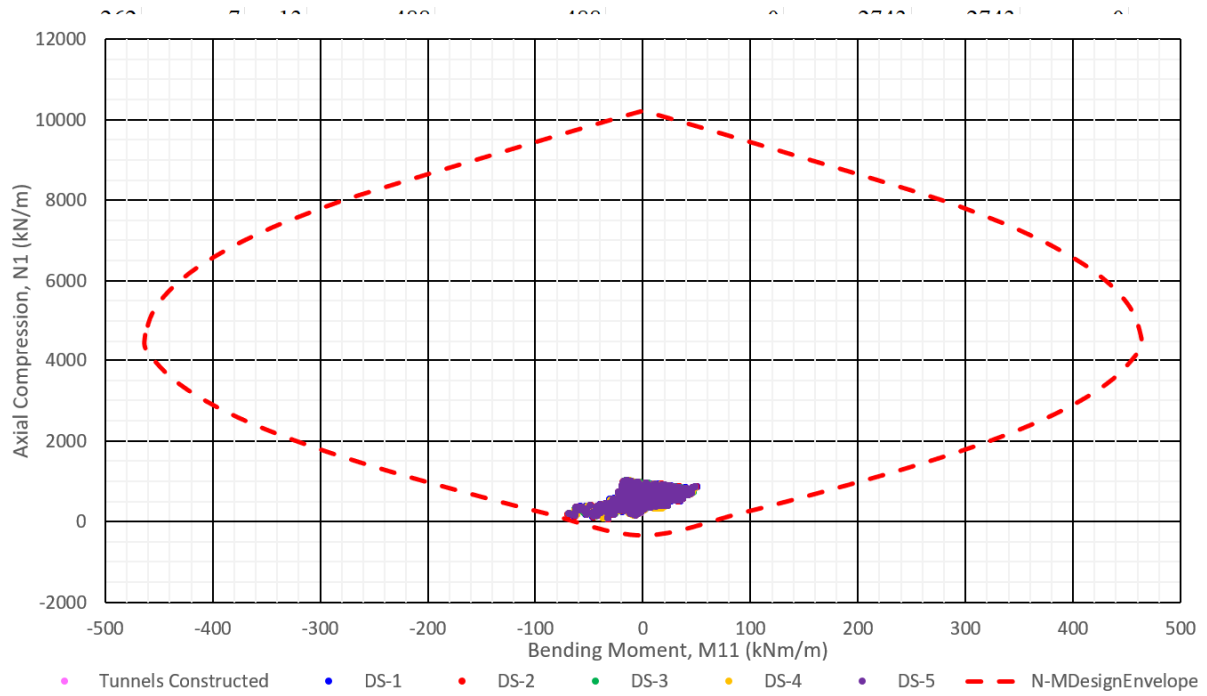


Figure 8-5: Design N-M Interaction Chart for tunnel lining along longitudinal direction with Plaxis 3D results plotted - MC NB

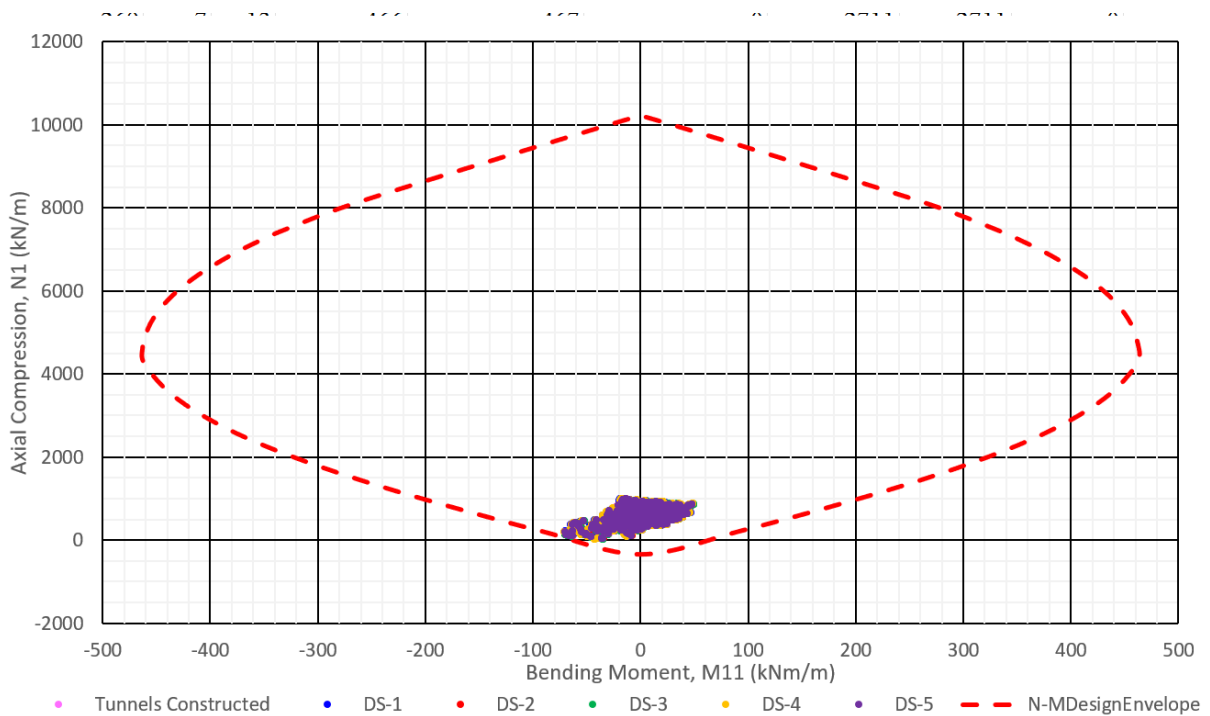


Figure 8-6: Design N-M Interaction Chart for tunnel lining along longitudinal direction with Plaxis 3D results plotted - MC SB

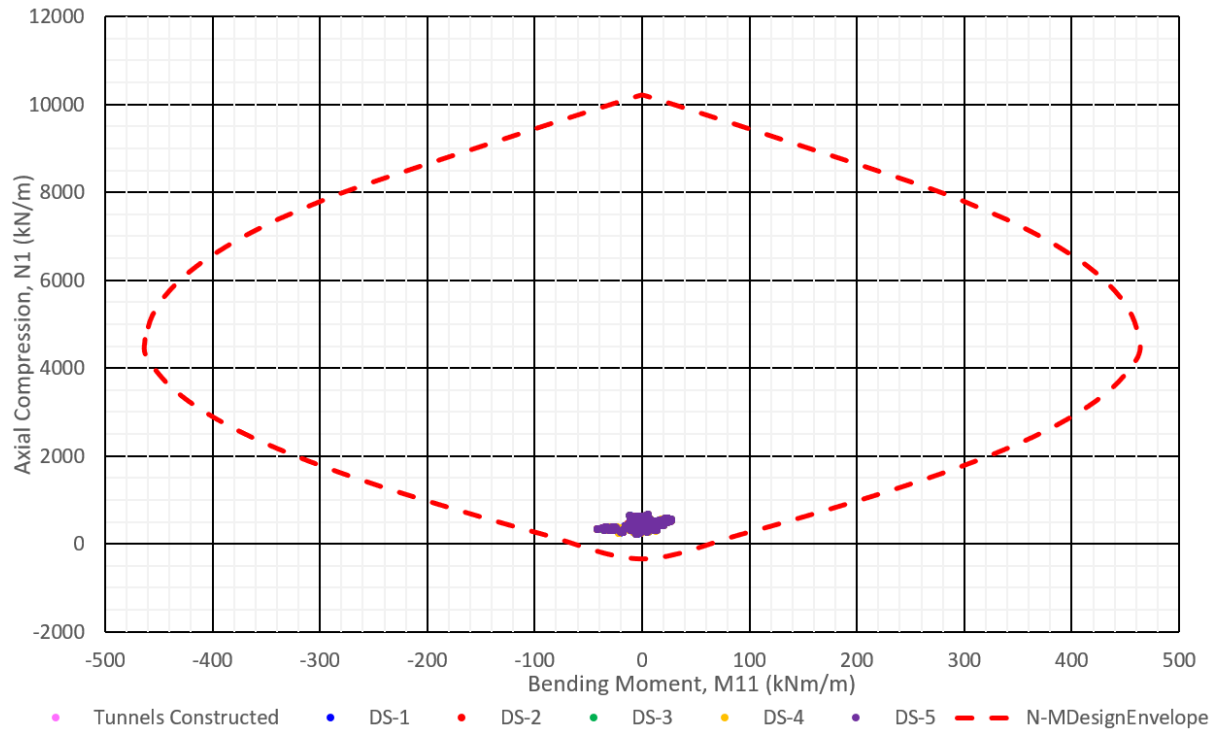


Figure 8-7: Design N-M Interaction Chart for tunnel lining along longitudinal direction with Plaxis 3D results plotted - HSS NB

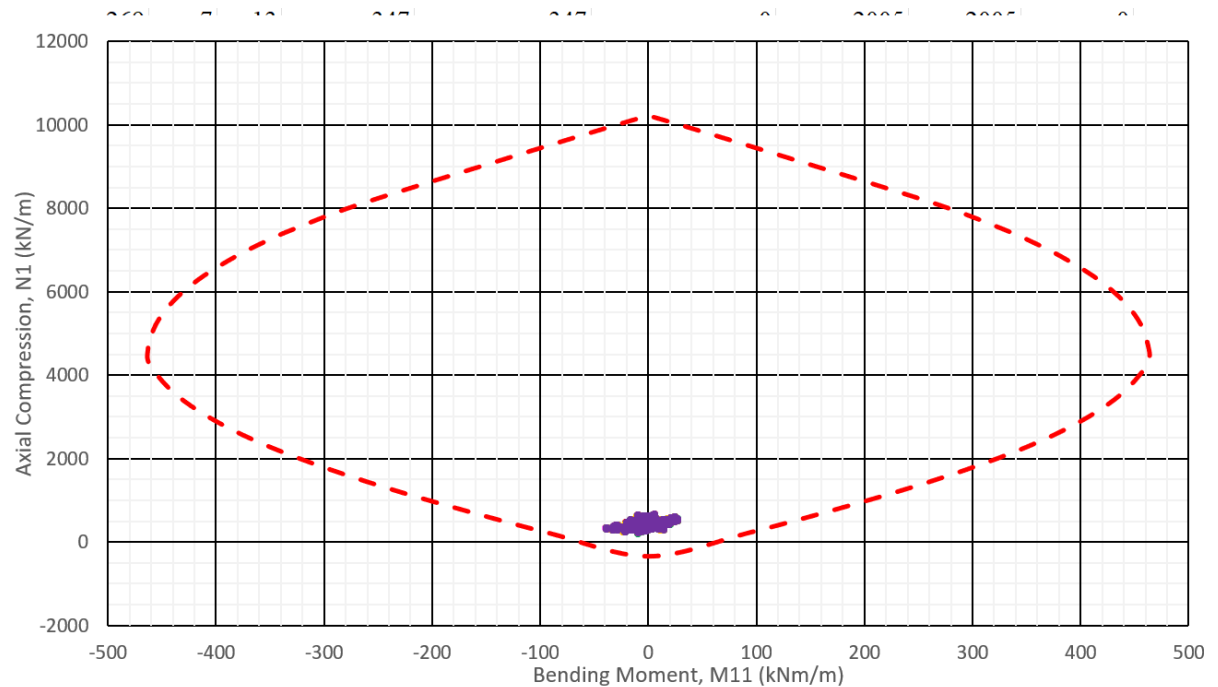


Figure 8-8: Design N-M Interaction Chart for tunnel lining along longitudinal direction with Plaxis 3D results plotted - HSS SB

8.3 Tunnel Lining Shear Forces

8.3.1 Transverse Joints

The shear force exerted on the tunnel lining in the transverse direction has been assessed to determine that the force can be taken by the tunnel lining. The tunnel lining remains in compression in all the design stages, therefore the shear force exerted by the earth pressures would be taken by the shear capacity of the bolts in the transverse direction and the friction between the concrete segments due to the axial load (N_2).

There are 2 No. bolts over the segment width of 1.7m. the bolts are M24 Grade 8.8 spear bolts as shown on drawing no DR/HA/BT/C11/41001/09/X. The design shear resistance of the bolts per m width is 155 kN/m.

The characteristic axial force (N_2) on the segment is at the location of the maximum shear force (Q23) 2614kN/m, which gives a design resistance due to friction of 1046kN/m, assuming a frictional coefficient of 0.4 for a smooth construction joint and a partial factor of 1 applied to the axial force assuming a variable favourable action.

The Total Design Shear Resistance of the primary lining joints is **1201 kN/m**.

The maximum characteristic shear force (Q23) from the Plaxis 3D program was 250kN/m. Conservatively assuming this is a variable unfavourable action, the design shear force is **375kN/m** which is less than the Design Resistance, and is therefore acceptable.

8.3.2 Longitudinal Joints

The shear force exerted on the tunnel lining in the longitudinal direction has been assessed to determine that the force can be taken by the tunnel lining. The tunnel lining remains in compression in all the design stages, therefore the shear force exerted by the earth pressures would be taken by the shear capacity of the bolts in the longitudinal direction and the friction between the concrete segments due to the axial load (N_1). However, the contribution of the friction between the concrete segments has been conservatively ignored in this assessment.

There are 19 No. bolts over the tunnel perimeter length. The bolts are M24 Grade 8.8 spear bolts as shown on drawing no DR/HA/BT/C11/41001/09/X. The design shear resistance of the bolts on the longitudinal joint is **2508 kN** assuming a material factor γ_{m0} of 1.0.

The average characteristic shear force (Q13) over the full tunnel perimeter of 35.2m is 21.75kN/m. Assuming a variable unfavourable action, a partial factor of 1.5 is applied, giving a design longitudinal shear force over the tunnel perimeter of **1147kN**. This is less than the Design Shear Resistance and is therefore acceptable.

8.4 Tunnel Lining Ovalisation & Joint Rotation & Eccentricity

The calculations referred to in this section are included in Appendix A and are based on the calculations provided by Haswell Consulting Engineers in document no. CA_HA_BT_C11_54026_02_O_BORED_LINING_CALCS.

Tunnel Ovalisation/Squatting

The ovalisation/squatting of the tunnels refers to the increase (ovalisation) or decrease (squatting) of the tunnel diameter from its original circular state.

There is no information available on the as-built ovalisation of the Dublin Tunnels. The tunnels were constructed in accordance with the British Tunnel Society Tunnel Specification (1987) which specifies a max construction tolerance of 50mm. This would be equivalent an ovalisation strain of **0.46%** (i.e. $50/(10.84*1000)$).

The maximum vertical and horizontal deflection of the tunnels calculated for DS-1 to DS-5 was 2.1mm, which equates to an ovalisation strain of **0.019%**. This is significantly less than the ovalisation of 0.46% for the permitted construction tolerance of 50mm. Therefore, the ovalisation exerted on the tunnels is considered to have negligible effect on the Dublin Tunnels.

Joint Rotation and Radial Joint Eccentricity

The construction tolerance of 50mm equates to a joint rotation of 0.581 degrees. The maximum vertical and horizontal deflection of the tunnel lining is calculated to be 2.1mm which equates to a joint rotation of **0.024 degrees** which is well below the construction tolerance of 0.581 degrees. Therefore, the joint rotation induced in the tunnel lining due to the construction of the development is considered to have negligible effect on the integrity of the Dublin Tunnels.

The maximum Radial Joint Eccentricity due to the construction tolerance of 50mm equates to 41mm. The maximum deflection of the tunnel lining is calculated to be 2.1mm which is much lower than the 50mm construction tolerance and corresponds to an eccentricity of 28.1mm which is the minimum eccentricity assuming a linear load distribution – see calculations in Appendix A. Consequently, this will have negligible affect on the tunnel lining.

8.5 Tunnel Lining Longitudinal Curving & Joint Opening

The axial forces and bending moments exerted on the tunnels in the longitudinal direction were assessed in Section 8.2.2 and indicate that the forces and bending moments on the tunnel are within the design limits. The results also indicate that the tunnel is in compression along its length and does not go into tension. Therefore, there would be no additional forces exerted on the bolts.

The potential joint opening at the segment connections due to longitudinal distortion has been checked to ensure that any joint opening will not adversely affect the hydrophilic seal at the lining connections. The hydrophilic seal comprises a single hydrophilic strip which is 22 mm wide and 5 mm thick.

The maximum relative displacement between points of inflection due to the curvature of the tunnel in the longitudinal directional in the x and z plane is 0.3mm and occurs over a distance of 8m (DS-2 MC SB western tunnel edge). The maximum theoretical joint opening caused due to the construction on the development is estimated to be 0.74mm. This can be accommodated by the hydrophilic seal which expands when it comes into contact with water. The calculations are included in Appendix A.

9 ASSESSMENT OF PEDESTRIAN CROSS PASSAGE

The maximum vertical stress increase on the Pedestrian Cross Passage is 16.0kPa for the Mohr-Coulomb model and 11.3kPa for the HSS model. These are both well below the 22.5kPa recommended surcharge increase on the tunnel for the tunnel to remain within the Serviceability Limit State.

10 CONSTRUCTION SEQUENCE

Consideration has been given to the impact on the tunnel of the different construction sequences that could be adopted during construction. For example, should Blocks F and G be constructed before Blocks A to E (DS-2) and should the basement be constructed with Blocks F and G (DS-3).

Inspection of the results has shown that the worst-case impact on the tunnels occurs under Block G at the location shown on Figure 7-31, for Design Situations DS-5 (full site loading condition) and DS-2 (Loads applied to Block G and F only).

Any intermediate stages such as DS-1 (excavation of Blocks F and G) and DS-3 (load applied to Block G and F with excavation for basement) were found to be less onerous. The full unloading condition (DS-4) was also found to have no detrimental effect on tunnel lining. The analyses of the situation where Block F was constructed prior Block G and vice versa confirmed that the most onerous condition was as stated above, i.e. DS-2 and DS-5. The plots showing the results of these assessments are included in Appendix F. Assessment of the model also showed that Blocks B and C (which are greater than 55m from the northbound tunnel) and attenuation tanks 1, 2 and 3, were outside zone of influence of the tunnel, hence these elements can be constructed at any stage – see plots included in Appendix F.

Therefore, the model was not found to be sensitive to the construction sequence adopted.

Table 10-1 presents the construction sequences analysed as part of this report, that must be adopted by the Contractor during the works. No other construction sequences shall be permitted.

Table 10-1: Construction Sequences analysed (see notes 1 & 2)

Step	Sequence A	Sequence B	Sequence C	Sequence D
1	Excavation for Foundations of Block F and Block G ²		Excavation for basement, foundations for Blocks F and G ² , and basement access ramp	
2	Construction of Block F and G ²	Excavation of basement, and basement access ramp	Construction of Block F and G ²	Construction of Blocks A, D, E, F & G
3	Excavation of Basement carpark below Blocks A, D & E, access ramp	Construction of Blocks F and G ²	Construction of Blocks A, D & E	
4	Construction of Blocks A, D & E			

Note

1. Blocks B and C (which are greater than 55m from the northbound tunnel) and attenuation tanks 1, 2 and 3, were outside zone of influence of the tunnel, hence these elements can be constructed at any stage
2. Blocks F and G can be excavated and constructed in any order i.e. Block F can be constructed before Block G and vice versa.

11 SUMMARY & CONCLUSION

The 3D finite element program, PLAXIS, has been used to assess the impact on the Dublin Port Tunnels due to the excavation and building loads for the Hartfield Place Development.

The Plaxis 3D program enables structural elements as well as soils to be modelled to develop sophisticated soil/structure interaction analyses and the 3D modelling allows for the combined effect of the development on the Dublin Port Tunnels (DPTs) to be analysed. The assessment takes into account all aspects of the development including the excavation for the basement carpark under Blocks A to E, the loads for the buildings Blocks A to G and the unloading due to construction of the attenuation tanks.

The Hardening Soil model with small-strain stiffness (HSS) and the Mohr Coulomb (MC) material models have been used to model the behaviour of the Boulder Clays. The latter model (MC) provides a more conservative estimate of the impact of the development on the tunnel, however, the HSS model has been shown to closely model the behaviour of the very stiff Dublin Boulder Clays (Lawlor et. al, 2011).

The NRA (now TII) has set out criteria to be met for any development proposed to be constructed in the vicinity of the Dublin Port Tunnels in the document titled *Guidance Notes for Developers, The assessment of surface and sub-surface developments in the vicinity of the Dublin Port Tunnel*. This document states the following with regards to surcharge loading and unloading of the DPTs:

- *“Surcharge Loading: The NRA requires the developer to demonstrate that a development does not incur a surcharge loading on the tunnel in excess of 22.5kNm² either during construction or at completion. Cognisance must be taken of any surcharge loading at depth due to anchors or piles.*
- *Unloading: The NRA requires the developer to demonstrate that the method and sequencing of construction of the development minimises or eliminates the potential for tunnel deformation”*

Section 2.5 of the GND also states the following:

- *The NRA will consider: A comprehensive submission from the developer which demonstrates that surcharge loads, during construction and on completion, exceeding 22.5kNm² are not detrimental to the lining and its components with respect to the Ultimate Limit and Serviceability Limit States*

The analysis carried out in this report assesses the results with respect to the criteria set out by TII above. In addition, checks of the tunnel lining for Ultimate Limit and Serviceability Limit State have been made in respect to tunnel distortion such as ovalisation/squatting and longitudinal tunnel deformations, as well as shear force, axial force and bending moment in the tunnel lining (both in the longitudinal and transverse directions) and the tunnel lining bolt connections.

The analysis has been carried out for various design situations (DS-1 to DS-5) to account for the different excavation depths and loading combinations for the development that would have an impact on the Dublin Port Tunnels which includes the following:

- DS-1: Excavation of Block F and Block G
- DS-2: Excavation & Loading of Block F and Block G with no benefit from unloading due to the basement excavation
- DS-3: Excavation & Loading of Block F and Block G with excavation of basement

- DS-4: Full unloading of site due to excavation for basement, access ramp, Block F, Block G and the attenuation tanks.
- DS-5: Excavation & Loading of the site for Blocks A to G and the basement carpark i.e. final development

The following is a summary of the results of the assessment of the proposed development on the tunnels from the numerical analysis presented herein:

1. The analyses showed that the increase in vertical total stress on the tunnel lining does not exceed the limit of 22.5kPa at any point on the main tunnels or pedestrian cross passage. The maximum increase in stress on the tunnel lining is calculated to be 19.3kPa for Design Situation DS-2 for the Mohr Coulomb material model. We note that TII does not require any further assessment of the tunnel lining and its components (i.e., in respect to the Ultimate Limit and Serviceability Limit States) where the surcharge loading on the tunnel does not exceeded. 22.5 kN/m².
2. The design bending moments and axial forces derived from the Plaxis 3D model indicate that the combined design axial forces and bending moments plot within the design envelope for the tunnel lining both in the transverse and longitudinal directions and are therefore acceptable.
3. The design shear forces exerted on the tunnel lining in the transverse and longitudinal directions are less than the design shear resistance of the tunnel lining and are therefore acceptable.
4. The change in ovalisation, joint rotation, radial joint eccentricity and longitudinal curving of the tunnel due to the proposed development are considered to have negligible effect on the integrity of the Dublin Tunnels.
5. Based on the results of the 3D finite element analysis, the impact on the Dublin Port Tunnels of different construction sequences (modelled by the design situations DS-1 to DS-5) was found to be negligible.
6. Consideration has been given to the impact on the tunnel of the different construction sequences that could be adopted during construction. The construction sequences analysed as part of this report must be adopted by the Contractor during the works. No other construction sequences shall be permitted.

In conclusion, it is found that the construction of the proposed residential development at Hartfield Place does not exceed the TII surcharge limit on the tunnels and is also found to have no detrimental effect on tunnel lining.

12 REFERENCES

1. CA/HA/BT/C11/54026/02/O titled Bored Tunnel Lining Definitive Design Calculations.
2. Gillarduzzi (2013), Proceedings of the Institution of Civil Engineers Forensic Engineering 167 August 2014 Issue FE3 Pages 119–142
3. Guidance Notes for Developers, The assessment of surface and sub-surface developments in the vicinity of the Dublin Port Tunnel
4. Myles L. Lawler, Eric R. Farrell, and Andrew L.E. Lochaden 2011. Comparison of the measured and finite element–predicted ground deformations of a stiff lodgement till, Canadian Geotechnical Journal Volume 48: 98–116 (2011) (Lawlor et al, 2011)
5. Specification for Tunnelling, Third Edition, British Tunnelling Society and The Institution of Civil Engineers, ICE, British Tunnelling Society.
6. The bearing capacity of Dublin Black Boulder Clays, E.R. Farrell, N.G. Bunni & J. Mulligan (1988) IEI Transactions 1987-1988 IEI. Vol 112 (Farrell et al., 1988)
7. Long, Brangan, Menkiti, Looby and Casey, Retaining walls in Dublin Boulder Clay, Ireland, Geotechnical Engineering Volume 165 Issue GE4, ICE Publishing, 15/05/2012

APPENDIX A

CALCULATIONS

APPENDIX B

AS-BUILT DRAWINGS OF DUBLIN PORT TUNNELS

APPENDIX C

PLAXIS 3D RESULTS

APPENDIX D

**COMPARISON OF MOHR COULOMB (MC) AND HARDENING SOIL
MODEL WITH SMALL-STRAIN STIFFNESS (HSS) MATERIAL MODELS**

APPENDIX E

PUNCH CONSULTING CHARACTERISTIC BEARING PRESSURES BELOW BUILDINGS & BASEMENT

APPENDIX F

PLAXIS 3D RESULTS – CONSTRUCTION SEQUENCE

APPENDIX G

GII 2010 GROUND INVESTIGATION REPORT

APPENDIX H

GII 2020 GROUND INVESTIGATION REPORT